Models of Sub-Components and Validation for the IEA SHC Task 44 / HPP Annex 38

Part C: Heat Pump Models

A technical report of subtask C

Report C2 Part C – Final Draft

Date: 10 Jun 2013

By Ralf Dott[1], Thomas Afjei[1], Andreas Genkinger[1], Antoine Dalibard[2], Dani Carbonell[3], Ricard Consul[3], Andreas Heinz[4], Michel Haller[5], Andreas Witzig[6], Jorge Facão[7], Fabian Ochs[8], Peter Pärisch[9]

[1] Institut Energie am Bau - Fachhochschule Nordwestschweiz, IEBau - FHNW,
St. Jakobs-Strasse 84, 4132 Muttenz, Switzerland

Phone : +41 61 467 45 74
E-mail : ralf.dott@fhnw.ch

[2] University of Applied Sciences Stuttgart, Schellingstraße 24, 70174 Stuttgart, Germany

[3] RDmes Technologies S.L., IPCT, Ctra. Nac. 150, km 14.5, 08227 Terrassa, Spain

[4] Graz University of Technology, IWT, Inffeldgasse 25/B, 8010 Graz, Austria

[5] Institut für Solartechnik SPF - HSR, Oberseestr. 10, 8640 Rapperswil, Switzerland

[6] Vela Solaris AG, Stadthausstrasse 125, 8400 Winterthur, Switzerland

[7] LNEG, Estrada do Paço do Lumiar, 22, Edifício H, 1649-038 Lisboa, Portugal

[8] UIBK, Universität Innsbruck, Technikerstr. 13, 6020 Innsbruck, Austria

[9] ISFH GmbH, Am Ohrberg 1, 31860 Emmerthal, Germany

SOLAR HEATING & COOLING PROGRAMME
INTERNATIONAL ENERGY AGENCY

IEA Solar Heating and Cooling Programme

The *International Energy Agency* (IEA) is an autonomous body within the framework of the Organization for Economic Co-operation and Development (OECD) based in Paris. Established in 1974 after the first "oil shock," the IEA is committed to carrying out a comprehensive program of energy cooperation among its members and the Commission of the European Communities.

The IEA provides a legal framework, through IEA Implementing Agreements such as the *Solar Heating and Cooling Agreement*, for international collaboration in energy technology research and development (R&D) and deployment. This IEA experience has proved that such collaboration contributes significantly to faster technological progress, while reducing costs; to eliminating technological risks and duplication of efforts; and to creating numerous other benefits, such as swifter expansion of the knowledge base and easier harmonization of standards.

The *Solar Heating and Cooling Programme* was one of the first IEA Implementing Agreements to be established. Since 1977, its members have been collaborating to advance active solar and passive solar and their application in buildings and other areas, such as agriculture and industry. Current members are:

Australia	Finland	Singapore
Austria	France	South Africa
Belgium	Italy	Spain
Canada	Mexico	Sweden
Denmark	Netherlands	Switzerland
European Commission	Norway	United States
Germany	Portugal	

A total of 49 Tasks have been initiated, 35 of which have been completed. Each Task is managed by an Operating Agent from one of the participating countries. Overall control of the program rests with an Executive Committee comprised of one representative from each contracting party to the Implementing Agreement. In addition to the Task work, a number of special activities—Memorandum of Understanding with solar thermal trade organizations, statistics collection and analysis, conferences and workshops—have been undertaken.

Visit the Solar Heating and Cooling Programme website - www.iea-shc.org - to find more publications and to learn about the SHC Programme.

Current Tasks & Working Group:

Task 36	*Solar Resource Knowledge Management*
Task 39	*Polymeric Materials for Solar Thermal Applications*
Task 40	*Towards Net Zero Energy Solar Buildings*
Task 41	*Solar Energy and Architecture*
Task 42	*Compact Thermal Energy Storage*
Task 43	*Solar Rating and Certification Procedures*
Task 44	*Solar and Heat Pump Systems*
Task 45	*Large Systems: Solar Heating/Cooling Systems, Seasonal Storages, Heat Pumps*
Task 46	*Solar Resource Assessment and Forecasting*
Task 47	*Renovation of Non-Residential Buildings Towards Sustainable Standards*
Task 48	*Quality Assurance and Support Measures for Solar Cooling*
Task 49	*Solar Process Heat for Production and Advanced Applications*

Completed Tasks:

Task 1	*Investigation of the Performance of Solar Heating and Cooling Systems*
Task 2	*Coordination of Solar Heating and Cooling R&D*
Task 3	*Performance Testing of Solar Collectors*
Task 4	*Development of an Insolation Handbook and Instrument Package*
Task 5	*Use of Existing Meteorological Information for Solar Energy Application*
Task 6	*Performance of Solar Systems Using Evacuated Collectors*
Task 7	*Central Solar Heating Plants with Seasonal Storage*
Task 8	*Passive and Hybrid Solar Low Energy Buildings*
Task 9	*Solar Radiation and Pyranometry Studies*
Task 10	*Solar Materials R&D*
Task 11	*Passive and Hybrid Solar Commercial Buildings*
Task 12	*Building Energy Analysis and Design Tools for Solar Applications*
Task 13	*Advanced Solar Low Energy Buildings*
Task 14	*Advanced Active Solar Energy Systems*
Task 16	*Photovoltaics in Buildings*
Task 17	*Measuring and Modeling Spectral Radiation*
Task 18	*Advanced Glazing and Associated Materials for Solar and Building Applications*
Task 19	*Solar Air Systems*
Task 20	*Solar Energy in Building Renovation*
Task 21	*Daylight in Buildings*
Task 22	*Building Energy Analysis Tools*
Task 23	*Optimization of Solar Energy Use in Large Buildings*
Task 24	*Solar Procurement*
Task 25	*Solar Assisted Air Conditioning of Buildings*
Task 26	*Solar Combisystems*
Task 27	*Performance of Solar Facade Components*
Task 28	*Solar Sustainable Housing*
Task 29	*Solar Crop Drying*
Task 31	*Daylighting Buildings in the 21st Century*
Task 32	*Advanced Storage Concepts for Solar and Low Energy Buildings*
Task 33	*Solar Heat for Industrial Processes*
Task 34	*Testing and Validation of Building Energy Simulation Tools*
Task 35	*PV/Thermal Solar Systems*
Task 37	*Advanced Housing Renovation with Solar & Conservation*
Task 38	*Solar Thermal Cooling and Air Conditioning*

Completed Working Groups:

CSHPSS; ISOLDE; Materials in Solar Thermal Collectors; Evaluation of Task 13 Houses; Daylight Research

IEA Heat Pump Programme

This project was carried out within the Solar Heating and Cooling Programme and also within the *Heat Pump Programme*, HPP which is an Implementing agreement within the International Energy Agency, IEA. This project is called Task 44 in the *Solar Heating and Cooling Programme* and Annex 38 in the *Heat pump Programme*.

The Implementing Agreement for a Programme of Research, Development, Demonstration and Promotion of Heat Pumping Technologies (IA) forms the legal basis for the IEA Heat Pump Programme. Signatories of the IA are either governments or organizations designated by their respective governments to conduct programmes in the field of energy conservation.

Under the IA collaborative tasks or "Annexes" in the field of heat pumps are undertaken. These tasks are conducted on a cost-sharing and/or task-sharing basis by the participating countries. An Annex is in general coordinated by one country which acts as the Operating Agent (manager). Annexes have specific topics and work plans and operate for a specified period, usually several years. The objectives vary from information exchange to the development and implementation of technology. This report presents the results of one Annex. The Programme is governed by an Executive Committee, which monitors existing projects and identifies new areas where collaborative effort may be beneficial.

The IEA Heat Pump Centre

A central role within the IEA Heat Pump Programme is played by the IEA Heat Pump Centre (HPC). Consistent with the overall objective of the IA the HPC seeks to advance and disseminate knowledge about heat pumps, and promote their use wherever appropriate. Activities of the HPC include the production of a quarterly newsletter and the webpage, the organization of workshops, an inquiry service and a promotion programme. The HPC also publishes selected results from other Annexes, and this publication is one result of this activity.

For further information about the IEA Heat Pump Programme and for inquiries on heat pump issues in general contact the IEA Heat Pump Centre at the following address:

IEA Heat Pump Centre
Box 857
SE-501 15 BORÅS
Sweden
Phone: +46 10 16 55 12
Fax: +46 33 13 19 79

Visit the Heat Pump Programme website - http://www.heatpumpcentre.org/ - to find more publications and to learn about the HPP Programme.

Contents

1 Introduction

1.1 General Situation

Europe launched an ambitious program: 20-20-20 up to 2020, i.e. 20% less greenhouse gases, 20% higher energy efficiency and a share of 20% renewable energies until the year 2020. Ultra-low energy, near or net zero energy buildings are part of the solution. Many of them are equipped with heat pumps. Hence, in future highly energy-efficient buildings, heat pumps will play a key role. Annual efficiency calculation and optimization by means of simulating heat pump heating and cooling systems are very valuable, especially if building and building technology are coupled.

1.2 Heat Pump Modelling Group

The "Heat Pump Modelling Group" works in the frame of Subtask C "Modelling and Simulation" of the project "Solar and heat pumps" for the International Energy Agency IEA, conducted as joint project of the Solar Heating and Cooling Programme SHC as Task 44 and the Heat Pump Programme HPP as Annex 38 (IEA HPP A38 / SHC T44). Further information is available on the website task44.iea-shc.org. Working Group members of the Heat Pump Modelling Group in this frame are:

Thomas Afjei*	thomas.afjei@fhnw.ch	FHNW	CH	
Ralf Dott	ralf.dott@fhnw.ch	FHNW	CH	
Antoine Dalibard	antoine.dalibard@hft-stuttgart.de	HFT Stuttgart	DE	see Ch. A1
Dani Carbonell	rdmes@rdmes.com	RDmes	ES	see Ch. A2
Ricard Cònsul	rdmes@rdmes.com	RDmes	ES	see Ch. A2
Oscar Camara	oscar.camara@aiguasol.coop	Aiguasol	ES	
Anja Loose	loose@itw.uni-stuttgart.de	ITW	DE	
Andreas Heinz	andreas.heinz@tugraz.at	IWT	AT	see Ch. A3
Michel Y. Haller	michel.haller@solarenergy.ch	SPF	CH	see Ch. A3
Jeremy Sager	Jeremy.Sager@NRCan-RNCan.gc.ca	NRCan	CA	
Sara Eicher	sara.eicher@heig-vd.ch	HEIG	CH	
Peter Pärisch	p.paerisch@isfh.de	ISFH	DE	see Ch. A8
Marc Bätschmann	marc.baetschmann@3s-pv.ch	3S	CH	
Pierre Hollmuller	pierre.hollmuller@unige.ch	Uni Geneva	CH	
Fabian Ochs	fabian.ochs@uibk.ac.at	Uni Innsbruck	AT	see Ch. A7
Cedric Paulus	cedric.paulus@cea.fr	CEA INES	FR	
Matteo D'Antoni	matteo.dantoni@eurac.edu	EURAC	IT	
Jorge Facao	jorge.facao@lneg.pt	LNEG	PT	see Ch. A6
Andreas Genkinger	andreas.genkinger@fhnw.ch	FHNW	CH	see Ch. A5

* Leader of the group

1.3 This Report

This report gives an overview on existing models and a categorization with pros and cons in terms of generic approach, validation and quality of documentation. Most common are simple performance map based models for seasonal performance factor calculations, sometimes improved by adding PT1 inertia for heating up and cooling down. Especially for heat pump design, refrigerant cycle based physical grey-box models can encourage new developments. Furthermore first results of the work in connection with heat pump modelling for IEA HPP A38 / SHC T44 are presented. Further contributions are welcome to be integrated.

2 Purpose of heat pump modelling

Depending on the use of the heat pump model, there are mainly three different classes of models corresponding to the required level of detail and the amount of work accepted for their application. Table 1 shows a qualification of the three model classes according to their application, which are described in the following.

2.1 Calculation methods

The aim of calculation methods is to provide a fast but sufficiently precise calculation of heat pump system performance, in order to compare different heat pump products using a seasonal coefficient of performance (SCOP) or to calculate a building specific seasonal performance factor (SPF). Both, the best choice and most commonly used, are calculation methods using simplified performance maps and an energy or time related weighting of representative operating conditions.

2.2 Dynamic system behaviour

Going into more detail, the next step is dynamic analyses of whole heat supply systems. Therein, mostly performance maps for the heat pump behaviour are both in use and in most cases appropriate, but now with more detailed performance data. However, the time-dynamic influence of the boundary conditions, such as climate or user behaviour, is now considered as a temporal series of boundary conditions with fixed or dynamic time steps.

2.3 Heat pump design

The need in heat pump design processes is to optimize the heat pump unit on the level of the refrigerant cycle. Hence, the models need to calculate the refrigerant flows and states as well as to represent the heat pump components individually (evaporator, compressor, condenser and expansion valve) to be able to replace components and optimize the interaction of the heat pump components. Therein mostly component performance map models are in use. For further optimization of the individual heat pump components, e.g. the evaporator of an air-to-water heat pump, specialized physical models are necessary.

Table 1: General qualification of models

	Calculation methods		Dynamic simulation		Heat pump design models	
	SCOP	SPF	quasi steady state model	dynamic effect model	refrigerant cycle model	heat pump component
Flexibility of use	- -	-	o	+	++	o
Level of detail	- -	-	o	o	+	++
Amount of work for application	- -	-	o	o	++	++
Computation time	- -	- -	o	+	++	++
Required knowledge	-	-	o	+	++	x

- - = very low - = low o = medium + = high ++ = very high x = specialized

3 Heat pump model overview

3.1 Calculation methods

In standards, mostly easy to use calculation methods are required for the seasonal performance factor of commonly used heat pumps. They are in use for the purpose of comparison between different heat pumps or with other heat generating technologies. Therein two different applications of calculation methods can be distinguished, product comparison with standard ratings and system evaluation applied to individual buildings. Both types of calculation methods usually use simplified performance maps of heat pumps while time and energy are taken into account by weighting factors for representative operating conditions.

3.1.1 Product Comparison

Product comparison with standard ratings (e.g. SCOP) uses simplified calculation methods under uniform standard conditions and boundaries not related to a real but only to an artificial reference building and furthermore indicated only for a single or a restricted number of representative climatic conditions. For Northern America, the standard ANSI/AHRI 210/240-2008 defines the measurement conditions and calculation procedure of the seasonal energy rating for the heating period as heating seasonal performance factor (HSPF) and for the cooling period as the seasonal energy efficiency ratio SEER. In the European standardization there is up to now no finalized standard for a seasonal energy rating on product comparison level. Until now, product labelling and hence comparison is referred to single operating conditions by the coefficient of performance (COP) based on measurements according to EN 14511:2011.

The standard EN 14825:2012 will provide a standard rating by a SCOP for the heating season and by a SEER for the cooling season. The standard defines one reference climate for cooling and three reference climatic conditions for heating, i.e. average, warmer and colder climate. It defines furthermore one procedure for heat emission systems in cooling mode and three types of heat emission systems for heating, i.e. low, medium and high temperature application.

3.1.2 Comparison of individual building technology

The comparison of an individual building technology solution with required minimum performance (e.g. SPF) or maximum primary energy consumption requires calculation methods that are more detailed and have as far as possible realistic boundary conditions, but also take into account some standard assumptions e.g. for the user behaviour. On the European level, this provides the standard EN 15316-4-2:2008 named “Heating systems in buildings – Method for calculation of system energy requirements and system efficiencies – Part 4-2: Space heating generation systems, heat pump systems”. Therein, the calculation method bases on a temperature class approach (bin-method shown in Figure 1), where representative operating conditions are weighted with individually derived factors based on time and energy. This could be extended by a ventilation system and eventually installed solar components that are considered by subtracting the fraction of the heat recovery / solar input of the fraction of space heating (SH) or domestic hot water (DHW, in figure 1 also W is used) energy, respectively, to be covered by the heat pump. The fraction of back-up energy is calculated by an energy balance, which is evaluated by the running time of the heat pump. The heat pump fraction is subsequently weighted with the respective COP of the bin derived

by the testing, and added-up. An energy weighting of the heat pump and back up delivers the SPF for the SH mode. In a similar way, the SPF of the DHW-mode is calculated and energy weighting of both SPF numbers delivers the overall SPF of the unit.

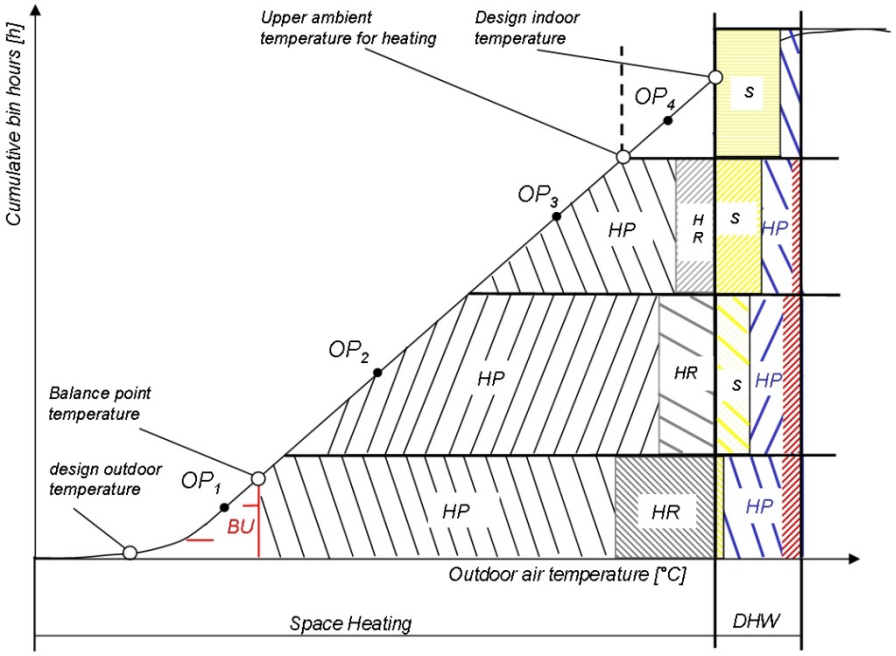

Figure 1: Principle of the bin method for space heating, domestic hot water and ventilation with heat recovery systems
(OP - operating point, BU – back-up, HR – heat recovery unit, HP – Heat Pump, S – Solar heat)
(from Afjei et al. 2007)

The described static calculation methods are well suited for known components in known system configurations that are covered by the respective calculation procedure and allow for a very fast and sufficiently precise result for a broad group of users. However, they are also restricted to the above-mentioned application and are not suitable for new system configurations, applications or an extrapolation of the application range.

3.2 Dynamic system simulation

For the evaluation of new more sophisticated system concepts, a more detailed modelling is required to be able to consider system dynamics or to evaluate the systems under varying boundary conditions. Therein the interaction of heat loads like building or domestic hot water demand with heat storages and heat sources, e.g. borehole heat exchangers or solar heat, play a key role for the evaluation of the system behaviour over long-term periods like full years or short-term periods to evaluate for example the control behaviour. Empirical models are quite widespread, because the representation of the component behaviour in the system is sufficiently precise and furthermore the required data of individual products are mostly available. Physical models, or better models based on physical effects, are rather available for less complex components like solar collectors or borehole heat exchangers, but not for such complex units as heat pumps since the required computation time rises significantly if solving the states and flows of the refrigerant cycle for each simulation time step.

3.2.1 Performance map models

Quasi steady state performance map models are the most widespread heat pump models in dynamic simulation programs like e.g. TRNSYS, ESP-r, Insel, EnergyPlus, IDA-ICE or Matlab/Simulink Blocksets (as e.g. described in Afjei 1989) and Polysun (see Witzig 2008). Therein, a restricted number of sampling points from performance map measurements are used either to interpolate in-between those points or to fit a two-dimensional polynomial plane. These models use the inlet-temperature of the heat source to the heat pump and the desired outlet-temperature on the heat sink side of the heat pump to calculate the thermal output of the heat pump and its electricity demand. Figure 2 shows an exemplary COP performance map of an air-to-water heat pump.

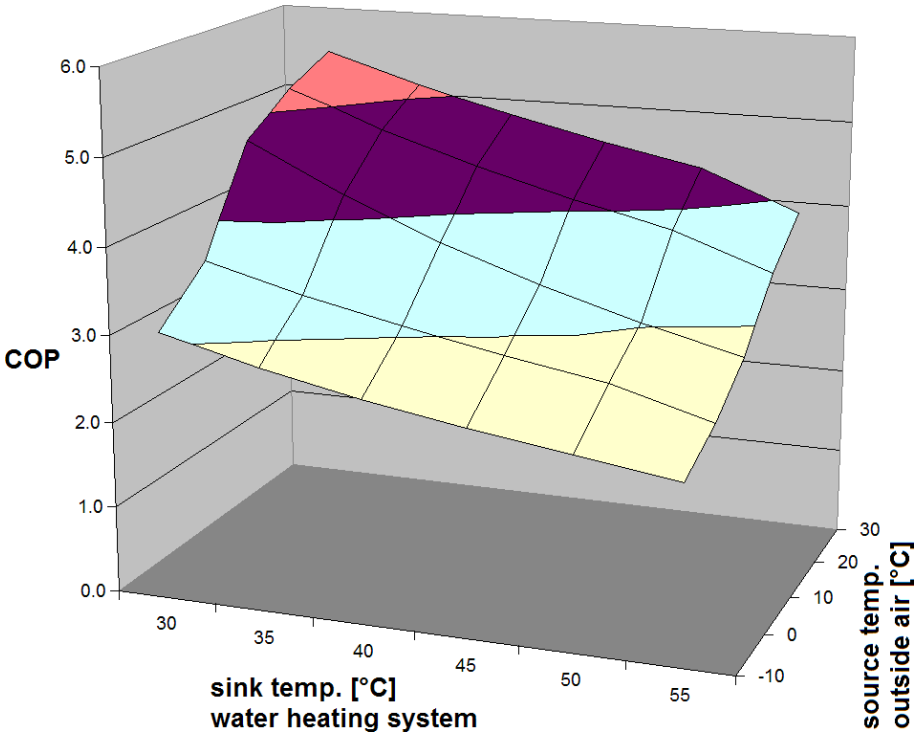

Figure 2: Exemplary COP performance map of an air-to-water heat pump from Dott et al. 2011

Typical implementations of quasi steady state performance map models for heat pumps in simulation software packages are for example the TRNSYS Types 504, 505, 665 and 668 from the TESS library 2011. Furthermore, these kinds of models can also represent a more complex heat pump, if they still have defined characteristics like a two stage heat pump that has been described by Afjei et al. 1997. The following equation shows exemplarily for the heat capacity of a heat pump, a biquadratic curve-fit equation model as it is used in the Afjei 1989 model description:

$$\dot{Q}_{HP} = C_{q1} + C_{q2} * T'_{evap,in} + C_{q3} * T'_{cond,out} + C_{q4} * T'_{evap,in} * T'_{cond,out} + C_{q5} * {T'_{cond,out}}^2 + C_{q6} * {T'_{evap,in}}^2 \quad \text{with } T' = \frac{T+273.15}{273.15}$$

Usually only the standard measurements according to EN 14511:2011 are available as input for this kind of simulation models. Therein standard rating conditions, that are mandatory, and application rating conditions, which provide additional information (in the following given in brackets), are declared. For water source heat pumps the rating conditions, representing typical heat source conditions, are 10 °C (15 °C), and for brine source heat pumps, 0 °C (-5 °C / 5 °C). For air source heat pumps the inlet dry bulb temperature of the outdoor air is 7 °C (2 °C / -7 °C / -15 °C / 12 °C). The corresponding heat sink temperatures represent the desired outlet temperature, i.e. the supply temperature to the heating system. EN 14511:2011 defines standard rating points for low temperatures at 35 °C e.g. for floor heating, for medium temperatures at 45 °C e.g. for radiator heating in low energy buildings, for high temperatures at 55 °C e.g. for other radiator heating systems and for very high temperatures at 65 °C. Both, look-up table and polynomial fit models, represent the behaviour quite well in the range of the given sampling points. However, if extrapolating the range, the user has to check the results carefully, since the gradients at the boundary of the modelled performance map do not necessarily correspond to the gradient of the real heat pump. This effect has especially shown relevance on the one hand for very low sink temperatures, e.g. in ultra-low energy houses with thermally active building elements using flow temperatures in the range of 25 °C to 30 °C, and on the other hand for solar assisted heat pumps with high source temperatures, when the maximum operating pressure of thermostatic expansion valves can be reached. Furthermore air source heat pumps show a significant drop in performance at source temperatures below 5-7 °C. There, the moisture in the heat source air can start forming ice on the evaporator, which needs to be defrosted, if too much ice has formed. This effect decreases the COP of the heat pump by a few decimal points below the mentioned source temperatures. Therefore, especially for air source heat pumps, the gradients at the boundary of the measured performance maps are very important for extrapolating the performance map in simulation. The measurements according to EN 14511:2011 include the icing / defrosting effect for air source heat pumps by averaging the performance measurements over operating periods that include heat pump operation with and without icing. Hence, it will be considered correctly for annual performance simulations, but the short time dynamic effect influencing the control or flow temperature fluctuations will not be represented.

3.2.2 Dynamic effects

Dynamic effects like described above for icing / defrosting can be an extension to quasi steady state models. The effect of icing / defrosting has been described by Afjei 1989 based on a semi empirical model approach. Therein, the COP reduction due to the icing effect could be considered separately as addition to performance map based on compressor data, where icing / defrosting is not taken into account. Furthermore, the model described in Afjei 1989 includes extensions for thermal inertia in condenser or evaporator. A PT1 element with

defined time constant represents the dynamic effect during the start-up or shutdown of the heat pump. The first order differential equation models the heating of the heat pump components and the pressurising of the heat pump cycle as well as releasing the stored heat after shutdown.

In conclusion, the dynamic system simulation models rely also on reference measurements according to EN 14511:2011, like the calculation methods, which are very well suited for most applications that operate in the range of the underlying measurement data. Important is a good fitting of the performance map to the real characteristic that could be achieved by look-up tables as well as with polynomial fits. Compared to static calculation methods, dynamic system simulations consider time dynamically and hence are free to combine a wider range of surrounding system components. Furthermore, they are able to implement additional short time dynamic effects.

3.3 Heat Pump Design models

The most sophisticated class are models for the design of heat pumps. Their aim is to be able to build up a theoretical heat pump out of known component characteristics, i.e. for condenser, expansion valve, evaporator and compressor. Therefore, they need to represent the interaction of the internal heat pump components on the refrigerant cycle level and calculate the refrigerant states and flows. On the heat pump assembly design level, the interaction of the refrigerant cycle components, their sizing and the refrigerant types are of main interest. Again, performance map models are mostly used, but now performance maps for the refrigerant cycle components. For the optimization of single components, some models go even to a more detailed level to optimize the component design and behaviour like e.g. icing of an air-to-water heat pump evaporator or inverter driven compressors. On this level of detail, physical models are sometimes in use or, albeit rarely, 3D-CFD models.

3.3.1 Refrigerant Cycle models

Refrigerant cycle models aim to optimize the heat pump by choosing the right components for evaporator, compressor, condenser and expansion valve or by integrating additional components into the refrigerant cycle like subcooler, desuperheater or internal heat exchanger. Therein, the aim is mainly not to optimize components in detail but to exchange components and find the right components for an optimized interaction. Hence, the refrigerant cycle models require performance characteristics of the heat pump components from measurements, where a good representation of their behaviour in the heat pump cycle is important. These models are again mainly quasi steady state models, but now on component level.

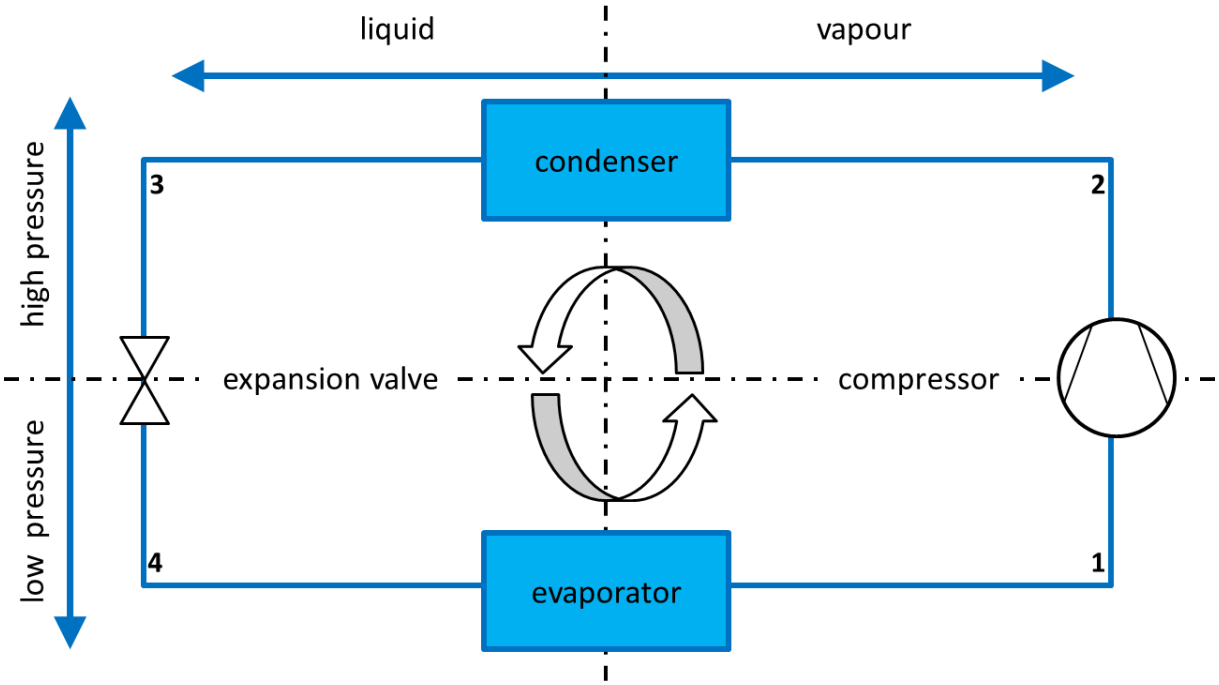

Figure 3: Schematic heat pump process

The development of refrigerant cycle models starts from rather simple representations of the refrigerant cycle, as shown in Figure 3. Therein, pressure drop is neglected and hence constant refrigerant temperatures are assumed over the evaporator and condenser and they are calculated based on the average logarithmic temperature difference in the heat exchangers. A heat transfer characteristic of the heat exchangers (NTU-model) allows for the

adaption to varying mass flow rates, flow temperatures and compressor capacity. Hence, the evaporator and the condenser are calculated with one averaged heat transfer efficiency, summarizing the parts of the heat exchanger, where desuperheating, subcooling or superheating of the refrigerant takes place or only separating the desuperheating part in the condenser. Fourth degree polynomials can be found for the evaporator and condenser NTU-models. The compressor model bases on a characteristic of its isentropic efficiency.

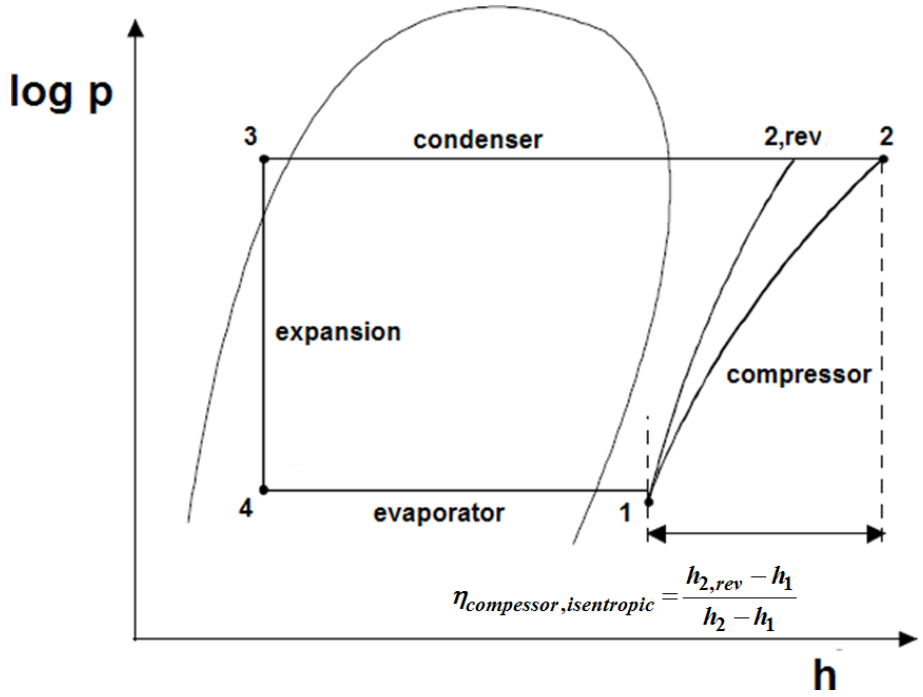

Figure 4: Heat pump process in log-p-h-diagram with isentropic compressor efficiency

The isentropic efficiency is calculated as quotient of the isentropic enthalpy difference for an ideal and hence reversible compression divided by the real, polytropic enthalpy difference, c.f. Figure 4. The models used for the isentropic efficiency range from an assumed constant isentropic efficiency to 3rd degree polynomials of the compression ratio over the compressor. For the volumetric efficiency of the compressor, 2nd degree polynomials or exponential functions of the compression ratio can be found. The process in the expansion valve is commonly assumed adiabatic, since the heat transferred across the small surface is negligible. All parameters of the above-mentioned curve fit models have to be derived from measurements or catalogue data. The above-described models can be found for example in detail in Hornberger 1994 or Schraps 2001.

The development of refrigerant cycle models in detail goes into more detailed representations of heat pump components, the integration of more physical effects and the consideration of time dynamic effects. For example, Bühring 2001 extended in his doctoral thesis the commonly used quasi-static heat pump design models with the integration of two condensers in series, an air source evaporator considering icing on the evaporator with a simplified model and with an internal heat exchanger. With using two condensers in series it is necessary to differentiate the parts of the condenser where the refrigerant desuperheats, condenses or subcools, to be able to calculate the heat flows in the two heat exchangers that work with only one expansion valve behind both. Thus every condenser, and accordingly every evaporator, is calculated with a moving boundary, which defines the three named parts of the heat exchanger dynamically. The model for icing on the air source evaporator adds the

heat gain caused by the phase change of the humidity in the air and enables the model to estimate the point in time when defrosting would be necessary. An internal heat exchanger in the refrigerant process can enhance the heat pump performance by transferring heat from the condensed refrigerant at high pressure before the expansion valve to the evaporated refrigerant at low pressure before the compression. Albert et al. 2008 furthermore examined the icing on air source evaporators in detail and developed a model for the formation of ice on the evaporator of an air source heat pump depending on its geometry, surface structure and the state of the entering moist air.

Alternatively to the above-mentioned isentropic efficiency model for the compressor, a polynomial equation fit for the compressor performance map using the same model as described for the heat pump performance in Afjei 1989 gives an equal good representation of the compressor characteristic. Ohyama et al. 2008 gives an overview on the last year's development in capacity controlled scroll compressor technology. Especially the capacity controlled scroll compressors improved their performance due to development of enhanced electronic controlled interior permanent magnet motor technology. Although most of the compressor models were developed for single speed compressors, some empirical curve fit models for part load operation have been described e.g. in Bühring 2001, Jin 2002 or Jin et al. 2003.

Afjei 1993 went a step further and examined the behaviour of inverter driven scroll compressors in detail. In his doctoral thesis, he describes a model for an inverter driven scroll compressor and the determining effects for its efficiency, i.e. the fixed volume ratio, leakages, friction, motor losses, inverter losses and shell losses. One essential characteristic is the fixed built-in compression ratio or volume ratio of the scroll compressor. Especially air source heat pumps work over a wide range of operating conditions with varying refrigerant pressure ratios between condenser and evaporator. Only in one operating point, this external pressure ratio of the heat pump cycle is equal to the internal pressure ratio of the scroll compressor. In all other operating points over- or under-compression lead to reduced efficiency. Madani et al. 2011 describe a similar approach for the compressor model in a capacity controlled ground source heat pump system. One other essential influence on the inverter compressor efficiency is the part load efficiency of the electric motor and the inverter. The development in the motor technology from inverter driven induction motors (IM) over surface permanent magnet synchronous motors (SPMSM) to interior permanent magnet synchronous motors (IPMSM) over the last 15 years combined with inverter improvements has resulted in a significant enhancement of the part load efficiency (c.f. Figure 5). In today's high efficiency capacity controlled compressor motors, the motor efficiency stays above 90% over the part-load operating range.

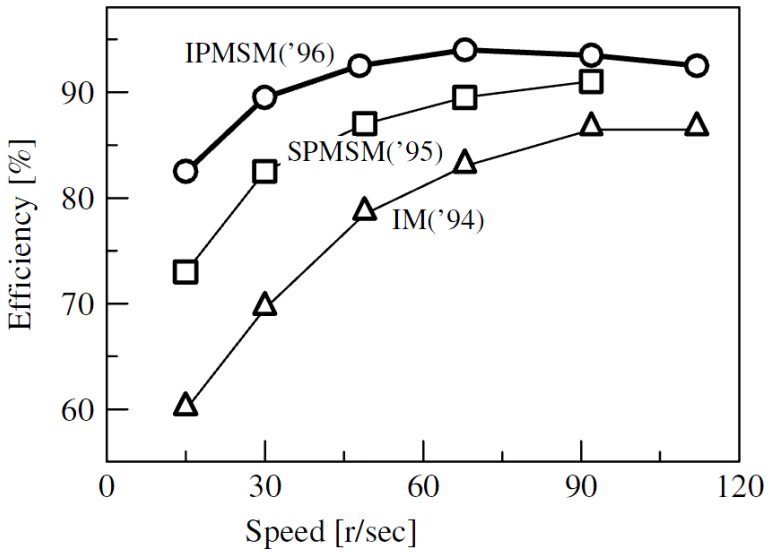

Figure 5: Comparison of compressor motor efficiency from Ohyama et al. 2008

Jin 2002 and Brandemuehl et al. 2009 conducted an extensive literature review on heat pump and chiller models and available manufacturer data. They further developed the found model descriptions and defined heat pump models based on a parameter identification methodology for the fit to catalogue data. The aim of this approach is to benefit from the detailed compressor model developments and derive a model that is still suitable for annual performance simulations. For this, the most important parameters of detailed heat pump design models are identified and the detailed calculation methods are simplified so far, that a parameter estimation procedure can fit these parameters from manufacturer catalogue data. Although, the derived approach requires only catalogue data from manufacturers, the model results are as precise as detailed design models and furthermore may be extended beyond the catalogue data with a more stable and precise extrapolated prediction.

Heat pump design models usually include models on the refrigerant cycle level. They are in use and suited mainly for the design of heat pumps, requiring a high level of knowledge, computation time and amount of work for application and on the other hand delivering very specialised or detailed results. In newer developments, the experiences with heat pump design model application lead to improved dynamic system simulation models in the form of complex models that are easier to access by parameter identification techniques or give advice for the integration of relevant effects into empirical models.

4 Model Verification

4.1 Calculation method against field measurements

The results of the calculation according to EN 15316-4-2:2008 have been compared to field measurements in Afjei et al. 2007 (also published in Wemhoener et al. 2008) for a ventilation compact unit air source heat pump (SH, DHW and ventilation mode). The measured performance has been compared to the calculated values for the different operation modes and different system boundaries. For the calculation the local outdoor temperature conditions monitored with the field monitoring equipment have been used as input data for the calculation in order to refer to the same boundary conditions as in field testing, which is necessary for validation purposes. Figure 6 gives an overview of the results.

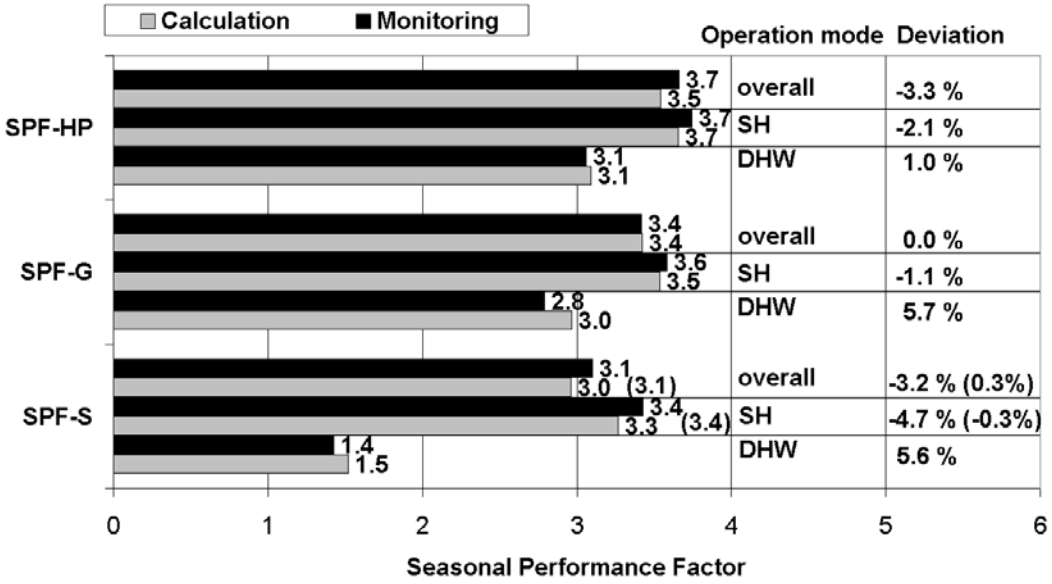

Figure 6: Seasonal performance factors of the field monitoring compared to the calculated values (from Afjei et al. 2007)

Since controller settings are usually not known in detail and therefore cannot be evaluated, two operation modes of the circulating pump on the sink side have been considered for the calculation of the electricity demand: pump is running when heat pump is on and pump is running throughout the whole heating period, which is given by the values in brackets. However, the impact on SPF values is marginal. Regarding the comparison of the field monitored performance to the calculation results, the space heating part is generally reproduced better than the DHW part. For the DHW calculation a constant daily consumption has been assumed, while in reality the tapping volumes are not so evenly spread over the year. Further differences occur due to control effects. For instance, the back-up heating supports the DHW heating by the heat pump after large draw-offs to accelerate the hot water availability. These controller settings are too case-specific to be reproduced by a hand calculation.

Calculated overall seasonal performance factor values deviate in the range of ±4% from measured values, which is a satisfactory result for a hand calculation, where certain simplifications are inevitable. The single operation modes show with ±6% a slightly higher deviation from the measured results for this ventilation heat pump compact unit.

4.2 Calculation method against dynamic simulations

The same calculation method according to EN 15316-4-2:2008 has been compared in Dott et al. 2011 to dynamic simulations for a brine-to-water heat pump coupled to a low energy single family house. Exemplary results of this study for the generator seasonal performance factor (SPF-G) are shown in Table 2. The SPF-G assesses the energetic quality of the heat generation and is calculated as sum of the generated heat divided by the required expenditure in the heat generator including the expenditure for the heat source. In Dott et al. 2011, on the one hand the functions space heating (SPF-G_H) and domestic hot water preparation (SPF-G_W), as described in the standard, and on the other hand an additional SPF-model for a passive cooling function (SPF-G_C) with borehole heat exchanger passively coupled to the low temperature floor heating system have been considered. The calculation model for the passive cooling function only considers a daily heat storage of the space cooling heat rejected into the ground and the increase in the heat pump source temperature in domestic hot water operation, whereas the dynamic simulation uses a detailed physical model of the borehole and the surrounding ground for all operation modes. The calculation method without passive cooling according to EN 15316-4-2:2008 leads to very good agreement of the SPF-G compared to detailed simulation results.

Table 2: Comparison of the generator SPF from dynamic simulation and calculation method (from Dott et al. 2011)

generator SPF without passive cooling			
	simulation	bin-method	
SPF-G_H	4.4	4.6	5%
SPF-G_W	3.3	3.2	-3%
SPF-G_{HW}	4.0	4.1	2%
generator SPF with passive cooling			
	simulation	bin-method	
SPF-G_H	4.4	4.6	5%
SPF-G_W	3.5	3.5	-1%
SPF-G_C	12.9	12.6	-2%
SPF-G_{HWC}	4.7	4.8	2%

The added passive cooling function, neglecting the heat storage effect on the space heating operation in the calculation method, leads to equal good agreement like without heat injection into the borehole and confirms the simplification to neglect the effect of heat injection into the borehole on the winter heat withdrawal. The increase of the domestic hot water seasonal performance factor by the heat injection from passive cooling could be reproduced by a very simple calculation model based on a short time adiabatic ground heat storage model. The performance factor of the passive cooling could be reproduced with good agreement also by a simplified calculation based on average electric power consumption as long as the assumption of full cooling need coverage is valid.

4.3 Comparison of Parameter-Estimation and Equation-Fit models

Jin 2002 compared the results of the derived parameter estimation model and of a quasi-static performance map model against catalogue data. Table 3 shows the results as relative error.

Table 3: Comparison of the relative error by parameter estimation and equation-fit models (from Jin 2002)

Catalogue Data Used	relative Error					
	Maximum (abs. value)		average (abs. value)		RMS	
	Parameter estimation	Equation fit	Parameter estimation	Equation fit	Parameter estimation	Equation fit
	electric power consumption					
234 points	16.1%	29.1%	4.2%	6.3%	5.8%	7.8%
16 points	22.0%	33.5%	4.2%	6.9%	5.8%	8.5%
	heating capacity					
234 points	8.2%	38.5%	2.5%	7.4%	3.1%	9.7%
16 points	8.8%	49.2%	2.8%	12.6%	3.4%	16.5%

4.4 Validation of heat pump design models

Bühring 2001 conducted a validation of the derived detailed heat pump design model. Therein, the bi-quadratic polynomial curve fit for the compressor thermal capacity and electric power consumption according to Afjei 1989 reaches deviations smaller than 0.4% compared to manufacturer data. The electricity consumption and the heat capacity of the whole heat pump model achieve inaccuracies smaller 5%.

5 Work in IEA HPP Annex 38 / SHC Task 44

5.1 HP-Model List

The heat pump modelling working group collected a list of well documented heat pump model descriptions that are actually available and gives an overview on the state of the art heat pump models. Chapter A9 shows the complete list of collected heat pump models.

5.2 Insel-HP-Model Description

Antoine Dalibard and Felix Thumm from HFT Stuttgart implemented a refrigerant cycle heat pump model in their simulation environment INSEL and carried out first elements of validation. Furthermore they wrote a model description which is attached to this report in Chapter A1.

5.3 Comparison of Parameter-Estimation and Equation-Fit model

Dani Carbonell implemented two heat pump models in the RDmes simulation environment and conducted a validation of the parameter estimations based model (PBE) developed by [Jin et al., 2002] as well as a comparison between the PBE and YUM model from [Afjei, 1989]. The models have been validated by the authors using some commercial catalogue heat pumps data. In the present paper the validation and comparison between models is provided for different mass flow rates and under non-standard conditions using experimental data obtained at ISFH. The documentation of his work is attached to this report in Chapter A2.

5.4 Description of TRNSYS Type 877

The basis for the heat pump model Type 877 is an EES-model that has originally been developed by Stefan Bertsch of NTB Buchs, Switzerland. Based on this EES model a TRNSYS model was programmed at SPF. This model is further developed in cooperation between the Institute of Thermal Engineering, Graz University of Technology and SPF. A model description is attached to this report in Chapter A3.

5.5 Description of the heat pump model capabilities of Polysun

The goal of integrating heat pump model capabilities is to provide a tool for planners, which also covers arbitrary hydraulic systems. In particular, the combination with ground probes, buildings or the integration of several heat pumps in one system is covered in the heat pump version of Polysun (Witzig et al. 2008). Furthermore, there is a comprehensive database of heat pumps available on the market which is shipped with the Polysun software. Vela Solaris is constantly extending this database. The general goal of Polysun is to provide a capability to compare different heat pump machines with one another based on dynamic calculations with statistical weather data and an annual performance analysis based on dynamic system calculations.

In Polysun, the combination of heat pumps with solar thermal is provided with the modular system design capability of Polysun Designer. Furthermore, a continuously growing set of

predefined templates is integrated on all user levels. Since 2012, Polysun Online is offering a very easy access to the simulation kernel through a simple browser interface. Combined solar and heat pump systems are also integrated in this version and are continuously extended. The Polysun heat pump model has been extended to cover solar cooling with absorption and adsorption cooling machines (Rezaei 2009). A detailed description of the Polysun models is given in Chapter A4.

5.6 Heat pump model of EFKOS

The European Union's energy efficency strategy lead to a series of requirements for products which have a major impact on Europe's energy consumption. The implementation of this so called 'ErP' (Energy related products) or 'ecodesign' directive 2009/125/EG for heat pumps is based on standard EN 14825:2012, which defines a variety of conditions under which a heat pump shall be rated and how an expected seasonal performance of the unit shall be evaluated therewith. According to legal texts, it is allowed to calculate required input data from a few testing points available from well established EN 14511 rating measurements. In the EFKOS project, a possible calculation process how this can be done has been described. This process is based on a semi-empirical model which has been validated for an air-to-water heat-pump. As the model is mostly based on widely available data, it can be used to simulate many heat-pumps available on the european market. It is however a drawback of such an empirical model that it's based on steady state conditions, which is why complex behaviour like defrosting operation of air-to-water heat pumps cannot be implemented in a realistic manner. On the other hand, the model originally has been developed for the use in standard calculations. It's therefore a strength that results of such assessments and simulations can directly be compared. A model description is attached to this report in Chapter A5.

5.7 Direct expansion solar assisted heat pumps

In direct expansion solar assisted heat pump it is difficult to model dissociated the heat pump, evaporator and storage tank. The strategy adopted was to model the heat pump according the data provided by compressor manufacturer as a function of evaporating and condensing temperature. The evaporator was model as an uncovered solar collector and the storage tank with a help of TRNSYS Type for stratified tanks. Since the system was tested without intrusive measurements the evaporator and condenser temperature are unknowns, as well as refrigerant mass flow rate. The model of the global system simulates the evaporating and condensing temperature and calculates the useful heat flux. A model description is attached to this report in Chapter A6.

5.8 Calculation of primary energy and SPF of heat pumps in Passive Houses

The increasing number of heat pumps worldwide and especially their widespread applications in Passive Houses created the requirement for a calculation tool that allows predicting the annual electrical energy consumption and the seasonal performance factor (SPF) of heat pumps with high accuracy. Until now, calculation tools such as JAZcalc (or WPesti) [1], SIA 384/3 [2] and VDI 4650 [3] are available. Their applicability is restricted e.g. due to limited availability of climates and/or because of non-satisfying accuracy.

The new algorithm is based on the algorithm of 'Compact' sheet [4] for so called compact units (heat pump and ventilation with heat recovery in one device), which is already available

in Passive House Planning Package (since PHPP 2004). The goal of the new heat pump tool is the achievement of high accuracy and the improvement of flexibility with regard to heat pump sources (air, water, brine), sinks (air heating, radiators, floor heating), functionality (heating, domestic hot water, both), heating distribution system (air heating, floor heating, radiators), store options and control strategies. A model description is attached to this report in Chapter A7.

5.9 Measurement and model validation regarding a typical solar assisted ground source heat pump by Peter Pärisch

At ISFH stationary and dynamic tests of a brine-water heat pump have been carried out in order to analyse the behaviour under varying temperature and flow rate conditions and to validate the YUM-model for TRNSYS Type 401 (Afjei and Wetter 1997). Furthermore a flow rate correction from (Pahud and Lachal 2004) for Type 401 was tested successfully. Further information is given in Chapter A8.

6 Conclusion

The transition from fossil to renewable energy sources leads as one aspect to new heat supply systems in buildings. Therein heat pumps with ambient or solar heat sources play an important role. Therefore detailed knowledge of their behaviour and numerical methods are required.

This report gives at the present state mainly an overview on heat pump models in literature and current development that are sufficiently described to be implemented in a program. Therefore the typology of required models for the three applications "simplified calculation methods", "dynamic simulation" and "heat pump design" is described. Simplified calculation methods require simple but robust calculation schemes relying on easily available product data that are focussed and therewith may be also restricted to the desired application. These methods give seasonal efficiency results for usual applications in a fast and easy way. The application in dynamic simulation programs mostly still relies on easily available product data but gives the opportunity to change the system configuration and time dependent the boundary conditions. Therefore the mathematical model for dynamic simulation needs to represent the time dynamic behaviour of the heat pump also for a wider range. Heat pump design models aim to design the components of a heat pump and therewith need to represent their behaviour on the level of the refrigerant cycle. This report gives a categorization with pros and cons in terms of generic approach as well as a view on the validation of these heat pump models.

For combined solar and heat pump systems most of the existing models are applicable as far as the solar system and the heat pump work like one beside the other without too strong interaction. But further system integration for possibly enhanced energetic system performance influences the refrigerant cycle, where mathematical models up to now mainly exist for design purposes and rather seldom for annual efficiency calculation. The demand is here on the one side to be able to calculate the behaviour of more complex heat generation systems using solar irradiation and heat pump technology where the interaction is on a hydraulic or on the refrigerant cycle level and on the other side to be able to represent these systems in more simple calculation or simulation methods for a broader application. Furthermore general questions need to be answered during the work in A38T44. Those are e.g. the questions how to integrate solar heat and heat pump technology in heat generation systems, the use of capacity modulation of heat pumps or how to handle highly integrated systems.

7 References

Afjei T., 1989. YUM a yearly utilization model for calculating the seasonal performance factor of electric driven heat pump heating systems - Technical Form. Eidgenössische Technische Hochschule Zürich, IET-LES, Zürich CH.

Afjei T., 1993. Scrollverdichter mit Drehzahlvariation. Dissertation, Eidgenössische Technische Hochschule, IET-LES, Zürich CH.

Afjei T., Wetter M., Glass A., 1997. TRNSYS type: Dual-stage compressor heat pump including frost and cycle losses - Model description and implementation in TRNSYS. TRNSYS user meeting, Stuttgart DE.

Afjei T., Wemhoener C., Dott R., Huber H., Helfenfinger D., Keller P. and Furter R., 2007. Calculation method for the seasonal performance of heat pump compact units and validation - Final report. Swiss Federal Office of Energy, Bern CH.

Albert M., Sahinagic R., Gasser L., Wellig B., Hilfiker K., 2008. Prediction of Ice and Frost Formation in the Fin Tube Evaporators of Air/Water Heat Pumps. 9th International Energy Agency Heat Pump Conference, Zurich CH.

ANSI/AHRI 210/240-2008. Performance Rating of Unitary Air-Conditioning & Air-Source Heat Pump Equipment. Air-Conditioning, Heating, and Refrigeration Institute AHRI, Arlington USA.

ANSI/ARI Standard 540-1999 [2] "Positive Displacement Refrigerant Compressors and Compressor Units", 1999.

Brandemuehl M.J. and Wassmer M.R., 2009. Updated Energy Calculation Models for Residential HVAC Equipment, ASHRAE, Atlanta GA USA

Bertsch, S.S. & Groll, E.A., 2008. Two-stage air-source heat pump for residential heating and cooling applications in northern US climates. International Journal of Refrigeration, 31(7).

Bühring A., 2001. Theoretische und experimentelle Untersuchungen zum Einsatz von Lüftungs-Kompaktgeräten mit integrierter Kompressionswärmepumpe. Dissertation, Technische Universität Hamburg-Harburg, Hamburg DE.

Dott R., Wemhöner C. and Afjei T., 2011. Heating and Cooling with heat pumps in Swiss residential buildings. 10th International Energy Agency Heat Pump Conference, Tokyo JP.

EN 14825:2012 Air conditioners, liquid chilling packages and heat pumps, with electrically driven compressors, for space heating and cooling - Testing and rating at part load conditions and calculation of seasonal performance. European Committee for Standardization CEN, Brussels BE.

EN 15316-4-2:2008 Heating systems in buildings – Method for calculation of system energy requirements and system efficiencies – Part 4-2: Space heating generation systems, heat pump systems. European Committee for Standardization CEN. Brussels, BE

EN 14511:2011 Air conditioners, liquid chilling packages and heat pumps with electrically driven compressors for space heating and cooling – Parts 1 to 4. European Committee for Standardization CEN, Brussels BE.

Hornberger M., 1994. Solar unterstützte Heizung und Kühlung von Gebäuden. Dissertation, Institut für Thermodynamik und Kältetechnik, Universität Stuttgart, Stuttgart DE.

Jin H., 2002. Parameter estimation based heat pump models. PhD thesis, Oklahoma State University, Stillwater OK USA.

Jin, H. and Spilter, J.D., 2002. A parameter estimation based model of water-to-water heat pumps for use in energy calculations programs, ASHRAE Transactions, Vol 108 (1), pp 3-17, 2002.

Jin H. and Spitler J.D., 2003. A parameter estimation based model of water to water heat pumps with scroll compressor and water/glycol solutions. Building services engineering research and techpnology August 2003 Vol 24 nº3 (203-219)

Madani H., Claesson J. and Lundquist P., 2011. Capacity control in ground source heat pump systems part I: modeling and simulation. International Journal of Refrigeration, Volume 34, Issue 6, Pages 1338-1347.

Ohyama, K. and Kondo, T., 2008. Energy-Saving Technologies for Inverter Air Conditioners. IEEJ Transactions on Electrical and Electronic Engineering, Vol. 3, pages 183–189, Tokyo JP.

Rezaei S. H., Witzig A., Pfeiffer M., Lacoste B., Wolf A., *Modeling and analyzing solar cooling systems in Polysun*, Proc of the 3rd international conference Solar Air-Conditioning by OTTI, Palermo, 2009.

Schraps S., 2001. Kombinierter Einsatz von Elektrowärmepumpe und Solarkollektor in Wohngebäuden. Dissertation, Institut für Energietechnik, Universität Hannover, Hannover DE.

TESS 2011. Thermal Energy System Specialists Component Libraries for TRNSYS. Madison WI USA.

Witzig A., Marti J., Brüllmann T., Huber A., *Systemoptimierung der Kombination von Solarkollektoren mit Wärmepumpenanlagen*, proc. 18th Symp. on solar thermal energy of OTTI, Bad Staffelstein,April 2008

Wemhoener C., Afjei T. and Dott R., 2008. IEA HPP Annex 28 – standardised testing and seasonal performance calculation for multifunctional heat pump systems. Applied Thermal Engineering, Volume 28, Issue 16, Pages 2062–2069.

A1. Insel-HP-Model Description by Antoine Dalibard

HFT Stuttgart

University of Applied Sciences

Date: 23/05/2011

Authors: Antoine Dalibard, Felix Thumm

1. Introduction

A simple physical heat pump model has been developed and implemented in the simulation environment INSEL[1]. The present document gives a short description of the model, underlines its limitations, gives a first step of validation and shows the possible further steps to improve the model.

2. Inputs/parameters/outputs of the model

Table 1 shows the inputs and parameters required for the model.

Table 1: Inputs/parameters of the model

Inputs	Parameters
Inlet fluid temperature at the evaporator side (°C)	Fluid specific heat capacity at evaporator side (kJ/(kg. K))
Mass flow rate at the evaporator side (kg/s)	Fluid specific heat capacity at condenser side (kJ/(kg. K))
Inlet fluid temperature at the condenser side (°C)	UA value of the heat exchanger at evaporator side (kW/K)
Mass flow rate at the condenser side (kg/s)	UA value of the heat exchanger at condenser side (kW/K)
Mode (heating / cooling)	Refrigerant used (-)
Set point temperature (°C)	Compressor electrical efficiency (-)
Superheating ΔT in evaporator (K)	Coefficient A_0 isentropic efficiency (-)
Subcooling ΔT in condenser (K)	Coefficient A_1 isentropic efficiency (C^{-1})
	Coefficient A_2 isentropic efficiency (C^{-2})
	Coefficient A_3 isentropic efficiency (C^{-1})
	Coefficient A_4 isentropic efficiency (C^{-2})
	Coefficient A_5 isentropic efficiency (C^{-2})

The model can be used to simulate both heat pump and electrical compression chiller. Mode 0 refers to heat pump mode and mode 1 to compression chiller. The set point temperature is the temperature required by the user. The UA values of both heat exchangers are assumed constant and have to be given by the user. The isentropic efficiency of the compressor is calculated using a cross-term correlation depending on condenser and evaporator temperatures (see Mathematical description).

[1] www.insel.eu

Table 2 shows the outputs provided by the model.

Table 2: Outputs of the model

Outputs
Outlet fluid temperature at the evaporator side (°C)
Outlet fluid temperature at the condenser side (°C)
Evaporator temperature (°C)
Condenser temperature (°C)
Power at condenser side (kW)
Power at evaporator side (kW)
Mechanical work of the pump (kW)
Electrical power of the pump (kW)
Coefficient of performance (-)
Isentropic compression efficiency (-)

3. Mathematical description

The thermodynamic states of the refrigerant is calculated using the REFPROP[2] subroutines for each points shown in figure 1 and table 3:

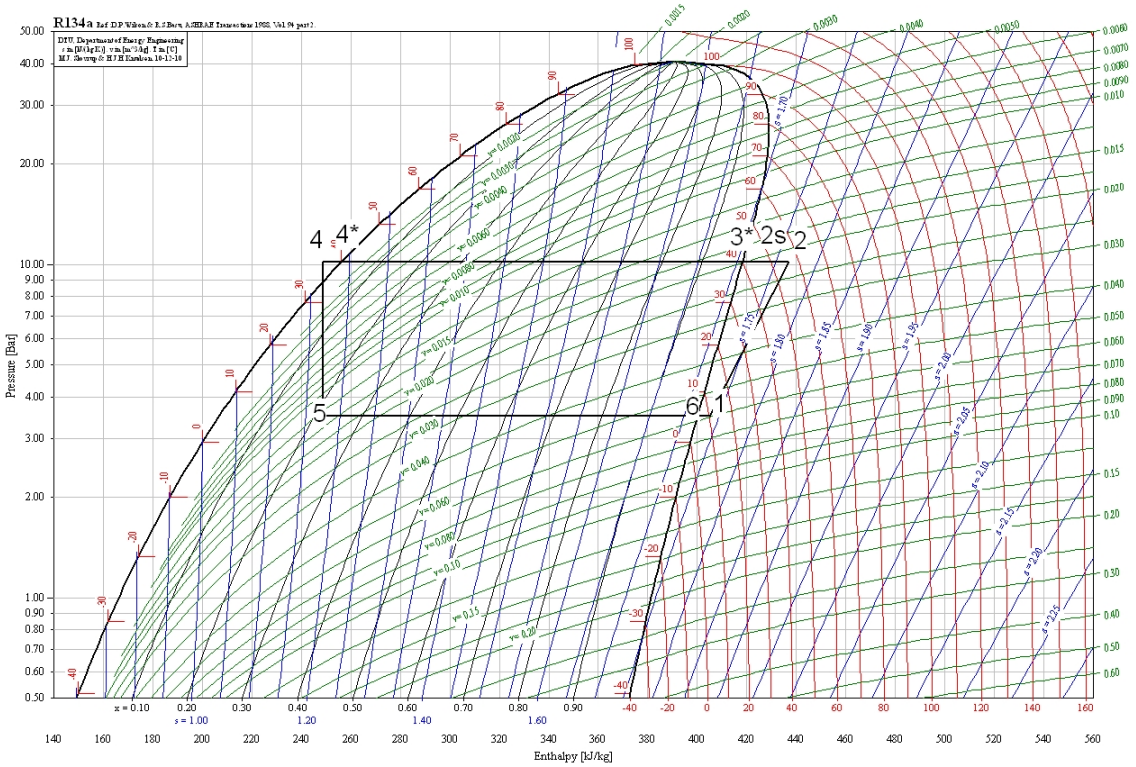

Figure 1: Thermodynamic cycle of the refrigerant

[2] Refprop: http://www.nist.gov/srd/nist23.htm

The polytropic compression is calculated by introducing the isentropic compression efficiency:

$$\eta_{isen} = \frac{h_{2s} - h_1}{h_2 - h_1}$$

The isentropic compression efficiency is calculated using a correlation of the following type:

$$\eta_{isen} = A_0 + A_1 T_{cond} + A_2 {T_{cond}}^2 + A_3 T_{eva} + A_4 {T_{eva}}^2 + A_5 T_{eva} T_{cond}$$

The coefficients of this correlation can be obtained if the compressor performance data are known. Some manufacturers provide these data with polynomials according to EN12900[3]. With these polynomial functions and with the help of the software EES the coefficients A_0 to A_5 can be calculated.

Table 3: Calculated thermodynamic states

Calculated points	Description
Point 1	Entry of the compressor
Point 2s	End of the isentropic compression
Point 2	End of the polytropic compression
Point 3*	Entry of the condenser
Point 4*	Exit of the condenser before subcooling
Point 4	Entry of the expansion valve (after subcooling)
Point 5	Entry of the evaporator valve
Point 6	Exit of the evaporator before superheating

In order to relate heat transfer fluid temperatures with refrigerant temperatures, the two heat exchangers were treated as simple heat exchangers with phase change on one side using the NTU method.

$$T_{cond} = T_{c,in} + \frac{\dot{Q}_{cond}}{\varepsilon_{cond}.\dot{m}_c.c_p} \quad with \quad \varepsilon_{cond} = 1 - \exp\left(\frac{-UA_c}{\dot{m}_c.c_p}\right)$$

$$T_{eva} = T_{e,in} + \frac{\dot{Q}_{eva}}{\varepsilon_{eva}.\dot{m}_e.c_p} \quad with \quad \varepsilon_{eva} = 1 - \exp\left(\frac{-UA_e}{\dot{m}_e.c_p}\right)$$

NB: for the moment, it is assumed that the heat pump can always supply the set point temperature. For the given inputs, the model calculates how much electricity it is needed to reach the set point temperature.

3 For example, Bitzer and Copeland provide for free in their website a software where these polynomials can be obtained.

4. First elements of validation

The model has been compared with measurement data of a brine/water heat pump VITOCAL 300 from the manufacturer Viessmann. The type of compressor used is known (Copeland ZR 40 K3E TFD) as well as the two heat exchangers (from the manufacturer SWEP: V25-40 for the evaporator and B25-30 for the condenser). With the polynomial functions from Copeland software and a small program written in EES, the isentropic efficiency can be calculated and then correlated to determine parameters A_0 to A_5 (see figure 2).

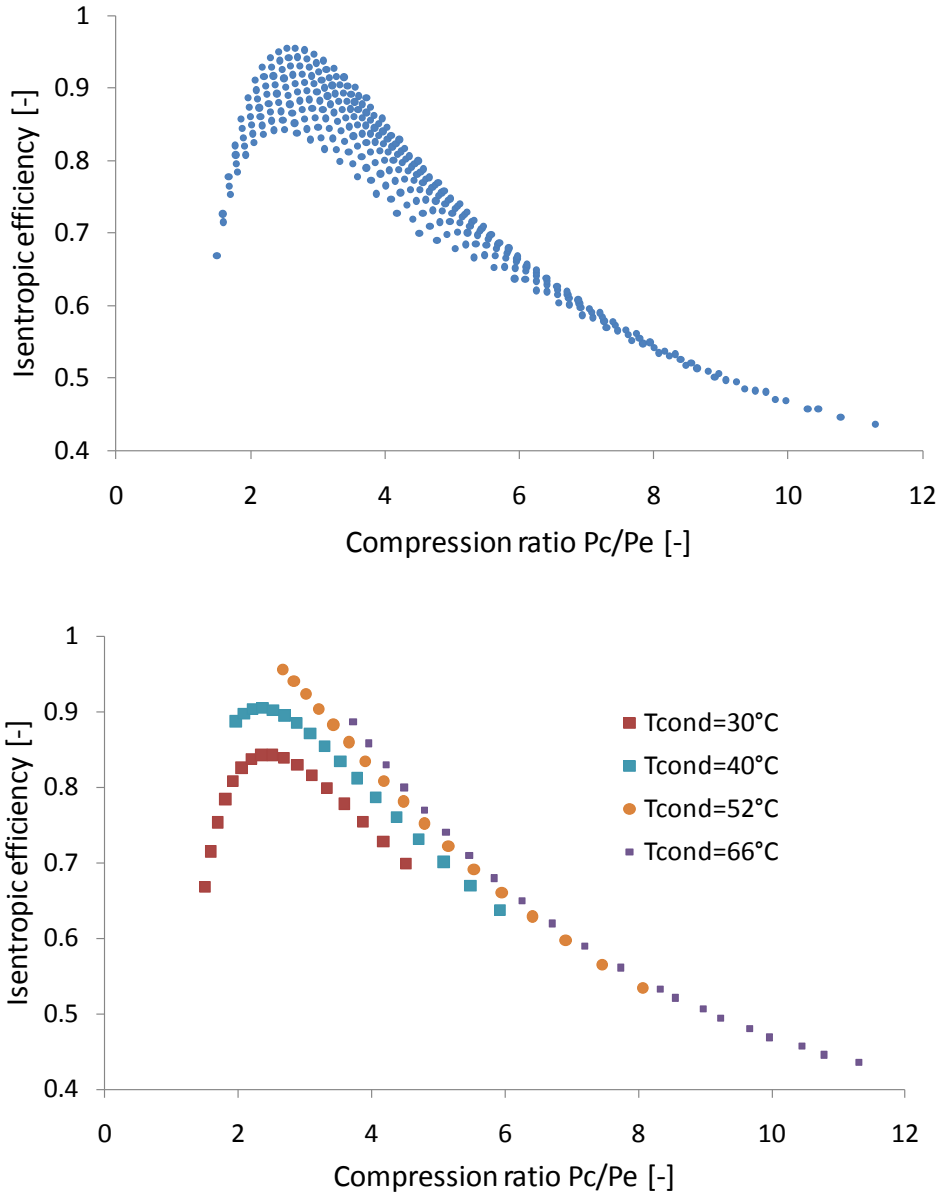

Figure 2: Isentropic efficiency calculated with EES and EN12900 polynomial functions for different operating conditions

Figure 3 shows the comparison between measurement and simulated data for one day. This show the typical daily operation of the heat pump when there is heat demand. The outlet water temperature at the condenser has been taken as set point and the model calculates the outlet brine temperature at the evaporator side as well as the electrical power needed by the heat pump.

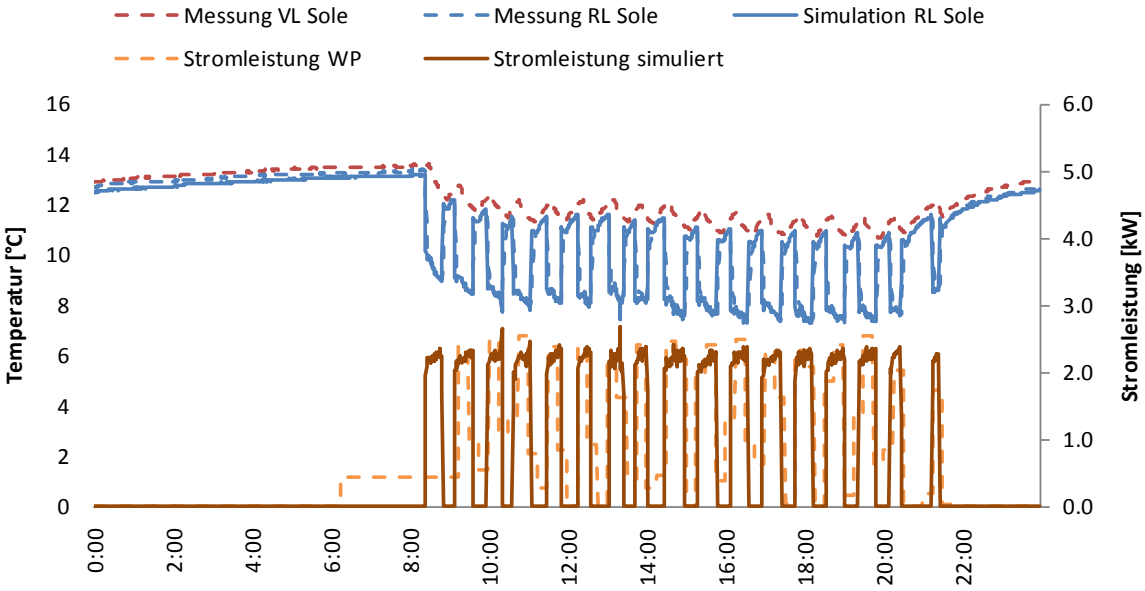

Figure 3: Comparison measurement/simulated values (21/02/2011).

Other days have been simulated and compared with measurement data (Table 4 and Figure 5). The 3 days in February correspond to typical winter days with heat demand whereas the days in March and April correspond to spring days with lower heat demand.

Table 4: Comparison simulation/measurements

Day	Qheat (kWh)	Qbrine (kWh)	Qbrine sim (kWh)	Pelec (kWh)	Pelec sim (kWh)	COP (-)	COP sim (-)
22/02/2011	86.3±3.2	74.8±4.0	76.9	18.2±0.9	17.6	4.7±0.4	4.9
23/02/2011	98.3±3.5	83.8±4.3	86.4	20.5±1.0	20.4	4.8±0.4	4.8
24/02/2011	80.9±3.1	69.1±3.9	73.1	16.9±0.8	16.7	4.8±0.4	4.8
20/03/2011	10.6±0.4	9.2±0.5	12.0	2.4±0.1	2.1	4.4±0.4	4.9
01/04/2011	17.7±0.7	14.4±0.8	16.1	4.0±0.2	3.6	4.4±0.4	4.9

NB: here the COP are defined as followed: COP=Qheat/Pelec where Pelec includes only the electricity consumption of the compressor + internal controllers.

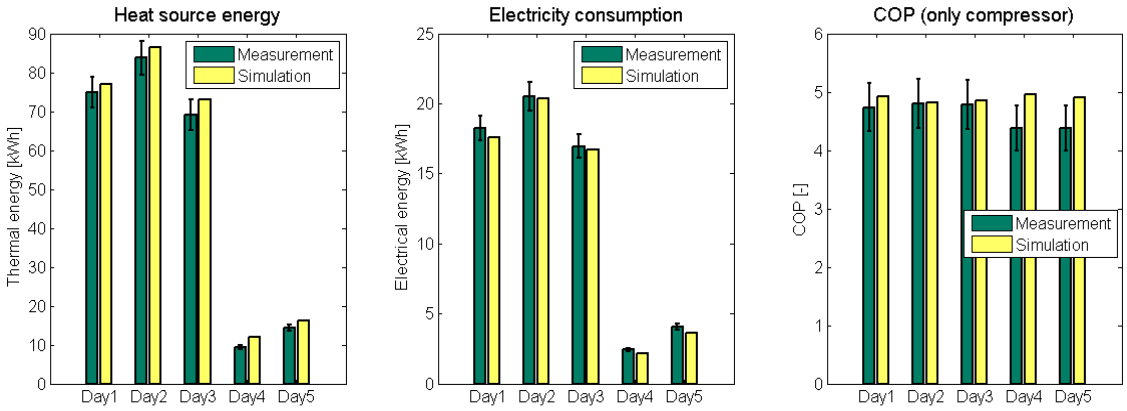

Figure 4: Comparison measurement/simulation for 5 different days

5. Limitations

This model is really simplified although it calculates the thermodynamic cycle of the refrigerant. It can theoretically simulates all kind of heat pumps with the following limitations (Table 5)

Table 5: Limitations of the heat pump model

Physical /empirical	Thermal capacitance	Kind of heat pump	Defreezing of heat exchanger	Detailed compressor model
Mixed	No	All	No	Yes (but no physical description)

6. Computational time: problem with zeotropic refrigerant mixture

The model is quite fast when pure fluids are used as refrigerant (ex: R134a). Nevertheless, for zeotropic refrigerant mixtures (ex:R407C), since the evaporation and condensation do not occur at constant temperature, an extra computational effort is required for finding the mean condenser/evaporator temperature (see figure 5). Furthermore, the Refprop subroutines for refrigerant mixtures are also slower, which make the model quite slow.

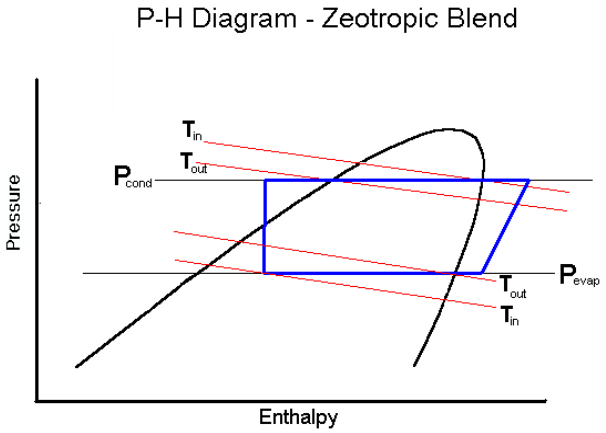

Figure 5:P-H Diagram - Zeotropic Blend

7. Model availability

The model has been programmed in Fortran for implementation in INSEL. The code could be shared with others.

8. Further steps

- Add thermal capacitance to both heat exchangers in order to take into account for the dynamics.
- Add more complex compressor models.

A2. Numerical analysis of heat pump models. Comparative study between equation-fit and refrigerant cycle based models.

D. Carbonell[1], J. Cadafalch[2], P.Pärisch[3] and R. Cònsul[1]

[1]RDmes Technologies S.L., Ctra. Nac. 150, km 14.5, Institut Politècnic, 08227, Terrassa, Spain

[2]Universitat Politècnica de Catalunya (UPC), Departament de Màquines i Motors Tèrmics (MMT), Terrassa, Spain

[3]Institut für Solarenergieforshung Hameln GmbH (ISFH), Am Ohrberg 1, 31860 Emmerthal, Germany

Contact: rdmes@rdmes.com

1. Introduction

Heat pumps are becoming an important technology in the renewable energy field. Studies of capabilities and limitations of existing models in order to choose appropriately which models to use for specific situations is considered to be of importance. Validation and analysis of an equation-fit and a refrigerant cycle based models for a brine to water heat pump in heating mode is provided in this paper. A very important feature that the models must fullfill is that the necessary inputs are to be estimated only from catalogue data typically provided by manufacturers.

The so-called YUM model [1] has been selected as a representative of the equation-fit (EF) based models. A water/brine source heat pump parameter estimation model described in [2] is chosen to represent the refrigerant cycle (RC) based models.

The models have been implemented in two modes: i) estimation and ii) prediction. The estimation mode calculates the input parameters needed for the models using catalogue or experimental data. The prediction mode solves the heat pump model with defined inputs.

These models have been validated by the authors under the framework of IEA SHC Task 44 / HPP A38 : Solar and Heat Pumps in [3] using some commercial catalogue heat pumps data. The RC model was validated for scroll and reciprocating compressors using several refrigerants. Moreover a heat pump using a double circuit with two compressors were included in the analysis. In all analyzed cases, the estimation procedure of the EF model was proved to be easier and more accurate compared to the RC model, not matter which type of heat pump, refrigerant or compressor were used. Therefore, in order to calculate steady state conditions in normal catalogue data range, the EF model was shown to be the best alternative. In the present paper the validation and comparison between models is provided for different mass flow rates and under non-standard conditions using experimental data obtained at ISFH.

2. Mathematical formulation

Equation fit based model

The YUM model [1] is a black-box model based on quasi steady state performance maps. The mathematical formulation is simplified to a two-dimensional polynomial plane able to describe air and water/brine source heat pumps. This model is based on a biquadratic polynomial fit of the condenser heat power Q_c and the compressor work W_{cp}:

$$Q_c = bq_1 + bq_2\bar{T}_{e,in} + bq_3\bar{T}_{c,out} + bq_4\bar{T}_{e,in}\bar{T}_{c,out} + bq_5\bar{T}_{e,in}^2 + bq_6\bar{T}_{c,out}^2 \quad (1)$$

$$W_{cp} = bp_1 + bp_2\bar{T}_{e,in} + bp_3\bar{T}_{c,out} + bp_4\bar{T}_{e,in}\bar{T}_{c,out} + bp_5\bar{T}_{e,in}^2 + bp_6\bar{T}_{c,out}^2 \quad (2)$$

where $\bar{T}_{e,in}$ is the fluid inlet temperature in the evaporator and $\bar{T}_{c,out}$ the fluid outlet temperature in the condenser. The normalized temperature $\bar{T}$ is obtained from $\bar{T}=T[^{o}C]/273.15+1$. In the estimation mode, the polynomial coefficients are calculated using the multidimensional least square fitting algorithm of GSL (GNU Scientific library, [4]). In prediction model a brent solver [4] is employed.

Refrigerant cycle based model

The model solves the refrigerant circuit using simple models for evaporator, condenser, expansion valve and compressor. The inputs of the models are obtained by means of multidimensional parameter minimization from catalogue or experimental data. A reciprocating [2] and scroll [5] compressor models have been implemented to cover most of the heat pumps. Physical properties of refrigerants are calculated using a pre-processed matrix data obtained from NIST calculations to speed up the computational time. Moreover, a method to estimate the performance for different brine solutions has also been included in the present work as explained in [5].

The two heat exchangers are solved using the ε−*NTU* model [6] assuming negligible pressure lost. For a phase change process at constant temperature the efficiency of the heat exchanger ε can be obtained from:

$$\epsilon = 1 - e^{\frac{UA}{c_p\dot{m}}} \quad (3)$$

where the exponent term represents the number of transfer units *NTU*, *UA* is the global heat transfer coefficient in [*W*/*K*], c_p is the fluid specific heat capacity in [*J*/*kgK*] and $\dot{m}$ is the fluid mass flow rate in [*kg*/*s*]. Since this model uses only catalogue data, the configuration, length and other details of the heat exchangers are unknown. Therefore, the *UA* value is estimated from experiments or from catalogue data. Once the efficiency is obtained, the condensing and evaporating temperatures, T_c and T_e respectively, can be calculated:

$$\mathrm{T_e} = \mathrm{T_{fe,i}} - \frac{\mathrm{Q_e}}{\varepsilon \mathrm{c_p} \dot{\mathrm{m}}_\mathrm{e}} \quad (4)$$

$$\mathrm{T_c} = \mathrm{T_{fc,i}} - \frac{\mathrm{Q_c}}{\varepsilon \mathrm{c_p} \dot{\mathrm{m}}_\mathrm{c}} \quad (5)$$

where $\mathrm{T_{fe,i}}$ is the fluid inlet temperature in [*K*], *Q* is the heat power in [*W*] and the subscript *e* and *c* stand for evaporator and condenser respectively. At this stage, in prediction mode, Q_c and Q_e are unknown, thereby an iterative procedure is needed. In the estimation mode these values are obtained from the experiments or catalogue data and no iterations are necessary.

In prediction mode, the heat in the evaporator is obtained from the refrigerant side as:

$$Q_e = \dot{m}_r(h_{re,out} - h_{re,in}) \quad (6)$$

Here, $\dot{m}_r$ is the refrigerant mass flow rate, $h_{re,out}$ and $h_{re,in}$ are the outlet and inlet enthalpy of the refrigerant in the evaporator in [*J/kg*]. The condenser heat is then obtained from the global heat balance of the heat pump:

$$\mathrm{Q_c} = \mathrm{Q_e} + \mathrm{W_{cp}} \tag{7}$$

where $\mathrm{W_{cp}}$ is the compressor work. The enthalpy values used in Eq.6 are obtained from saturation values at the respective temperatures of the condenser and evaporator assuming and adiabatic expansion process. Moreover, the $h_{re,out}$ is actually neglecting the superheating effect but this should be compensated with and underpredicted UA_e value estimated by the model [2]. The same reasoning also applies to the neglected superheating and subcooling values of the condenser.

In order to calculate the compressor work needed in Eq.7 the following expression is used:

$$\mathrm{W_{cp}} = \frac{\mathrm{W_{cp,t}}}{\eta} + \mathrm{W_{loss}} \tag{8}$$

where $W_{cp,t}$ is the theoretical compressor work, η the electro-mechanical efficiency and W_{loss} the constant part of the electro-mechanical power loss. The electro-mechanical parameters η and W_{loss} are inputs of the model and thereby calculated in the estimation mode.

The values of $\dot{m}_r$ of Eq.6 and $W_{cp,t}$ of Eq.8 are obtained from the compressor model, which is the key aspect in the RC based model. In this paper, only a heat pump with a scroll compressor has been analyzed.

Scroll compressor

The scroll compressor model has been described in [5]. The compressor mathematical description distinguishes between the external pressure ratio π defined as:

$$\pi = \frac{\mathrm{p_c}}{\mathrm{p_e}} \tag{9}$$

where p_c and p_e are the condensing and evaporating pressures in [*Pa*], and the build-in pressure ratio π_i defined as:

$$\pi_\mathrm{i} = \frac{\mathrm{p_{in}}}{\mathrm{p_e}} = \upsilon_\mathrm{i}^{\gamma} \tag{10}$$

where the build-in volume ratio $\upsilon_\mathrm{i}^{\gamma}$ is an input of the model. In design conditions ($\pi = \pi_\mathrm{i}$) the compressor work is calculated using the theoretical isentropic work [2]. For under-compression ($\pi < \pi_\mathrm{i}$) and over-compression ($\pi > \pi_\mathrm{i}$) the theoretical compressor work is higher than that of the isentropic process and can be calculated with:

$$\mathrm{W_{cp,t}} = \frac{\gamma}{\gamma-1}\mathrm{p_e}\dot{\mathrm{m}}_\mathrm{r}\rho_\mathrm{in}\left[\frac{\gamma-1}{\gamma}\frac{\pi}{\upsilon_\mathrm{i}} + \frac{\pi^{\frac{\gamma-1}{\gamma}}}{\gamma} - 1\right] \tag{11}$$

where ρ_{in} is the density of the refrigerant at the suction state. The refrigerant mass flow rate is obtained from:

$$\dot{\mathrm{m}}_\mathrm{r} = \mathrm{V_r}\rho_\mathrm{r} - \mathrm{C}\pi \tag{12}$$

where the last term represents the reduction of the mass flow rate due to the leakage. The refrigerant volumetric mass flow rate $\mathrm{V_r}$ in [m^3/s] and the dimensionless coefficient *C* are inputs of the model.

Brine model

If the inputs of the model are obtained from a fluid in the evaporator and afterwards it is necessary to predict the heat pump behavior with a different fluid, for example if the inputs

are estimated with water and predicted with brine, a model is necessary. Following [5], the global heat transfer coefficient can be obtained from:

$$\mathrm{UA_e} = \frac{1}{\frac{\mathrm{C_3}}{\mathrm{D_f}}\left(\frac{\dot{\mathrm{m}}_\mathrm{e}}{\rho}\right)^{-0.8} + \mathrm{C_2}} \tag{13}$$

where the coefficients $\mathrm{C_2}$ and $\mathrm{C_3}$ are inputs of the model. The degradation factor $\mathrm{D_f}$ can be calculated as shown in [5]. When the fluid running through the evaporator is the same for the estimation and for the prediction mode, as in the present case, the $\mathrm{D_f}$ is equal to unity. However, the brine model is still used because th UA e depends on $\dot{m}$, it is calculated from two parameters and the estimation procedure is more accurate when more parameters are employed. The same procedure can be used for the condenser, but in the present work this model is only applied for the evaporator side. Unfortunately, a validation of this model when $\mathrm{D_f} \neq 1$ is not provided because no experimental data are available.

Summing up, the RC based model needs eight inputs C_2, C_3, UA_c, ΔT_{sh}, η, $\mathrm{W_{loss}}$, v_i and $\mathrm{V_r}$ that are to be obtained by multidimensional minimization algorithms. In the present paper these data are obtained from experiments using a Simplex Nelder minimization algorithm from GSL [4].

3. Results

In order to validate the models, experimental data obtained at ISFH are employed. The experimental set-up has been described in [7]. Experiments have been conducted in four cases depending on the mass flow rate defined here in [*kg/h*]: case-A) $\dot{\mathrm{m}}_\mathrm{c} = 500$ and $\dot{\mathrm{m}}_\mathrm{e} = 1900$; case-B) $\dot{\mathrm{m}}_\mathrm{c} = 700$ and $\dot{m}_\mathrm{e} = 1900$; case-C) $\dot{m}_\mathrm{c} = 900$and $\dot{m}_\mathrm{e} = 1900$ and case-D) $\dot{m}_\mathrm{c} = 700$ and $\dot{m}_\mathrm{e} = 1900$. Numerical calculations have been obtained with all possible combinations. For example, the parameters have been estimated at conditions of case-A and predicted in all conditions from case-A to case-C.

Experimental inlet fluid condenser temperatures range from 14^oC to 50^oC and inlet fluid evaporator temperatures from -5^oC to 30^oC with overlapping regions. The heat pump investigated has a scroll compressor with R410A as a refrigerant and the brine fluid of the evaporator side is *Tyfocor*®.

In this work the experimental data are referred as non-standard conditions when the measured inlet temperature difference between the condenser and evaporator, $\Delta T_{diff} < 5^oC$ or when $T_{fe,i} > 20^oC$. All the other data are considered to be at standard conditions that represents the data typically provided by commercial catalogues.

Validation at standard conditions

For the validation procedure of this section, only the cases were the prediction mode is the same than that of the estimation mode are considered. Moreover, only experimental standard data are used.

Numerical results compared agains experimental data calculated at case-A are shown in Fig. 1a for the coefficient of performance (*COP*) and in Fig.1b for the compressor work W_{cp}. A relative error line band of 5%, calculated as $\varepsilon_r = 100 \cdot \left|\left(\phi_{num} - \phi_{exp}\right)/\phi_{exp}\right|$ being ϕ a generic variable, is also plotted in Fig. 1 for comparison purposes. In this case, both models predict experimental data with very satisfactory results with ε_r below 5%. In Table 1, the RMS (root mean square) error of all standard data are presented along with the maximum relative error $\varepsilon_{r,max}$ for Q_c, W_{cp} and *COP*. In this section only the data of the Table 1 with the same mass flow rates in the estimation and prediction mode are considered. The RMS and the $\varepsilon_{r,max}$ predicted for the EF model is always lower than that of the RC based model. Numerical results presented in Table 1 have been obtained for all mass flow rates used in

the experiments, but only some data are presented in this work. The analysis of all data for the cases studied in this section, does not provide a significant difference from the analysis of data shown in Table 1. All studies lead to the observation that the RC model predictions are typically below 10% while EF errors are always below 5%.

This conclusion is supported by our previous study [3] where catalogue data from several heat pumps were used for the comparison. For steady state calculations where the boundary conditions are equal in the estimation and prediction mode, the EF is recommended. The EF model is more accurate and it can adjust to any brine to water heat pump easily.

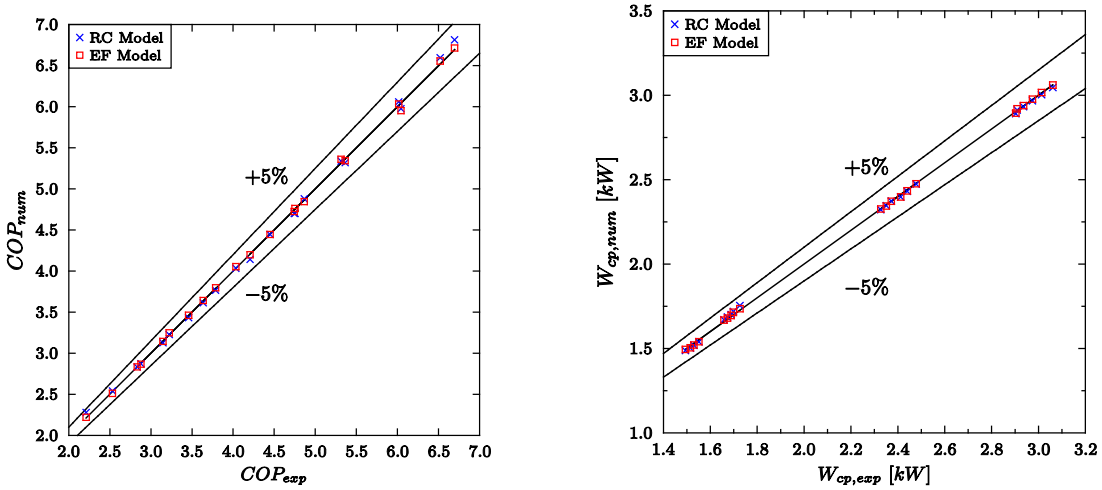

(a) (b)

Figure 1: Numerical results of a) COP and b) W_{cp}, compared with experimental data at case-A. Model inputs obtained from same conditions than that of experiments.

Table 1: Root mean square (RMS) and maximum relative error $\varepsilon_{r,max}$ of global variables as a function of the mass flow rates.

Estimation mode		**Prediction mode**			**RMS**			$\varepsilon_{r,max}$		
$\dot{m}_c$	$\dot{m}_e$	$\dot{m}_c$	$\dot{m}_e$	Model	Q_c	W_{cp}	COP	Q_c	W_{cp}	COP
[kg/h]	[kg/h]	[kg/h]	[kg/h]		[%]	[%]	[%]	[%]	[%]	[%]
500	1900	500	1900	RC	9.75	1.21	4.60	2.82	1.64	3.06
(Case-A)		(Case-A)		EF	4.08	0.82	2.72	1.10	0.95	1.50
		700	1000	RC	79.89	12.30	91.85	19.23	12.36	36.04
		(Case-D)		EF	173.15	7.38	128.39	33.58	7.51	44.43
900	1900	500	1900	RC	49.73	2.49	22.25	6.79	2.49	7.02

(Case-C)	(Case-A)	EF	51.70	16.13	48.90	8.37	9.24	15.83
	900 1900	RC	23.97	1.74	15.13	7.28	2.04	8.00
	(Case-C)	EF	10.90	1.17	8.80	2.72	1.60	4.22

One of the reasons of the better accuracy of the EF model is because it uses 12 parameters in the fitting procedure while the RC model is using only 8 inputs. To the author's opinion, a RC based model with 12 inputs will probably be as accurate as the EF model. However, the implementation of the RC model is much more complicated compared to the EF, specially for the model's input estimation procedure. Moreover, the algorithm used here to estimate the inputs of the RC model can not ensure the minimum absolute error, but only a relative. Therefore, the minimization process may change depending on initial values and some numerical parameters of the algorithm, which difficult the task of developing a robust tool to estimate the inputs. On the contrary, the input parameters of the EF model are much easier to be obtained and the estimation procedure does not depend on initial values and numerical parameters. Besides these, the RC model can only be accurate if the heat pump physical phenomena is considered. For example, a double circuit heat pump can be predicted with the present model but a higher errors than the ones shown here are obtained (see [3]).

It is also important to notice that if the RC based model is used in order to accurately match internal data of the heat pump, the inputs of the parameters can not be estimated from catalogue data, since a good prediction of $\mathrm{Q_c}$ and $\mathrm{W_{cp}}$ does not mean an accurate prediction of evaporative and condensing pressures, for example. The model was developed [2] to calculate global data such as $\mathrm{Q_c}$, $\mathrm{Q_e}$ and $\mathrm{W_{cp}}$, thereby internal heat pump data may not be accurately predicted using the present model without further improvements.

Mass flow rate analysis

Comparisons between the models for different mass flow rates in the evaporator and in the condenser have been analyzed. Predicted COP for inputs estimated at case-A and predicted at case-C have been plotted as a function of experimental data in Fig.2. In this case, predictions of both models are not as accurate as shown in the previous section with COP ε_r up to 15% for the EF model. The RC based model performs better than the EF model, which is something one might expect because the model is derived from physical concepts. All combination of cases from A to C have been studied but only some data are presented in Table 1. These results show that both RMS and $\varepsilon_{r,max}$ are usually better predicted by the RC compared to the EF model. Analysing all combination of cases defined in this section with different mass flow rates in the estimation and prediction mode, a general conclusion can be drawn: the greater the difference between the mass flow rate used for estimation and prediction modes, the greater the error of the models and also the larger the difference between them (in favor of the RC model). Results presented in this section confirm the generalized opinion that RC based models tend to extrapolate better. Moreover, the implementation of Eq.13 for the condenser side should improve RC predictions for varying mass flow rate.

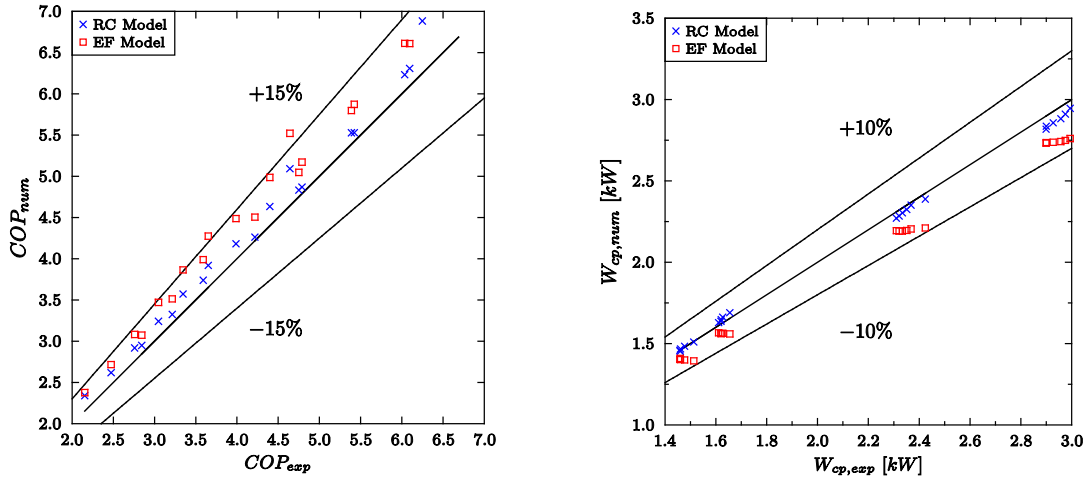

(a) (b)

Figure 2: Numerical results of a) COP and b) W_{cp} compared with experimental data at Case-C. Model inputs obtained from experiments at Case-A.

Model analysis at non-standard conditions

As explained in the previous sections, the experimental data obtained have been splitted into standard and non-standard data. The standard data have been used for estimation and prediction modes in all cases analyzed previously. In this section, the non-standard data have been used to analyse the behavior of the models under these conditions. Two cases have been considered: i) the standard data are used for estimation and the non-standard data for prediction and ii) all experimental data, including the non-standard values, are used for estimation procedure and the non-standard data are employed in the prediction mode. The first case is the most important, since typical catalogue data only include standard data and non-standard conditions may be found in system simulation calculations.

Numerical RMS and $\varepsilon_{r,max}$ for Q_c and W_{cp} have been presented in Table 2 for the two cases studied here. Surprisingly, the EF model extrapolates better to non-standard conditions in the two cases analyzed. Nevertheless, when the estimate procedure is only using standard data none of the models provide satisfactory results and relative errors up to 30% can be found.

Table 2: Root mean square (RMS) and maximum relative error $\varepsilon_{r,max}$ for predictions of non-standard data. Model inputs estimated at same conditions used in the prediction mode using only standard data or all experimental data for the estimating procedure.

			Using only standard data				**Using all experimental data**			
			RMS		$\varepsilon_{r,max}$		RMS		$\varepsilon_{r,max}$	
$\dot{m}_c$ [kg/h]	$\dot{m}_e$ [kg/h]	Model	Q_c [%]	W_{cp} [%]	Q_c [%]	W_{cp} [%]	Q_c [%]	W_{cp} [%]	Q_c [%]	W_{cp} [%]
500	1900	RC	228.56	8.21	33.82	8.90	129.40	5.99	22.19	6.95
(Case-A)		EF	185.64	5.88	27.93	5.18	21.48	1.08	2.69	0.94
900	1900	RC	177.84	16.50	29.69	11.52	130.77	3.00	24.21	3.30
(Case-C)		EF	95.81	2.68	15.59	1.85	9.49	1.85	1.30	1.92

The EF model performs very well if the non-standard data are used in the estimation procedure, with errors in the same range of accuracy as results presented in section "Validation at standard conditions". However, the RC predictions are not satisfactory even when all data for the estimation procedure are employed. For example, $\varepsilon_{r,max}$ of 34% in Q_c calculations are observed. When the compressor pressure ratio decreases because the evaporator and condenser inlet temperatures are close to each other, the COP increases until a certain point where the performance stabilizes (see [7]). This phenomena can be considered in the EF model if non-standard data are used for the fitting procedure. However, it is not considered in the mathematical description of the compressor of the RC based model. Therefore, if non-standard conditions have to be well predicted, the compressor model of the RC based approach should consider the compressor performance decrease at low pressure ratios.

4. Conclusions

An equation fit (EF) and a refrigerant circuit (RC) based heat pump models have been described, validated through comparisons agains experimental data, analyzed and compared to each other for varying mass flow rate and under non-standard conditions. From this work, the following conclusions can be drawn:

- When the same boundary conditions are used in the estimation and prediction mode, clearly, the EF model performs better and it is recommended, not only for its better accuracy, but also because the inputs of the model are much more easier to fit and the model is easier to implement.
- The RC based model extrapolates better when the mass flow rate is different in the prediction mode with respect the one employed in the estimation mode.
- The EF model extrapolates better for non-standard conditions. If the fitting procedure is done using non-standard data, the EF model would be as accurate as in standard conditions. Otherwise, $\varepsilon_{r,max}$ of Q_c in the range of 16% can be expected. For the RC model, even using non-standard data for estimating the inputs, high errors, with $\varepsilon_{r,max}$ up to 35% for Q_c, may be found.

5. Acknowledgments

This work has been partially supported by the Spanish Ministerio de Ciencia e Innovación (project reference ENE 2010-18994).

6. References

[1] Afjei, T. and Wittwer, D., 1995. Yearly Utilization Model YUM WP/Holz,Benutzerhandbuch mit Beispielen, INFEL/KRE, Zurich 1995, Schweiz.

[2] Jin, H. and Spitler, J.D., 2002. A parameter estimation based model of water-to-water heat pumps for use in energy calculations programs, ASHRAE Transactions, Vol 108 (1), pp 3-17.

[3] Dott, R., Afjei, T., Dalibard, A., Carbonell, D., Heiz, A., Haller, M. and Witzig, A., 2012. Models of sub-components and validation for the IEA SHC Task 44/ HPP Annex 38: Solar and Heat Pumps. Part C: Heat Pump Models.

[4] Galassi, M., Davies, J., Theiler, J., Gough, B., Jungman G., Booth, M. and Rossi, F., 2003. GNU Scientific Library Reference Manual (2nd Edition), ISBN 0954161734.

[5] Jin, H. and Spitler, J.D., 2003. A parameter estimation based model of water-to-water heat pumps with scroll compressor and water/glycol solutions, Building Services Engineering Research and Technology, Vol 24 (3), pp 203-219.

[6] Kuppan, T., 2000. Heat Exchanger Design Handbook. Marcel Dekker, Inc, New York, ISBN 0824797876.

[7] Pärisch, P., Warmuth, J., Kirchner, M. and Tepe, R., 2012. Durchfluss- und Temperaturabhängigkeit von Wärmepumpen im Project "Hocheffiziente wärmepumpen system mit geothermieund solarthermie nutzung", 22 Solarthermisches symposium, 9-11, Kloster Banz, Bad Staffelstein, OTTI.

A3. Description of TRNSYS Type 877 by IWT and SPF

TU Graz Graz University of Technology
HSR HOCHSCHULE FÜR TECHNIK RAPPERSWIL FHO Fachhochschule Ostschweiz
SPF INSTITUT FÜR SOLARTECHNIK

Date: 12th December 2012
Authors: Andreas Heinz, Michel Haller

1. Introduction and history

The basis for the heat pump model Type 877 is an EES-model, that has originally been developed by Stefan Bertsch of NTB Buchs (Bertsch, 2009), Switzerland and used the ARI model for the simulation of the compressor performance (ANSI/ARI 1999). Based on this EES model a TRNSYS model was programmed at Institut für Solartechnik SPF and further developed in a cooperation between the Institute of Thermal Engineering, Graz University of Technology and SPF. This document provides a short description of the model and its possibilities.

2. General description

The compression heat pump model Type 877 is a semi-physical model based on a calculation of the thermodynamic refrigerant cycle and the thermal properties of the used refrigerant. A performance map of the compressor is used for the simulation of the compressor efficiency and the electricity consumption (compare section 3). Figure 1 shows a schematic view of the refrigerant cycle that can be simulated with the model. It includes the possibility to use air, brine or both as a heat source (two evaporators) and the possibility to use an extra desuperheater heat exchanger in addition to the condenser for e.g. the preparation of domestic hot water.

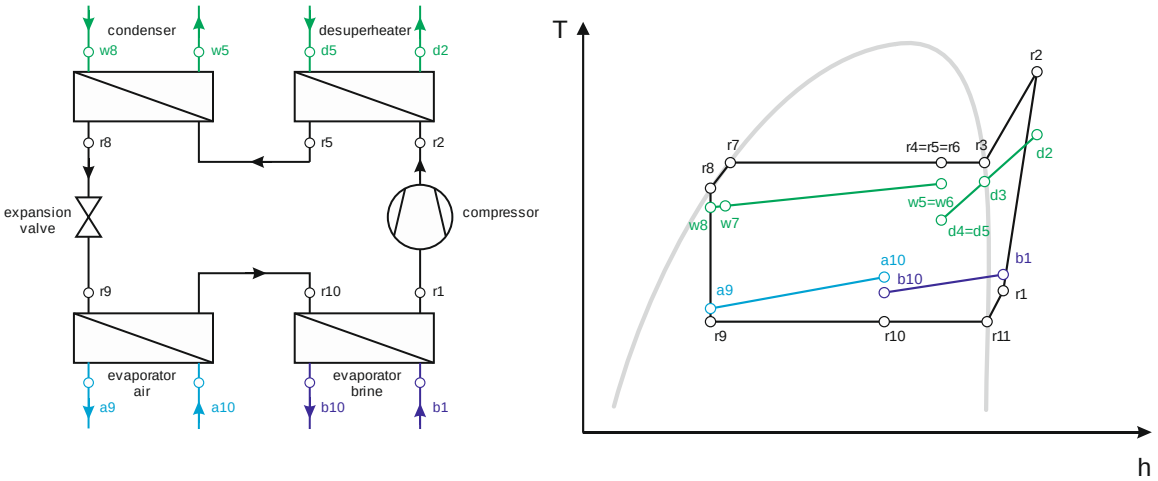

Figure 1: Left: Schematic of the heat pump cycle; Right: Schematic example process in the Th-diagram with all heat exchangers active

3. Mathematical description

Thermodynamic properties

The thermodynamic properties of the working fluid are obtained by polynomial curve fits, which have been determined separately for the two-phase and the superheated domain of the different refrigerants. The advantage of this approach compared to using a separate software for the determination of the thermal properties is a reduction of simulation time. As the model is doing a large number of iterations in every simulation time step, the number of necessary fluid property calculations is very high. A comparison to a first version of the model, which was using REFPROP (http://refprop.software.informer.com/) for the calculation of the thermal properties, showed a reduction in simulation time of about factor 50 to 100, while achieving minimal deviations between results.

Refrigerant data has up to now been integrated for R410A, R407C, R134a, R290 and R404A, but this list can be easily extended with additional working fluids.

Calculation of heat exchangers

Every heat exchanger in the cycle is calculated using the inlet conditions (m, p, T) of the fluids on both sides and the UA_{HX} (W/K) of the respective heat exchanger. For the calculation the heat exchanger is subdivided into sections with approximately constant properties as depicted in Figure 2. For every section a UA_i is calculated according to

$$UA_i = \frac{\dot{Q}_i}{\Delta T_{log,i}}$$

where $\dot{Q}_i$ is the heat transfer rate in the respective section and $\Delta T_{log,i}$ is the logarithmic mean temperature difference between the two fluid sides in the section. The refrigerant pressure in the heat exchanger is determined iteratively. Convergence is reached when

$$\Sigma UA_i = UA_{HX}$$

is fulfilled for the respective heat exchanger (with a certain tolerance).

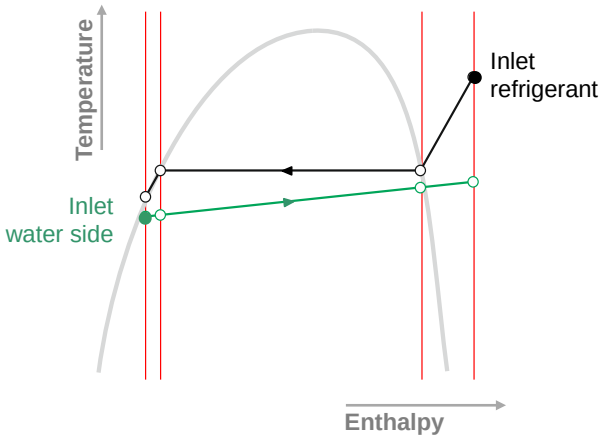

Figure 2: Subdivision of the condenser into sections

Compressor model

The model provides two possibilities for the simulation of the compressor:

a) Compressor data file

For the simulation of the compressor a performance map (bi-cubic curve fit) is used to determine the refrigerant mass flow rate and the electricity consumption. The coefficients of this performance map are provided to the model via a data file. The path and filename of the datafile have to be provided via Label 1 of the model. The datafile is an ASCII-file (e.g. *.txt) that contains lines made up of a tag in square brackets, and equal sign and a value for the tag in quotation marks. The order of the appearance of the tags is not relevant, but no tag should be missing. An example is given below. The bi-cubic curve fits for the electricity consumption and the refrigerant mass flow rate have the following form:

$$P_{el,comp} = x_{p1} + x_{p2}\cdot t_{F1} + x_{p3}\cdot t_{F2} + x_{p4}\cdot \left(t_{F1}\right)^2 + x_{p5}\cdot t_{F1}\cdot t_{F2} + x_{p6}\cdot \left(t_{F2}\right)^2 + x_{p7}\cdot \left(t_{F1}\right)^3 + x_{p8}\cdot \left(t_{F1}\right)^2\cdot t_{F2} + x_{p9}\cdot t_{F1}\cdot \left(t_{F2}\right)^2 + x_{p10}\cdot \left(t_{F2}\right)^3$$

$$\dot{m}_{wf,comp} = y_{m1} + y_{m2}\cdot t_{F1} + y_{m3}\cdot t_{F2} + y_{m4}\cdot \left(t_{F1}\right)^2 + y_{m5}\cdot t_{F1}\cdot t_{F2} + y_{m6}\cdot \left(t_{F2}\right)^2 + y_{m7}\cdot \left(t_{F1}\right)^3 + y_{m8}\cdot \left(t_{F1}\right)^2\cdot t_{F2} + y_{m9}\cdot t_{F1}\cdot \left(t_{F2}\right)^2 + y_{m10}\cdot \left(t_{F2}\right)^3$$

P [W], t [F], m[lbm/h]

Such curve fits can be obtained for many compressors from different manufacturers.

Example of a Compressor Performance Data ASCII-File:

```
[Compressor] = "Scroll ZP83KCE-TFD, 60Hz, 3 Phasen, Air Conditoning, 4.71 in3/rev, R410a"
[Pel_comp_1] = "-38.87"
[Pel_comp_2] = "-3.348"
[Pel_comp_3] = "75.24"
[Pel_comp_4] = "0.1096"
[Pel_comp_5] = "0.1775"
[Pel_comp_6] = "-0.5603"
[Pel_comp_7] = "0.001588"
[Pel_comp_8] = "-0.001553"
[Pel_comp_9] = "-0.001099"
[Pel_comp_10] = "0.003363"
[m_compr_1] = "405"
[m_compr_2] = "9.867"
[m_compr_3] = "5.402"
[m_compr_4] = "0.04198"
[m_compr_5] = "0.0235"
[m_compr_6] = "-0.05299"
[m_compr_7] = "0.0006481"
[m_compr_8] = "0.0001953"
[m_compr_9] = "-0.0000786"
[m_compr_10] = "0.0001347"
[T_sup_map] = "11.1"
[T_min_evap] = "-20"
[T_max_cond] = "65"
[T_max_evap] = "12"
[T_min_cond] = "30"
[Refrigerant] = "410"
[Phases] = "3"
[Volume] = "4.71"
[Size_factor] = "23.2"
```

The “size factor” provided in the file corresponds to the thermal heat capacity (heat output) at A2W35 in kW and is of informative character only.

b) Compressor calculation via η_{is}, η_{vol} and $\dot{V}_{swept}$

An alternative to using a compressor data file is to provide the model with the swept volume flow rate $\dot{V}_{swept}$ (Parameter 10) and the overall isentropic η_{is} and volumetric efficiency η_{vol} of the compressor (Inputs 26 and 27). In this case the mass flow rate of the working fluid and the electricity consumption of the compressor are calculated according to

$$\dot{m}_{wf} = \dot{V}_{swept} \cdot \rho_{wf,1} \cdot \eta_{vol}$$

and

$$P_{el,comp} = \frac{\dot{m}_{wf}\left(h_{wf,2,is} - h_{wf,1}\right)}{\eta_{is}}$$

The efficiencies η_{is} and η_{vol} are usually mainly dependent on the pressure ratio $\pi = p_{cond}/p_{evap}$ and can be determined from manufacturer data.

Additional functions

Defrosting losses: The losses caused by the icing of the air source evaporator and its defrosting are considered in a very simple way. The amount of ice that is expected to be built under the actual operating conditions is calculated depending on the evaporation temperature and the temperature and relative humidity of the air at the in- and outlet. The heating capacity needed for the melting of the ice is then subtracted from the condenser heating capacity, thus reducing the COP of the cycle. The dynamics of the defrosting are not considered by the model.

Variable capacity compressors: With input 1 of the model also the capacity of the compressor and the heating power of the heat pump can be controlled in a simple way. Changes in UA-values and electricity consumption of an air ventilator that go along with a change in compressor capacity are not calculated automatically but left to the user to change the corresponding inputs. Change in compressor performance is not considered for the compressor data based approach and is left to the user for changing the inputs in the case of the overall isentropic and volumetric efficiency approach.

Starting losses: The starting losses $\dot{Q}_{loss,start}$ are also considered in a rather simple way. Using a time constant τ_{start} (input 23) the starting losses are calculated depending on the simulation time step Δt and the fractional starting losses in the last time step $f_{loss,start,old}$. The starting losses are subtracted from the condenser heating capacity $\dot{Q}_{cond}$, thus reducing the COP of the cycle.

$$f_{loss,start} = f_{loss,start,old} \cdot e^{\frac{-\Delta t}{\tau_{start}}}$$

$$\dot{Q}_{loss,start} = \dot{Q}_{cond} \cdot f_{loss,start}$$

The time constant for the starting losses that is provided by the user is assumed to be valid for the maximum compressor speed (Input 1 = 1). For lower compressor speeds n_{Comp} the time constant is adapted according to the following equation in order to increase the duration of the start-up phase accordingly.

$$\tau_{start} = \frac{\tau_{start}}{n_{Comp}}$$

Stopping losses: After the compressor has switched off, the heat pump is assumed to cool out according to a time constant τ_{stop} (input 28). Thus the starting losses for the next start-up of the heat pump depend on the time the compressor was switched off.

$$f_{loss,start} = 1 - (1 - f_{loss,start,old}) \cdot e^{\frac{-\Delta t}{\tau_{stop}}}$$

Error function: Usually there are limitations concerning the maximum condensation pressure and the minimum and maximum evaporation pressure that a compressor can be operated with. If the maximum condensation pressure or minimum evaporation pressure is exceeded, the model will go into error mode. This means the compressor and the ventilator stay OFF for a certain time, which is provided by the user via Parameter 9.

4. Validation

Validation at Institut für Solartechnik SPF

Validation has been performed by the Institut für Solartechnik SPF by fitting model parameters and inputs to data that was measured by Daniel Philippen (SPF) for an air-to-water heat pump and by Robert Haberl (SPF) for a brine-to-water heat pump.

The compact outdoor mounted air source heat pump was tested in 2011, had a nominal heating capacity of 12 kW and used a reversed cycle for defrosting of the air-source heat exchanger. Measurements were performed in a climatic chamber at ambient temperatures from -8 °C to +30 °C (relative humidity 80-90%), and with flow temperatures of 35 °C and of 50 °C. Temperatures, flow and electric uptake were recorded in 1 second timesteps and then averaged over 1 minute.

The first attempt to model the heat pump with a constant delta-T for superheating resulted in a considerable overestimation of the performance of the heat pump at high ambient air temperatures. in a second approach, the superheating was calculated as a function of the outdoor temperature, based on measurements of the temperature of the refrigerant loop before and after the evaporator (Figure 3).

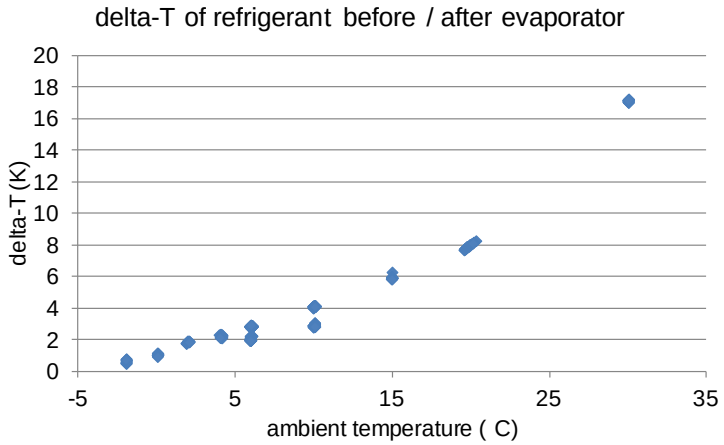

Figure 3: dependency of the superheating on the source temperature for an air-to-water heat pump

with thermostatic expansion valve.

The parameters and constant inputs of the heat pump were fitted using GenOpt. The resulting deviation between measured and simulated COP of the heat pump, including control device and electricity for the fan, but excluding the pump for the heating water, was 0.045 COP-point on average and is shown in Figure 4. The measured point at -8°C ambient air temperature was excluded from the fit because of additional electric uptake of the control unit for heating the fan-casing during defrosting that was not observed for any other measured points. An extra deduction from the COP would have to be done for ambient air temperatures <-5 °C to take this extra electric uptake into account.

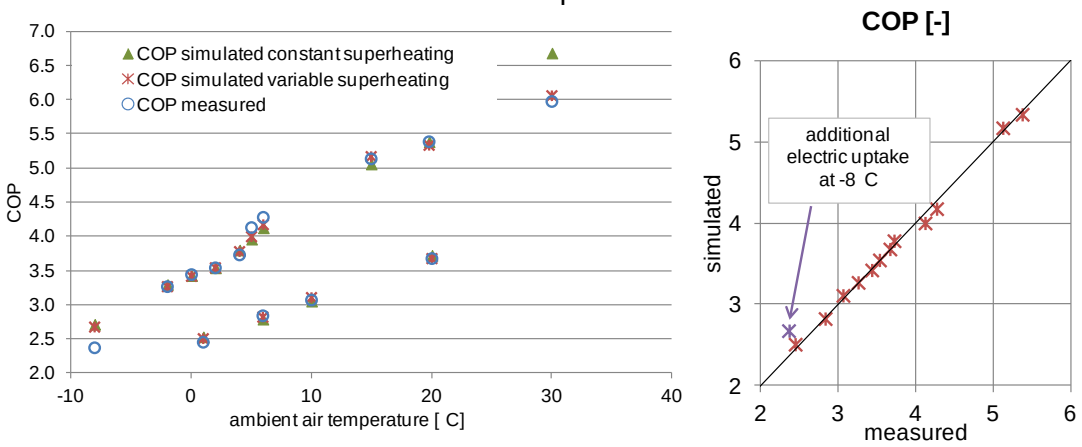

Figure 4: measured COP and COP simulated with constant superheating (green triangle) and with variable superheating (red cross).

A brine-to-water heat pump with a nominal heating capacity of 4 kW was measured during several charging processes of a storage tank. In a first step, the UA-values of the heat exchangers, superheating and subcooling where fitted by comparison of measured and simulated temperatures in the working fluid cycle. Figure 5 shows simulated and measured COP during a charging process with condenser outlet temperatures between 35 °C and 45 °C and the brine source inlet temperature at about 1.5 °C. If the heat pump is assumed to be without heat losses, the simulated COP is considerably higher than the simulated one (left). After fitting the heat losses (parameter 24 of the model) the simulated and measured COP match quite closely with the exception of the start phase (middle). Figure 5, right, shows the result after fitting the start heat losses with the start time constant (parameter 23).

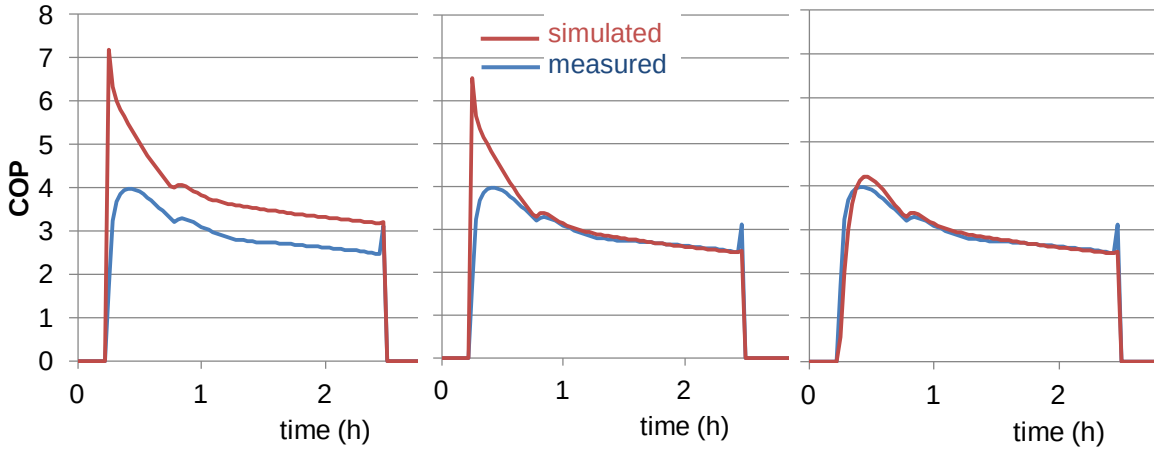

Figure 5: Simulated and measured COP over a boiler charging process with a brine-to-water heat

pump without taking into account heat losses (left), only taking into account steady state heat losses (middle), taking into account steady state and start heat losses (right).

No validation has been performed yet with variable capacity compressors and/or with the isentropic and volumetric efficiency approach.

Validation at IWT, TU Graz

At the Institute of Thermal Engineering, TU Graz, a comparison between measured results and simulations with the heat pump model was done. The measured data comes from an air-source heat pump with a speed controlled compressor and was provided by a heat pump manufacturer. A comparison of the simulated and measured results for the COP and the thermal power of the condenser is shown in Figure 6. In total 69 different operation points, including different heat source and sink temperatures, different compressor speeds and operation points with defrosting (average COP over several defrosting cycles) are represented.

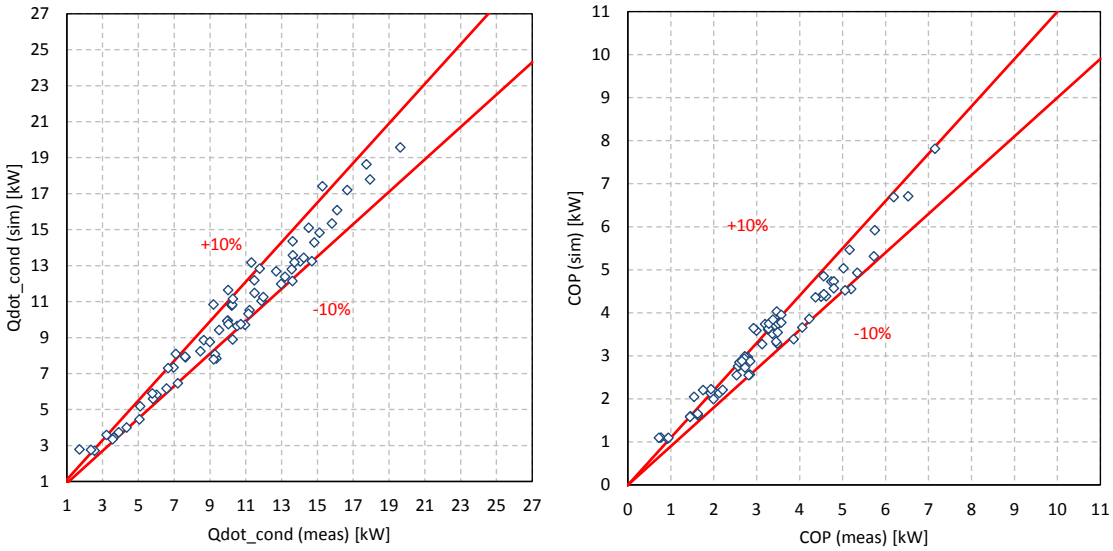

Figure 6: Comparison of measurement and simulation results for the condenser thermal power and the COP of an air source heat pump (69 points)

5. Parameters, Inputs and Outputs

Parameters

Nr.	*short*	*explanation*	*unit*	*range*
1	ref	Choice of working fluid / Refrigerant (1: R410A, 2: R407C, 3: R134a, 4: R290, 5: R404A)	-	[1;5]
2	Size Factor	Size_Factor for the thermal capacity of the heat pump. Only used if a compressor data file is used (if Par10=0). In this case the refrigerant mass flow and the electricity consumption of the compressor, which are calculated according to the compressor data in the file, are multiplied with this size factor	-	[0;+inf]
3	cp_{sink}	specific heat of the sink side fluid	kJ/kg.K	[0;+inf]
4	cp_{brine}	specific heat of brine (source)	kJ/kg.K	[0;+inf]
5	$P_{el,ctr}$	electricity consumption of controller	kW	[0;+inf]
6	$\dot{V}_{air,nom}$	Nominal air volume flow rate	m³/h	[0;+inf]
7	$T_{evap,defrost}$	Evaporation temperature below which defrosting of the evaporator (air heat source) is calculated	°C	[-Inf;+Inf]
8	$\eta_{defrost}$	efficiency of defrost-cycle	-	[0;1]
9	τ_{error}	Time that heat pump stays on error (compressor and ventilator OFF) if it has been tried to run it with inlet temperatures out of limits (max or min operating pressures of compressor reached)	h	[0;+Inf]
10	$\dot{V}_{swept,comp}$	Swept volume flow rate of the used compressor. If this Par is set to 0, the data from the provided Compressor data file (Label 1) will be used and all data provided at Par 11,12,13,14 and Inputs 25,26 will be neglected !	m³/h	[0;+Inf]
11	$T_{min,evap}$	Minimum evaporation temperature of the heat pump	°C	[-30;50]
12	$T_{max,evap}$	Maximum evaporation temperature of the heat pump	°C	[-30;50]
13	$T_{min,cond}$	Minimum condensation temperature of the heat pump	°C	[10;100]
14	$T_{max,cond}$	Maximum condensation temperature of the heat pump	°C	[10;100]

Inputs

Nr.	*short*	*explanation*	*unit*	*range*
1	$f_{comp,on}$	Control switch for turning heat pump (compressor / working fluid cycle) on; 0 .. off, 1 .. compressor on with 100% speed; speed control of compressor: 0.2 .. 1 → compressor speed 20 to 100%; 100% speed is the speed according to the compressor data file, or Par10 respectively	-	[0;1]
2	$f_{vent,on}$	Control switch for turning the air ventilator (heat source) on; 0 .. off, 1 .. ventilator on with 100% speed; speed control of ventilator: 0.1 .. 1 → ventilator speed 10 to 100%; 100% speed results in an air volume flow rate according to Par 6	-	[0;1]
3	ΔT_{sup}	Delta T superheating	K	[0;30]
4	ΔT_{sub}	Delta T subcooling	K	[0;30]
5	UA_{cond}	Heat transfer coefficient area product of the condenser (heat exchanger)	W/K	[0;+Inf]
6	$T_{cond,in}$	Temperature of sink inlet to condenser	°C	[-Inf;+Inf]
7	$\dot{m}_{cond,in}$	Mass flow rate of sink inlet to condenser (considered as signal / can be reset to zero due to internal evaporator or condenser pressure errors); only active if input 8 = 0	kg/h	[0;+Inf]
8	$mode_{cond}$	Mode for the control of the water flow through the condenser: 0...the water mass flow through the condenser is calculated externally and provided to the model via input 7 1...the water mass flow through the condenser is calculated by the model in order to reach the set temperature provided via input 9	-	[0;1]
9	$T_{cond,out,set}$	set water temperature at the outlet of the condenser (only active if input 8 = 1)	°C	[-Inf;+Inf]
10	UA_{desup}	Heat transfer coefficient area product of the desuperheater (heat exchanger)	W/K	[0;+Inf]
11	$T_{desup,in}$	Temperature of desuperheater heat sink inlet	°C	[-Inf;+Inf]
12	$\dot{m}_{desup,in}$	Mass flow rate of desuperheater heat sink inlet (only active if input13=0)	kg/h	[0;+Inf]
13	$mode_{desup}$	Mode for the control of the water flow through the desuperheater:	-	[0;1]

		0...the water mass flow through the desuperheater is calculated externally and provided to the model via input 12 1...the water mass flow through the desuperheater is calculated by the model in order to reach the set temperature provided via input 14		
14	$T_{desup,out,set}$	set water temperature at the outlet of the desuperheater (only active if input 13=1)	°C	[-Inf;+Inf]
15	$UA_{evap,brine}$	Heat transfer coefficient area product of the brine source heat exchanger	W/K	[0;+Inf]
16	$T_{brine,in}$	Temperature of brine (heat source) inlet	°C	[-Inf;+Inf]
17	$\dot{m}_{brine,in}$	Mass flow rate of brine heat source inlet	kg/h	[0;+Inf]
18	$UA_{evap,air}$	Heat transfer coefficient area product of the air source heat exchanger	W/K	[0;+Inf]
19	$T_{air,in}$	Temperature of air (heat source) inlet	°C	[-Inf;+Inf]
20	$p_{air,in}$	pressure of air	bar	[0;+Inf]
21	$RH_{air,in}$	relative humidity of air	-	[0;1]
22	$P_{el,vent}$	Electricity consumption of ventilator	kW	[0;+Inf]
23	τ_{start}	starting time constant (for a compressor speed of 100%); for lower compressor speeds the time constant will be adapted automatically	h	[0;+Inf]
24	UA_{loss}	The heat losses from the compressor to the ambient can be provided in two different ways: 1) as a positive value: heat transfer coefficient area product for the heat losses from the compressor to the ambient (ambient temperature is INPUT 25) 2) as a negative value: heat losses of the compressor are provided as a percentage of the electricity consumption of the compressor (e.g. if this input is "-0.2" then the heat losses will be 20 % of the compressor electricity consumption)	W/K or -	[0;+Inf]
25	T_{amb}	Ambient temperature, used for calculation of heat losses from the compressor	°C	[-Inf;+Inf]
26	η_{is}	Isentropic efficiency of the compressor Only used if Par 10<>0; otherwise the compressor calculation is done according to the data provided in the compressor data file	-	[0;1]
27	η_{vol}	Volumetric efficiency of the compressor Only used if Par 10<>0; otherwise the compressor calculation is done according to the data provided in the compressor data file	-	[0;1]
28	τ_{stop}	time constant for cooling out of the heat pump	h	[0;+Inf]

Outputs

Nr.	***short***	***explanation***	***unit***	***range***
1	$T_{cond,out}$	Temperature of the condenser (heat sink) outlet	°C	[-Inf;+Inf]
2	$\dot{m}_{cond,out}$	Mass flow rate of the condenser (heat sink) outlet	kg/h	[0;+Inf]
3	$T_{desup,out}$	Temperature of the desuperheater (heat sink) outlet	°C	[-Inf;+Inf]
4	$\dot{m}_{desup,out}$	Mass flow rate of the desuperheater (heat sink) outlet	kg/h	[0;+Inf]
5	$T_{brine,out}$	Temperature of brine (2nd heat source) outlet	°C	[-Inf;+Inf]
6	$\dot{m}_{brine,out}$	Mass flow rate of brine (2nd heat source) outlet	kg/h	[0;+Inf]
7	$T_{air,out}$	Temperature of the air (heat source) outlet	°C	[-Inf;+Inf]
8	$\dot{m}_{air,out}$	Mass flow rate of the air (heat source) outlet	kg/h	[0;+Inf]
9	$RH_{air,out}$	Relative humidity of the air (1st heat source) outlet	-	[0;1]
10	$h_{air,in}$	Specific enthalpy of air inlet	kJ/kg	[-Inf;+Inf]
11	$h_{air,out}$	Specific enthalpy of air outlet	kJ/kg	[-Inf;+Inf]
12	$\dot{m}_{H2O,cond,out}$	Mass flow rate of condensed water from air source heat exchanger	kg/h	[0;+Inf]
13	$P_{el,tot}$	Total electricity consumption rate of heat pump (includes compressor, air ventilator, and controller, does not include pumps for brine or water mass flows)	kW	[0;+Inf]
14	$P_{el,comp}$	Electricity consumption rate of compressor	kW	[0;+Inf]
15	$P_{el,vent}$	Electricity consumption rate of ventilator	kW	[0;+Inf]
16	$P_{el,ctr}$	Electricity consumption rate of controller	kW	[0;+Inf]
17	$\dot{Q}_{cond}$	Heat transfer rate of the condenser heat exchanger	kW	[0;+Inf]
18	$\dot{Q}_{desup}$	Heat transfer rate of the desuperheater heat exchanger	kW	[0;+Inf]
19	$\dot{Q}_{evap,brine}$	Heat transfer rate of the brine source evaporator (2nd evaporator)	kW	[0;+Inf]
20	$\dot{Q}_{evap,air}$	Heat transfer rate of the air source evaporator (1st evaporator)	kW	[0;+Inf]
21	$\dot{Q}_{loss,amb}$	Heat loss rate to ambient from compressor	kW	[0;+Inf]
22	$\dot{Q}_{loss,defrost}$	Average heat loss rate for defrosting	kW	[0;+Inf]
23	$\dot{Q}_{loss,start}$	Losses for start-up	kW	[0;+Inf]

24	$\dot{Q}_{balance}$	Energy balance (should always be zero)	kW	[-Inf;+Inf]
25	$\dot{m}_{wf}$	Mass flow rate of the working fluid in the refrigerant cycle	kg/h	[0;+Inf]
26	p_ratio	Pressure ratio (p_{cond}/p_{evap})	-	[1;+Inf]
27	Δt_{error}	Countdown time for blocking heat pump after error in evaporator or condenser	hr	[0;+Inf]
28..38	$T_{wf,1..11}$	Temperature of working fluid at point 1..11	°C	[-Inf;+Inf]
39..49	$h_{wf,1..11}$	Spec. enthalpy of the working fluid in point 1..11	kJ/kg	[-Inf;+Inf]
50..60	$p_{wf,1..11}$	Pressure of the working fluid in point 1..11	bar	[0;+Inf]
61..64	$T_{w,5..8}$	Water temperature in point 5..8	°C	[-Inf;+Inf]
65..68	$T_{dhw,2..5}$	DHW temperature in point 2..5	°C	[-Inf;+Inf]
69	IC_{glob}	Global convergence iteration counter (max=30)	-	[0;+Inf]
70	IC_{evap}	evaporator convergence iteration counter (max=25)	-	[0;+Inf]
71	IC_{cond}	condenser convergence iteration counter (max=25)	-	[0;+Inf]
72	IC_{desup1}	iteration counter for desuperheater case 1 (max=25)	-	[0;+Inf]
73	IC_{desup2}	iteration counter for desuperheater case 2 (max=25)	-	[0;+Inf]
74	$IC_{Tair,out}$	$T_{air,out}$ convergence iteration counter (max =25)	-	[0;+Inf]
75	Err_{evap}	Error in evaporator calculation: 0 = no error; 1 = evap. temp. too low; 2 = evap. temp. too high	-	[0;2]
76	Err_{cond}	Error in condenser: 0: o.k. 1: Low pressure error condenser 2: High pressure error condenser	-	[0;2]
77	Err_{desup}	obsolete	-	[-Inf;+Inf]

Literature

Bertsch, S., “Quasidynamischer Wärmepumpen-Simulator”, Computer - Code in EES (Engineering Equation Solver)

ANSI/ARI Standard 540-1999 [2] “Positive Displacement Refrigerant Compressors and Compressor Units”, 1999.

A4. Heatpump model of Polysun

1. Abstract

Polysun is a software program for the simulation of heating systems. The simulation kernel applies a time stepping algorithm and dynamically calculates all relevant system parameters over a one year period, based on statistical weather data. On the one hand Polysun draws out by physics-based simulation scheme and its modularity, which allows any arrangement of the system components. On the other hand, Polysun offers a unique set of component catalogues which cover a large number of comercially available system components.

In this project, three kinds of heat pumps have been integrated in Polysun, namely the air/water, water/water and brine/water heat pumps. Furthermore, the relevant heat sources have been implemented, namely ambient air, soil and groundwater. In consequence, Polysun now covers a larger, and almost complete, range of renewable energy systems.

Simulation parameters are the measured heat pump COP values (in accordance with EN 255 and 14511). A linear interpolation scheme has been developed in this project in order to simulate systems for arbitrary source and heat pump temperatures and to interpolate the power consumption.

For the dynamic simulation of the ground source heat pump, the numerical algorithm from the Program EWS (calculation module developed in 1997) has been integrated into Polysun. Groundwater wells are calculated with respect to the soil temperatures.

Heat pumps and probes were implemented as independent components in Polysun. In the graphical user interface, they can be arbitrarly placed and connected with other hydraulic components. The timestepping simulation calculates inlet temperature, electric power consumption and heat transfer in the entire system. The Polysun catalogs have been extended accordingly with total over 300 component entries and a number of relevant system templates.

2. Implementation

Polysun offers a modular concept for the design of heating systems. The flexibility of the software is only reached by more academic oriented tools like TRNSYS, but the operator convenience predestines Polysun for applications in the field of consulting operations in the industry.

Different operator levels are offered. In the highest level (operator level “designer”) the software provides absolutely freedom in system design to the system designer. The hydraulic components can be placed and recombined in an arbitrary way by means of graphical user interface. In a low-cost edition of the software (operator level “professional”), there is only offered an assistant which supports the selection of the default hydraulic components and enables a user-friendly and simple manipulation.

Beside the simulation, the databases of the system components and the system guidelines are an important part of *Polysun*. That way, the user saves time collecting all the performance parameters of each component out of the datasheets. The databases are continuously actualised by Vela Solaris and synchronised with the database of the user by an automatic update routine using internet. Therewith, it is guaranteed that the use of Polysun in the workflow process delivers a saving of time.

The heat pump is implemented as an autonomous component. It can be placed on the screen and connected arbitrary to other hydraulic components. Existing hydraulic models

with boilers can be connected to the air heat pump. In the simulation, for every time step the electric power consumption and the heat output to the circuit are calculated using the ambient temperature and the recirculation temperature. Statistical weather data, which is already included in Polysun, is used to calculate the heating load and the entry parameters of the air heat pump (Ambient temperature and humidity).

In the results, the electrical power consumption, heat transfer to the fluid, COP, temperatures (minimum, maximum and average) are presented on different time scales, namely hours, months and years. Figure 1 shows a simple hydraulic system for domestic warm water and building heating with an air heat pump, which is modelled in Polysun 4. Figure 2 shows a more complicated hydraulic system with a solar system. Up to now 14 hydraulic models in Polysun are integrated in a wide range of different combinations of hydraulic systems, like warm water, space heating, swimming pools, solar heating and photovoltaic.

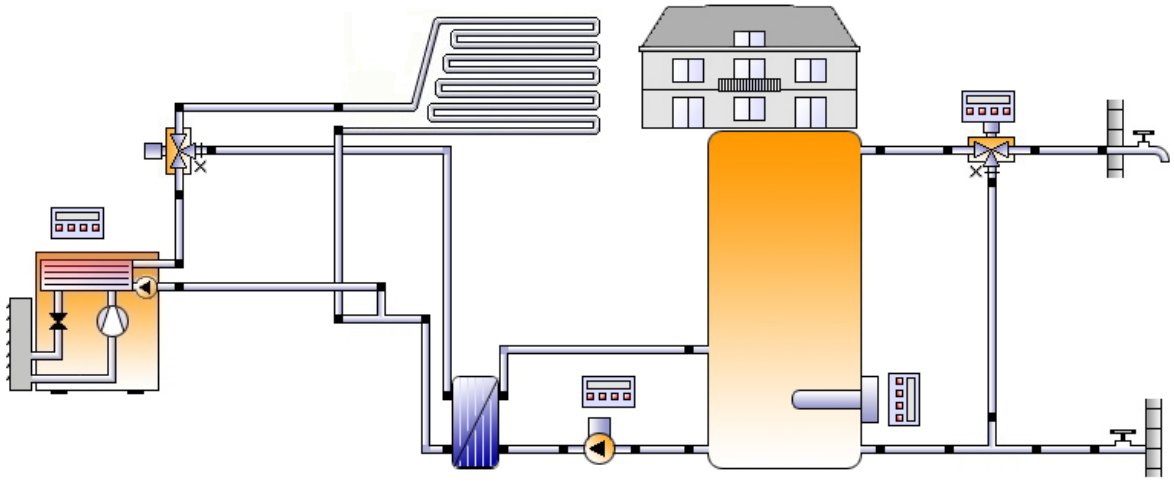

Figure 1: System for domestic hot water and space heating generation with heat pump.

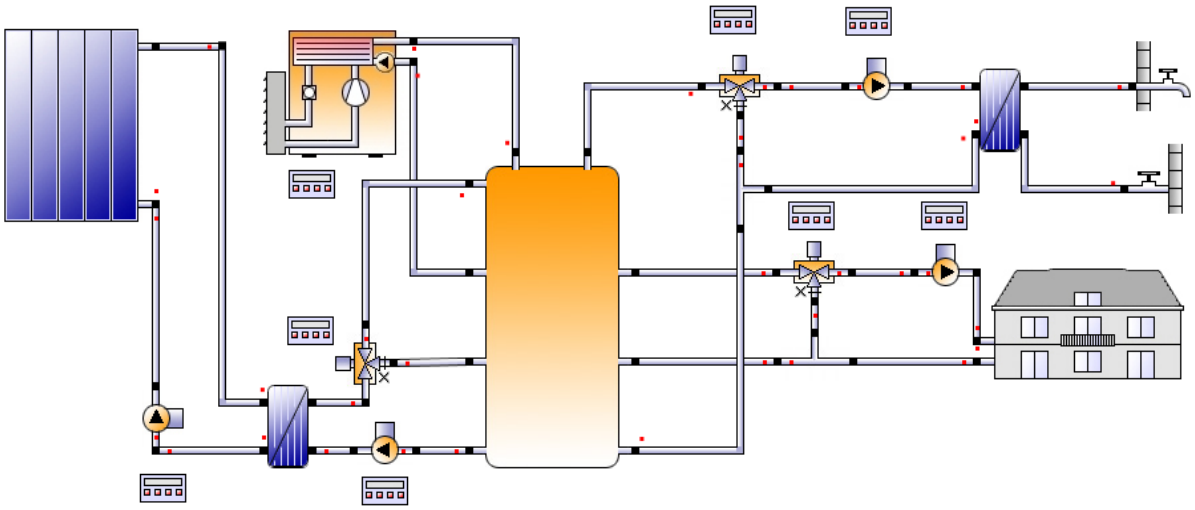

Figure 2: System for domestic hot water and space heating generation with solar heat and heat pump system.

Integration of heat pump in Polysun and linking to EWS

- *Already embedded weather data*, which is important for the calculation of the heat load as well as for the design of, e.g. air water heat pumps. If a location is not already deposited, Polysun interpolates the weather data of the new location using the geographical coordinates and the altitude (Meteonorm 6 from the company Meteotest is implemented in Polysun).
- *Variable time increment*: A one year simulation can be realised in one minute calculation time within a high accuracy.
- *Control behaviour*: An important component in the system optimization is the control unit. The control is implemented in a realistic way.
- *Building simulation*: Polysun 4 has an integrated building simulation for the calculation of the dynamic building load (based on Helios, which was developed at the EMPA).
- *Wide range of existing components*: The existing range of functions in Polysun includes all important components of a heating system (storage, boiler, pumps, heat exchanger, mixing valves, controls, buildings).
- *Results and visualization:* A wide range of results are visualized on a pleasant graphical user interface.

With the software *EWS* there is a further program available as a further basis for the project, which is focussed on the borehole heat exchanger and which has implemented the corresponding calculation equations and parameter rates for the most part. Due to the developers of this project, the know-how in modelling and the practical knowledge in the field of heat pumps exist.

The models were evaluated by short numerical investigations beyond *Polysun* framework and discussed in the project team. For the implementation, the *EWS* code was translated to programming language *Java* and could therefore implemented native in the *Polysun* code. The new functionality and parameters with relevance to the heat pump were added to the *Polysun* user interface and the databases.

For the delivery, the component database was expanded and corresponding hydraulic models were elaborated. The documentation was successively completed and the distribution/support partners were trained. Thereby, the standard functionality of *Polysun* was used for an efficient distribution of the heat pump features.

The publication of the new features on the designer level happens in an early stage, on the suggestion that only well trained users are using the new functionality. In a quarterly release cycle, the hydraulic guidelines and the documentations were delivered additionally, so that a widely user layer can be addressed.

3. Validation and Testing

For the validation and the testing of the physical models describing the heat pump functions, the procedure was proceed at the same well proven scheme as in the report request mentioned. At a first step, the models Vela-Solaris were validated internal. Following, external experts (project partner HETAG AG as a subcontractor) execute a function control with checking the quantitative results on its plausibility. Therefore, comparison calculations with standard version of the software *EWS* were made.

4. Results

Numerical model for air heat pump

Using linear interpolation of efficiency factors from the measured COP's (coefficient of performance) of air/water heat pumps, the COP values for different ambient temperatures and heat pump discharge temperatures can be calculated.

As a basic data for the interpolation the standardized measurements of the WPZ (Heat pump test facility) on air/water heat pumps are used. The from the WPZ covered measurement range of ambient temperatures T_a from -7°C to 20°C should be expanded from -14°C to 30°C. With further approximations, COP's standing outside this range can be calculated for arbitrary ambient temperatures. In Figure 3 an example for interpolated values is depicted.

By the indirect interpolation method of the COP, the COP is calculated with the help of the efficiency factor η_c. The efficiency factor η_c itself is calculated by linear interpolation from the variables T_a and T_v. Therefore, the COP measurement values are converted to efficiency factors η_c, which are interpolate linearly to T_a und T_v and finally recalculated to COP values. The different interpolation methods were compared with the conclusion that the interpolation of the efficiency factor leads in general to more accurate values of the COP's than the direct linear interpolation of the COP values to T_a und T_v (Figure 4 and Figure 5). The electric power consumption P_{el} of the heat pump is directly linearly interpolated out of the measurement values as a function of the ambient temperature T_a and the heat pump discharge temperature T_v.

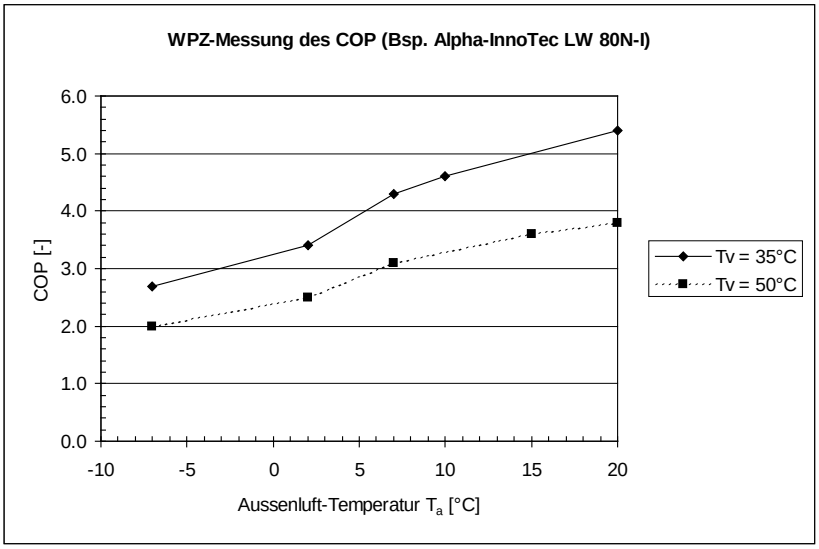

Figure 3: Example of a WPZ-Measurement of the COP on an Air/Water-heat pump according to EN 255 (HP-outlet-temperatures Tv = 35°C und Tv = 50°C).

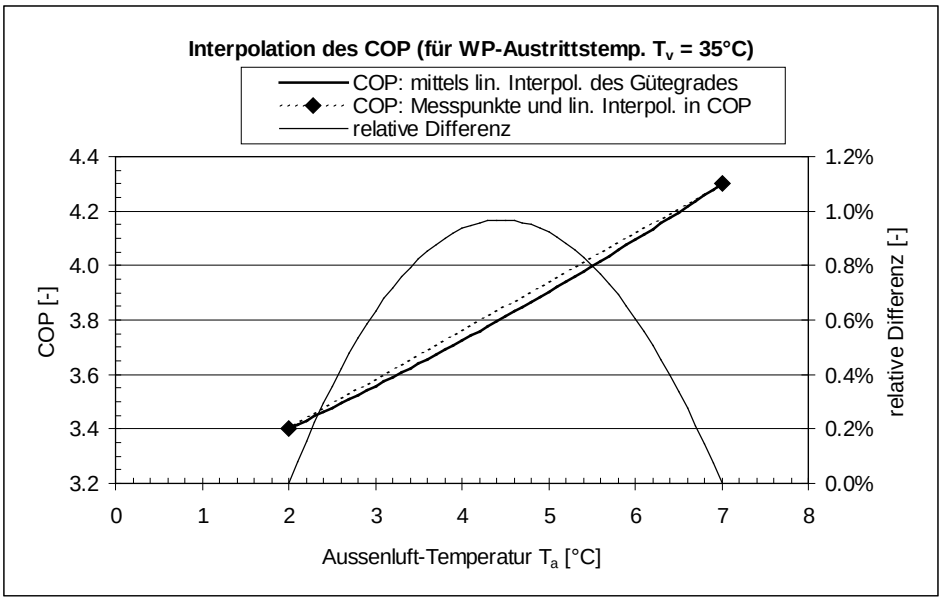

Figure 4: Calculation of the COP by using linear interpolation of the efficiency coefficient and comparison of the linear interpolation of the COP between the two measurement values. Additional, the relative difference between the two methods is depicted (Heat pump discharge temperature T_v=35°C).

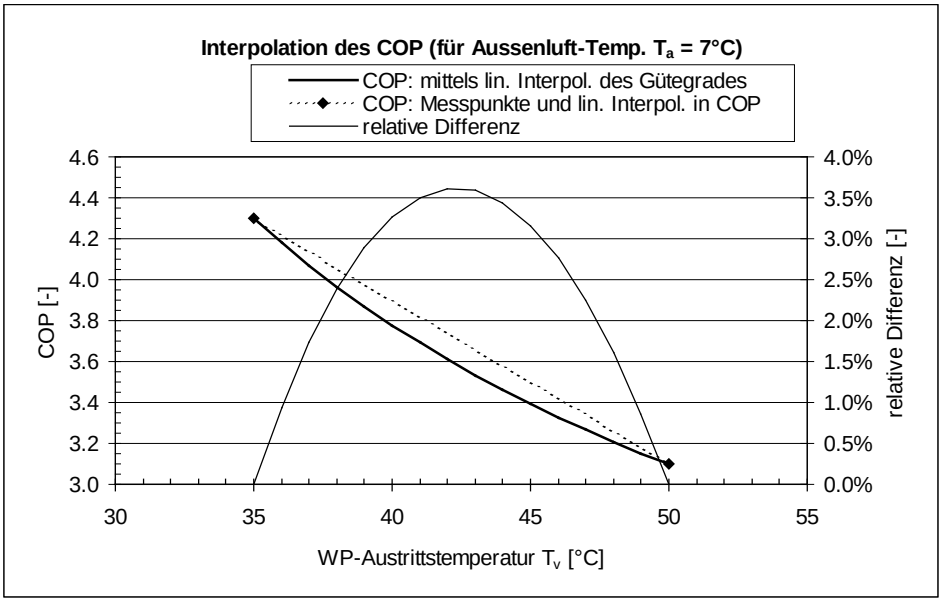

Figure 5: Calculation of the COP by using linear interpolation of the efficiency coefficient and comparison of the linear interpolation of the COP between the two measurement values. Additional, the relative difference between the two methods is depicted (Heat pump discharge temperature T_v=35°C).

Numerical model for water/water- and brine/water heat pumps

The HP-database in *Polysun* based on standardized measurements of the WPZ (Heat pump test facility) on brine/water- and water/water heat pumps. The majority of the current measurements are executed by using the old standard EN 255. Systems coming new on the market get tested by the actual standard EN 14511.

The heat pumps specified in the WPZ test report are tested as brine/water heat pumps, some of them additionally as water/water heat pumps. There are no heat pumps which are only tested as water/water- but not as brine/water heat pumps.

For brine/water heat pumps the duty points of the test measurement according to the old standard EN 255 are listed in Table 1, the ones according to the actual standard EN 14511 in Table 2.

For water/water heat pumps the duty points of the test measurement according to the old standard EN 255 are listed in Table 3, the ones according to the actual standard EN 14511 in Table 4.

measurement indicator / boundary condition	B-5/W35	B0/W35	B5/W35	B-5/W50	B0/W50	B5/W50
brine temp. T_s [°C]	-5	0	5	-5	0	5
HP-discharge temp. T_v [°C]	35	35	35	50	50	50

Table 1: Test points of the test measurement on brine/water heat pumps according to the old standard EN 255

measurement indicator / boundary condition	B0/W35	B5/W35	B-5/W45	B0/W45	B5/W45	B0/W55	B5/W55
brine temp. T_s [°C]	0	5	-5	0	5	0	5
HP- discharge temp. T_v [°C]	35	35	45	45	45	55	55

Table 2: Test points of the test measurement on brine/water heat pumps according to the actual standard EN 14511

measurement indicator / boundary condition	W10/W35	W15/W35	W10/W50	W15/W50
water temp. T_s [°C]	10	15	10	15
HP- discharge temp. T_v [°C]	35	35	50	50

Table 3: Test points of the test measurement on water/water heat pumps according to the old standard EN 255

measurement indicator / boundary condition	W10/W35	W10/W45	W15/W45	W10/W55	W15/W55
water temp. T_s [°C]	10	10	15	10	15
HP- discharge temp. T_v [°C]	35	45	45	55	55

Table 4: Test points of the test measurement on water/water heat pumps according to the actual standard EN 14511

At the indicated duty points the following measurement data is logged: *COP* (coefficient of performance), generated heating capacity $\dot{Q}_H$ and the electrical power consumption P_{el} of the heat pump. These measurements are executed by a constant volume flow of the brine and a constant temperature difference ΔT_{Nutzer} between the heat pump entry- and discharge temperature of the heating cycle fluid.

In the case of two step heat pumps the switching between the stages is detected in the WPZ measurement. The switch is detectable in the measurements due to the step in the generated heating capacity $\dot{Q}_H$ and the step in the electrical power consumption P_{el}. On the contrary, the COP is not affected.

As an example, in Figure 6 a typical COP-measurement according to the old standard EN 255 is and in Figure 7 a measurement of the electrical power consumption P_{el} is showed (both measurements for a one-step heat pump). The heat pump of this example is tested both as brine/water heat pump and water/water heat pump.

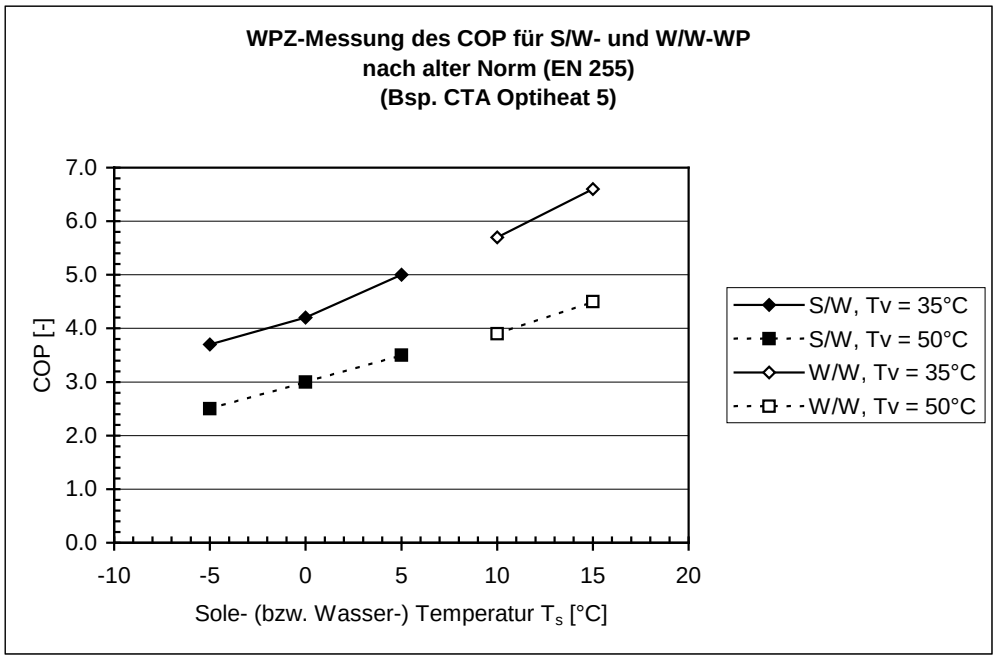

Figure 6: Example of a WPZ measurement of the COP of a heat pump, which is tested on brine/water (S/W) and water/water (W/W) service according to the old norm EN255 (Discharging temperature of the heat pump on the heat cycle T_v = 35°C und T_v = 50°C)

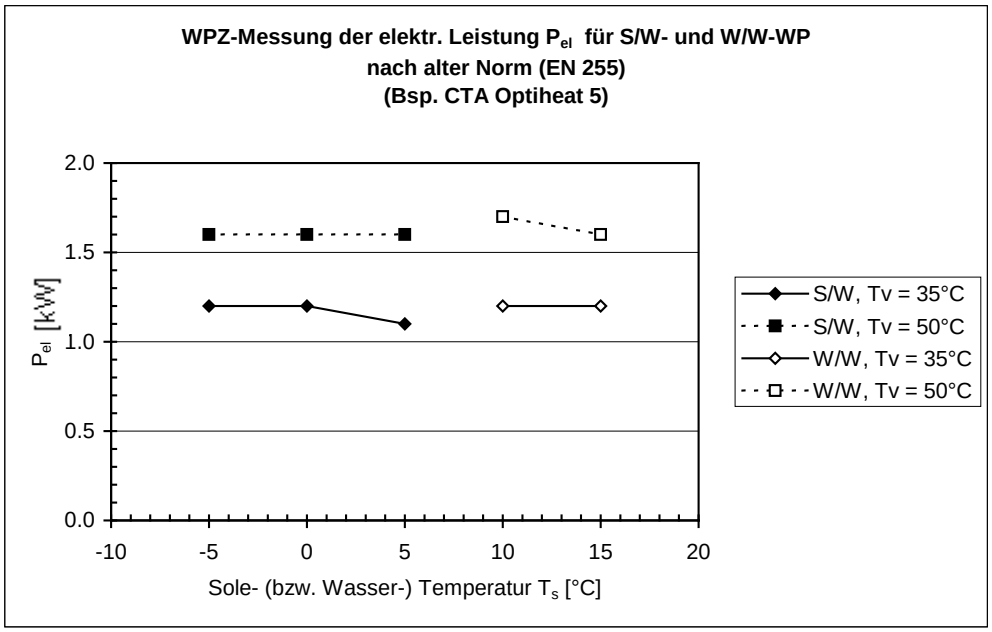

Figure 7: Example of a WPZ measurement of the electrical power consumption P_{el} of a heat pump, which is tested on brine/water (S/W) and water/water (W/W) service according to the old norm EN255 (Discharging temperature of the heat pump on the heat cycle T_v = 35°C und T_v = 50°C)

5. Modelling Literature

M. Vuolle, P. Sahlin: IDA Indoor Climate and Energy Application. EQUA Simulation Technology, http://www.equa.se.

Henning Schmidt, Integrierte Kopplung von Solarthermie und Wärmepumpe zur Wärmeerzeugung: Neues Konzept zur Wärmeerzeugung für Niedrigenergie-häuser, HLH Bd. 57, Heft 2, Februar 2006, S. 22 – 29.

Arthur Huber und Othmar Schuler: Berechnungsmodul für Erdwärmesonden.. Forschungsprojekt des Schweizerischen Bundesamtes für Energiewirtschaft (Schlussbericht). September 1997. Siehe auch http://www.hetag.ch → Referenzen → Forschungsprojekte: Erdwärmesonden

Arthur Huber und Daniel Pahud: Erweiterung des Programms EWS für Erdwärmesondenfelder. Forschungsprojekt des Schweizerischen Bundesamtes für Energiewirtschaft (Schlussbericht). Dezember 1999.

A5. Heatpump model of EFKOS

1. Abstract

The European Union's energy efficency strategy lead to a series of requirements for products which have a major impact on Europe's energy consumption. The implementation of this so called 'ErP' (Energy related products) or 'ecodesign' directive 2009/125/EG for heat pumps is based on standard EN 14825:2012, which defines a variety of conditions under which a heat pump shall be rated and how an expected seasonal performance of the unit shall be evaluated therewith. According to legal texts, it is allowed to calculate required input data from a few testing points available from well established EN 14511 rating measurements. In the EFKOS project, a possible calculation process how this can be done has been described. This process is based on a semi-empirical model which has been validated for an air-to-water heat-pump. As the model is mostly based on widely available data, it can be used to simulate many heat-pumps available on the european market. It is however a drawback of such an empirical model that it's based on steady state conditions, which is why complex behaviour like defrosting operation of air-to-water heat pumps cannot be implemented in a realistic manner. On the other hand, the model originally has been developed for the use in standard calculations. It's therefore a strength that results of such assessments and simulations can directly be compared. The following sections are referring to an electrically driven air-to-water heat-pump, while the actual model implementation in MATLAB Simulink simulation environment does not exclude water-to-water or brine-to-water units.

2. Basic assumptions and modelling

Available heat-pump data shows that there is no strong dependency between heating capacity and flow temperature, as long as conditions on the source side are kept identical. Table 1 shows exemplary data of an air-to-water heat-pump. As can be seen, heating capacity reduction of the unit is well below 5 % if flow temperatures increases from 35 ºC to 55 ºC.

Table 1: heating capacity vs. flow temperature of an air-to-water heat-pump. Data courtesy of Vaillant Deutschland GmbH & Co. KG (The unit does not necessarily correspond to a series production model).

		A-7	A2	A7	A12
W35	heating capacity	7.32	9.04	10.21	11.18
W55	heating capacity	7.05	8.78	9.98	10.98

This leads to the assumption, that a simple linear interpolation is more than accurate for the determination of heating capacity. Unfortunately, while rated data is based on outlet temperatures, usually return temperatures from the heating systems are given in a real-world application. This is important as today's heat-pump technology will lead to an over-temperature of the outlet when demand is low, that is at higher outdoor air-temperatures when heating capacity increases. To correctly model that effect, outlet temperature and heating capacity are calculated in an iterative process based on the given inlet temperature and massflow:

$$T_{sink,outlet} = T_{sink,inlet} + \frac{P_{heat}(T_{sink,outlet})}{\dot{m}_{sink} \cdot c}$$

Once sink and –given– source-temperatures are known, the COP can be found in a look-up table of rating points using linear interpolation for intermediate temperature values.

While this would already end up in fairly good results, it can be improved by taking some more care of the electric power consumption, which is much more influenced by outlet temperature (again considering equal source conditions). Comparisons between calculated an measured data show, that the improvement becomes evident especially at higher flow temperatures and low loads. Instead of simply looking up electrical power consumption, this value can be evaluated via a (linear) interpolation/extrapolation of the Carnot-efficiency η_{HP} from the nearest known values (and in fact, that's the way it is done in the EFKOS-model. For best results it's important to use rating data close to the operating limits):

$$P_{el} = \frac{P_{heat}}{COP_{carnot} \cdot \eta_{HP}}$$

The perfect (maximum) efficiency COP_{carnot} of a heat pump is discribed by carnot's law and is depending only on temperature levels of the cold and hot temperature reservoirs. The carnot process correspond's best to the refrigerant cycle of a real heat-pump, so temperatures at the refrigerant level are required. This introduces more values in the calculation process: Mean temperatures at the evaporator and condenser (that is both, inlet and outlet temperatures) and temperature drop across each of these heat exchangers. Using heating capacity, outlet temperature at the condenser, inlet temperature at the evaporator and corresponding flow rates as input values –given or calculated according to the section above– the temperatures at the refrigerant cycle can be calculated. Looking at the sink side:

$$T_{sink,refrigerant} = \frac{T_{sink,inlet} + T_{sink,outlet}}{2} - \Delta T_{cond}$$

While the mean temperature can easily be calculated, temperature drops which are depending on the actual heat-exchanger design are usually considered to be constant for the entire operating range. The model described here estimates actual temperature drop by assuming that this value is proportional to the power transmission at the actual operating point:

$$\Delta T_{cond} = \Delta T_{cond,rated} \cdot \frac{P_{heat,actual}}{P_{heat,rated}}$$

While shown here for the hot (sink) side of the heat-pump, the fourmulas above can be applied to the source side by just using corresponding values. Finally the carnot-COP at the actual operating point can be evaluated:

$$COP_{carnot} = \frac{T_{sink,refrigerant}}{T_{sink,refrigerant} - T_{source,refrigerant}}$$

Looking at the formulas above, it can be seen that another iteration process –at the cold side– is required to find outlet temperature and cooling capacity, which is implicitly required in the carnot COP calculation.

3. Implementation

The model has been implemented in MATLAB-Simulink environment and follows straightly the description from section 2. At each simulation time-step a few iterations are required (which could be defused by limiting the number of iterations as they add somewhat to the time-consumption of the whole simulation).

The following, essential parameters are required for the full description of a heat-pump in the EFKOS-model:

- Heating capacity (P_{heat}) and electrical power consumption (P_{el}) according to EN 14511:2011[4] at each rated point, evaluated for two different outlet temperatures (preferentially near the operation limits, e.g. at W35 and W 55).
- Temperature drop across the evaporator ($\Delta T_{evap,rated}$) and condenser ($\Delta T_{cond,rated}$) at specified source/sink temperatures
- Flow rates at sink ($\dot{m}_{sink}$) and source ($\dot{m}_{source}$) side according to EN 14511 rating conditions

A thermal capacity of the exchangers has been implemented to account for dynamic effects. Further, losses to the ambient are considered by a heat loss coefficient U_A. Both values are required, but can be set to zero for reasons of simpicity:

- Heat capacity of condenser (C_{cond}) and evaporator (C_{evap})
- Heat loss coefficient to ambient (U_A)

Input values that are required during runtime of the simulation are:

- Actual massflow at sink side
- Actual inlet temperature at sink side
- Actual massflow at source side
- Actual inlet temperature at sink side
- Ambient temperature at the place where the unit is installed

Figure 1 below shows some simulation outputs of the air-to-water heat-pump that has been used for validation of the model. The parameter $\Delta T_{cond,rated}$ was choosen to be 5 ºC (water sink) at A7/W35, while for the evaporator $\Delta T_{evap,rated}$ was assumed to be 10 ºC (air source) at A7/W35. While the simulation has been executed for different massflow rates on the sink side, all other input values except inlet temperature were kept constant. The picture shows the step response for a change of the inlet temperature (return from the heating system) fed to the heat-pump at t = 7200 s. As can be seen, COP and outlet temperature are both depending on actual massflow, as for 'real' heat-pumps. The depicted step in outlet temperature also shows the termal inertia simulated by a thermal capacity of some tens of kJ/K for both, evaporator and condenser.

[4] Of course, other rating points (e.g. according to 14511:2007) are also possible.

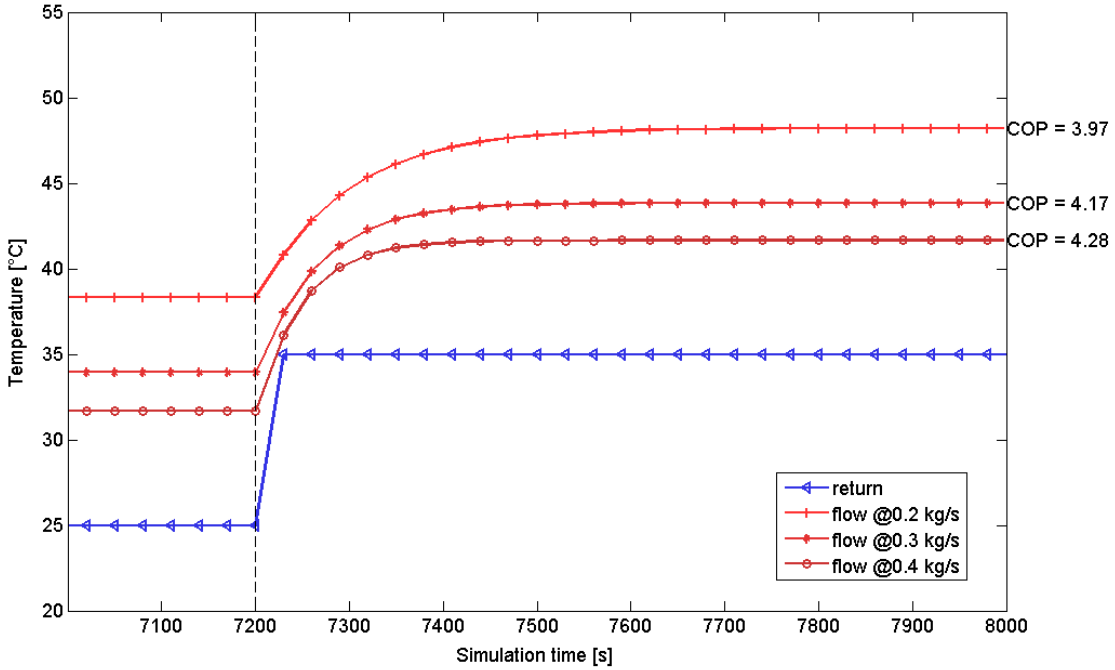

Figure 1: *Outlet temperature and COP for a given step of the inlet temperature (return). Dependency on massflow at A12 condition.*

4. Validation

For the validation process, EN 14511:2012 and EN 14825:2012 measurement data of an air-to-water heat-pump has been used (Table 2 and Table 3). Again, $\Delta T_{cond,rated}$ was choosen to be 5 °C while $\Delta T_{evap,rated}$ = 10 °C, both at A7/W35 rating conditions. Massflow at each measured operating point is know an has been set accordingly in the simulation.

Table 2: Comparison of measured and simulated performance data for average climate, low temperature application acc. EN 14825:2012 (0.5 kg/s massflow)

quantity	origin of data	unit	rating condition			
			A-7	A2	A7	A12
inlet temp.	measurement/ simulation	°C	30.6	27.8	25.7	23.5
outlet temp.	measurement	°C	34.0	32.1	30.5	28.8
outlet temp.	simulation	°C	34.1	32.1	30.6	28.9
heating capacity	measurement	kW	7.04	8.98	10.03	11.16
heating capacity	simulation	kW	7.34	9.08	10.26	11.24
el. Power	measurement	kW	2.35	2.28	2.11	2.01
el. Power	simulation	kW	2.36	2.29	2.09	1.98
COP	deviation from measurement	%	+3.7	+0.8	+3.6	+2.2

Table 3: Comparison of measured and simulated performance data for average climate, high temperature application acc. EN 14825:2012 (0.3 kg/s massflow)

quantity	origin of data	unit	rating condition			
			A-7	A2	A7	A12
inlet temp.	measurement/ simulation	°C	46.1	38.2	33.5	29.0
outlet temp.	measurement	°C	52	45.4	41.7	37.9
outlet temp.	simulation	°C	51.8	45,3	41.6	37.9
heating capacity	measurement	kW	7.24	8.99	10.3	11.25
heating capacity	simulation	kW	7.09	8.90	10.14	11.15
el. Power	measurement	kW	3.08	2.78	2.52	2.35
el. Power	simulation	kW	3.06	2.83	2.56	2.36
COP	deviation from measurement	%	-1.3	-2.9	-3.2	-1.5

The maximum deviation of the COP is below 4 %. Thus, the simulation shows good coincidence with measured values, especially when keeping in mind that measurement uncertainty according to EN 14511 is 6 % for COP and component tolerances may even be higher. The inclusion of power dependent temperature drop leads to somewhat better results at higher flow temperatures, but does show nearly no difference at low temperatures. Air-temperature drop at evaporator was assumed to be at a constant level of 5 K.

5. Modelling Literature

Genkinger, A., Jahresbericht EFKOS – Effizienz kombinierter Systeme mit Wärmepumpe, im Auftrag des BFE, Fachhochschule Nordwestschweiz FHNW, Muttenz, 2012, Schweiz

A6. Direct expansion solar assisted heat pumps

By Jorge Facão[1]

[1]LNEG

Address

Estrada do Paço do Lumiar, 22

Edifício H

1649-038 Lisboa

Portugal

Phone +351 210 924 600

Fax + 351 217 163 688

e-mail jorge.facao@lneg.pt

1. Nomenclature

A	aperture area of collector	m^2
b_0	constant for the calculation of the incident angle modifier	
b_u	collector efficient coefficient (wind dependence)	s/m
b_2	heat loss coefficient at (Te-Ta)=0	$W/(m^2K)$
c_2	collector efficiency coefficient	$Ws/(m^3K)$
E_L	long wave irradiance	W/m^2
G''	net irradiance	W/m^2
IAM	incident angle modifier	
$\dot{Q}_{evap}$	useful power extracted from evaporator collector	W
Q_{cond}	condensation power	W
$\dot{Q}_{cond}$	useful heat power in condenser	W
RH_a	relative humidity of air	
T_a	ambient air temperature	ºC
$T_{air,int}$	Indoor ambient temperature	ºC
T_c	refrigerant condenser temperature	ºC
T_{dp}	atmospheric dew point temperature	ºC
T_e	refrigerant evaporator temperature	ºC
$T_{air,int}$	Indoor ambient temperature	ºC
UA_{comp}	heat loss coefficient of the compressor	W/ºC
UA_{cond}	condenser heat transfer coefficient	W/ºC
u_{wind}	wind velocity	m/s
$\dot{W}$	compressor power consumption	W
β	tilted angle of the collector with respect to horizontal	degrees
σ	Stefan-Boltzmann constant	$W/(m^2K^4)$
ε_s	sky emissivity	
η_o	optical collector efficiency	
ν_a	humidity density of air	Kg/m^3
ν_{sat}	humidity density of saturated air	Kg/m^3
θ	angle of incidence	degrees

2. The model

In direct expansion solar assisted heat pump it is difficult to model dissociated the heat pump, evaporator and storage tank. The strategy adopted was to model the heat pump according the data provided by compressor manufacturer as a function of evaporating and condensing temperature. The evaporator was model as an uncovered solar collector and the storage tank with a help of TRNSYS Type for stratified tanks. Since the system was tested without intrusive measurements the evaporator and condenser temperature are unknowns, as well as refrigerant mass flow rate. The model of the global system simulates the evaporating and condensing temperature and calculates the useful heat flux. The model is according Morrison work [1].

Heat pump model

The work power absorbed by the compressor and the useful heat liberated in the condenser heat pump is a function of evaporator and condenser temperature, and available from compressor manufacturer data.

The curves from the manufacturer were fitted by second order polynomial regarding evaporator temperature and first order regarding condenser temperature.

$$\dot{Q}_{cond} = a + bT_e + cT_e{}^2 + dT_c + eT_eT_c + fT_e{}^2T_c \quad (1)$$

$$\dot{W}_{comp} = a_1 + b_1T_e + c_1T_e{}^2 + d_1T_c + e_1T_eT_c + f_1T_e{}^2T_c \quad (2)$$

The Energie system in analysis at LNEG uses a rotary compressor from Hitachi Higly, model WHP 01900 BSV. Table 1 presents the fitted polynomial constants for the compressor in analysis

Table 4 Polynomial fitting constants for the compressor.

a	1908,166	a_1	180,3259
b	63,21951	b_1	-4,99102
c	1,611799	c_1	-0,20506
d	-8,45291	d_1	4,891113
e	-0,29195	e_1	0,151518
f	-0,01848	f_1	0,002042

Collector model

The heat pump evaporator was simulated as an uncovered solar collector but with an influence of condensation when its temperature is below the dew point temperature.

The heat flux received by the evaporator was calculated by the equation 3.

$$\dot{Q}_{evap} = Q_{cond} + G^{"}A\eta_o(1 - b_u u_{vento})MAI - A[(b_2 + c_2u_{vento})(T_e - T_a)] \quad (3)$$

For the incidence angle modifier (IAM) equation 4 was considered.

$$\begin{aligned} MAI &= 1 - b_0\left(\frac{1}{cos\theta} - 1\right) && se\ \theta \leq 60 \\ MAI &= 0 && se\ \theta > 60 \end{aligned} \quad (4)$$

The condensation effect was introduced when the evaporator temperature was below dew point temperature [2].

$$\begin{aligned} Q_{cond} &= A1{,}7E3(2{,}8 + 3u_{vento})\left(v_a - v_{sat}(T_e)\right) && se\ T_e \leq T_{dp} \\ Q_{cond} &= 0 && se\ T_e > T_{dp} \end{aligned} \quad (5)$$

Where $v_a = v_{sat}(T_a).\mathrm{HR}_a$ and

$$v_{sat}(T) = 0{,}001(4{,}85 + 0{,}347T + 0{,}00945T^2 + 0{,}000158T^3 + 0{,}00000281T^4) \quad (6)$$

The net irradiance takes into account the relative long wave irradiance.

$$G^{"} = G + 0{,}85(E_L - \sigma(T_a + 273{,}15)^4) \quad (7)$$

$$E_L = \varepsilon_s \sigma (T_a + 273{,}15)^4 \frac{1+cos\beta}{2} \quad (8)$$

The sky emissivity can be quantified in terms of atmospheric dew point temperature

$$\varepsilon_s = 0{,}711 + 0{,}56\frac{T_{dp}}{100} + 0{,}73\left(\frac{T_{dp}}{100}\right)^2 \quad (9)$$

Tank model

To simulate the storage tank a modified type 4 was adopted with 11 nodes with the thermostat in node 10 and the heat exchanger in node 11. The heat loss coefficient was a function of storage tank ambient temperature.

The heat in condenser inside the storage tank is also a function of the global heat transfer coefficient and the temperature differential between the refrigerant temperature and water temperature in the storage tank.

$$\dot{Q}_{cond} = UA_{cond}(T_c - T_{water}) \quad (10)$$

Closure equation

The first law of thermodynamics applied of the system gives the following energy balance.

$$\dot{Q}_{cond} = \dot{W}_{comp} + \dot{Q}_{evap} - UA_{comp}(T_c - T_{air,int}) \quad (11)$$

For system simulation and considering the last equation we have to solve a system of non-linear equations. The unknown variables are: $\dot{Q}_{cond}$, $\dot{W}_{comp}$, $\dot{Q}_{evap}$, T_c e T_e. A Type developed in FORTRAN for TRNSYS [3] environment was developed. The type solves the system of non-linear equations by Newton-Raphson method with sub-relaxation factors. Figure 1 presents the flowchart of the new Type.

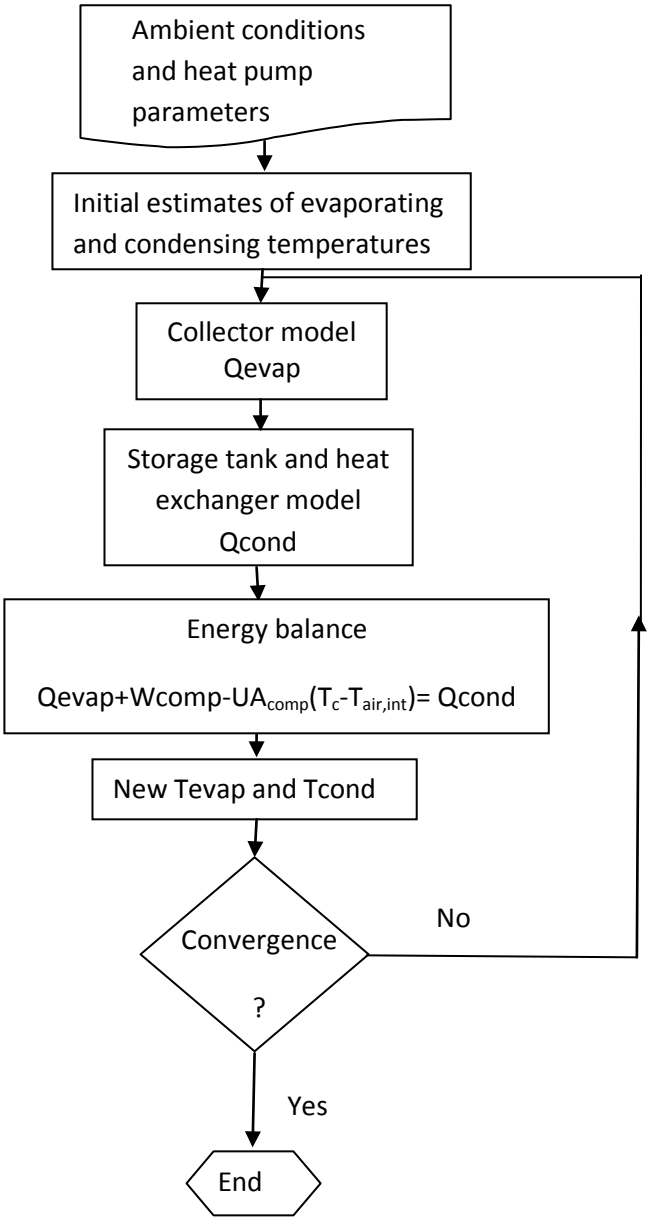

Figure 7 Procedure flowchart adopted.

3. Bibliography

[1] G. L. Morrison, Simulation of Packaged solar Heat-Pump Water Heaters, Solar Energy, Vol. 53, No. 3, pp. 249-257, 1994.

[2] B. Perers, An improved dynamic solar collector model including condensation and asymmetric incidence angle modifiers, Eurosun 2010, Graz.

[3] TRNSYS, A Transient Simulation Program. User's Manual, Version 16, Solar Energy Laboratory, University of Wisconsin-Madison, 2005.

A7. Calculation of primary energy and seasonal performance factor of heat pumps in Passive Houses.

Georgios Dermentzis, Fabian Ochs, Wolfgang Feist

Innsbruck 2012

1. Introduction

The increasing number of heat pumps worldwide and especially their widespread applications in Passive Houses created the requirement for a calculation tool that allows predicting the annual electrical energy consumption and the seasonal performance factor (SPF) of heat pumps with high accuracy. Until now, calculation tools such as JAZcalc (or WPesti) [1], SIA 384/3 [2] and VDI 4650 [3] are available. Their applicability is restricted e.g. due to limited availability of climates and/or because of non-satisfying accuracy (compare section 0).

The new algorithm is based on the algorithm of 'Compact' sheet [4] for so called compact units (heat pump and ventilation with heat recovery in one device), which is already available in Passive House Planning Package (since PHPP 2004). The goal of the new heat pump tool is the achievement of high accuracy and the improvement of flexibility with regard to heat pump sources (air, water, brine), sinks (air heating, radiators, floor heating), functionality (heating, domestic hot water, both), heating distribution system (air heating, floor heating, radiators), store options and control strategies.

2. PHPP 'Compact' sheet

PHPP is a calculation tool, implemented in Excel, which yields a building's heating, cooling and primary energy demand. The compact units consist of a heat pump and an air-to-air heat exchanger with heat recovery (mechanical ventilation system). The heat pump covers both the heating and hot water demand. The heat pump uses exhaust air as source and delivers heat for heating and domestic hot water at the same temperature level i.e. 55 °C. The heat is distributed to the building through the supplied air of the ventilation system. The 'compact' algorithm is a bin method in which the heating period (winter) is divided in two bins (time periods) and the non-heating period (summer) in one bin (see Figure 8). In each bin the demand for heating and domestic hot water and the mean Coefficient of Performance (COP) of the heat pump are calculated. The division of these two quantities gives the electrical energy consumption of the heat pump (W_{el_hp}). The total electrical energy consumption (W_{el}) is the sum of all bins plus the direct electrical energy.

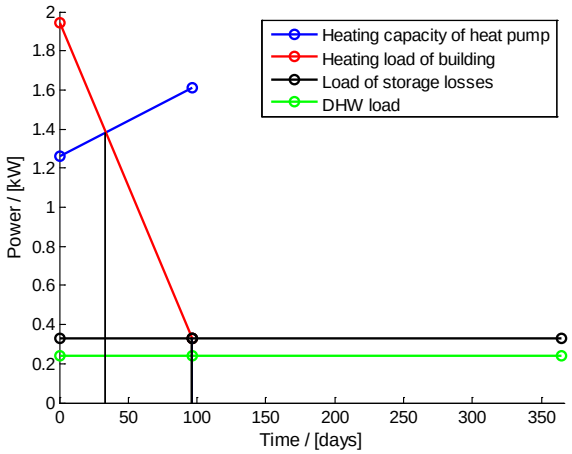

Figure 8: PHPP 'Compact' sheet [4].

3. Tool options

The new heat pump tool gives a range of additional opportunities, which are the followings:

- ✓ Several heat pump sources, such as ambient air, ground water, vertical or horizontal ground heat exchanger (GHX) can be chosen.
- ✓ Functionality options: The heat pump can cover either the heating demand or the domestic hot water (DHW) demand or both of them.
- ✓ Several heating distribution systems, such as radiators, floor heating and air heating are available.
- ✓ The possibility of two heat pumps in one building: One covering the heating demand and the other the domestic hot water demand.
- ✓ Two control systems: The first is the common 'on/off' and the second the 'ideal' control system (it yields the minimum possible electrical consumption).
- ✓ Variety of store options, e.g. same store for heating and DHW demand or two stores or heating distribution system without store. Furthermore, there is an option about the location of each store (inside or outside of the thermal envelope), since the store losses are gains in the heating period when the store is inside of the thermal envelope.
- ✓ Improvement of solar thermal, combined with a heat pump, for covering heating or domestic hot water demand.

4. Methodology

The method of the new heat pump tool is based on the method of 'compact' sheet. In the new algorithm more bins are implemented in order to improve the accuracy. The annual electrical energy consumption of the system is:

$$W_{el} = \sum W_{el\_hp}(bin) + W_{dir} \qquad (1)$$

Where W_{dir} is the direct electricity demand (Q_{dir}) in Figure 2(b).

Energy supplied by the heat pump (Q_{hp})

The heating capacity of the heat pump and the heating load of the building are assumed to be linear, as shown in Figure 9(a). The energy supplied by the heat pump (Q_{hp}) depends on the heating capacity of the heat pump and on the heating load of the building (Figure 2(b)).

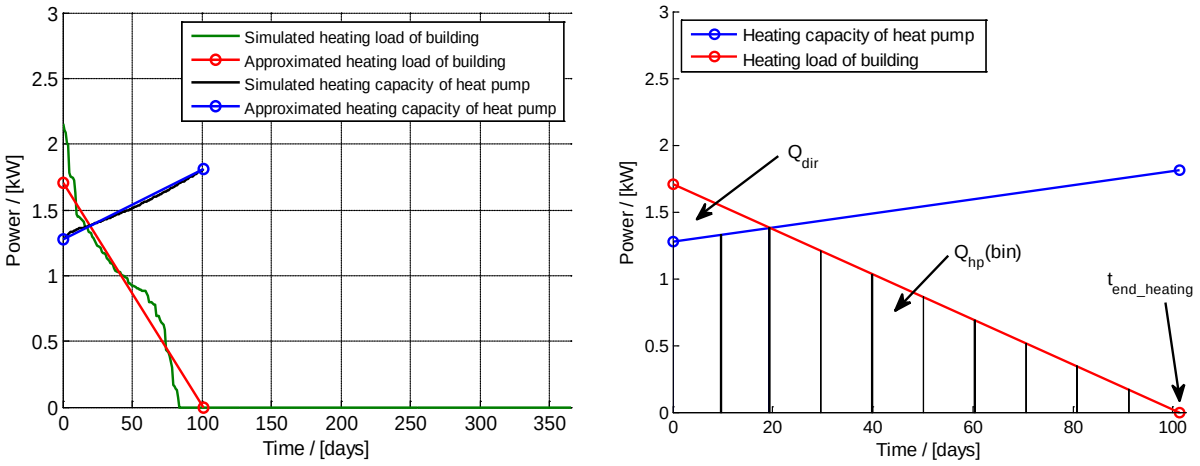

(a) (b)

Figure 9: Example of a family house in Passive House standard in Innsbruck. a) Simulated and approximated load duration curve and heating capacity of the heat pump [4]. b): Load duration curve and heating capacity of the heat pump in heating period.

Heating load line of the building

The duration of the heating period (Figure 2(b)) is calculated by the maximum heating load (P_{H_max}, 'Heating Load' sheet) for time equal to zero and by the area of the triangle (created by the red line) corresponding to the heating demand (Q_{HD}, 'Monthly Method' sheet):

$$t_{end\_heating} = 2 \cdot \frac{Q_{HD}}{P_{H\_max}} \quad (2)$$

Heating capacity of the heat pump (Php)

The heating capacity depends on the source temperature and the sink temperature of the heat pump. The correlation between these three quantities is defined by linear approximation using equation (3).

$$P_{hp} = a_1 \cdot \theta_{src} + a_2 \cdot \theta_{snk} + a_3 \quad (3)$$

Coefficient of performance (COP)

The COP significantly depends on the source temperature and the sink temperature of the heat pump. The Carnot efficiency can be applied to account for that:

$$COP = \eta_{ind} \cdot \frac{\theta_{snk} + 273.15}{\theta_{snk} - \theta_{src}} \quad (4)$$

The Carnot performance factor η_{ind} in equation (4) is calculated using the input measured test points (e.g. from [6]). The value of source temperature (ϑ_{src}) is limited to the maximum value of 20°C to account for more realistic behavior.

5. Validation

The validation of the new heat pump tool has been performed for four different systems using several sink temperatures (Table 5) and several heat pumps (data from [6]). The sink temperatures correspond to the appropriate heating distribution system. The selected sink temperature (ϑ_{snk}) is 24, 28 or 35 °C for floor heating, 40 °C for radiators and 55 °C for air heating. The validation models are presented in Table 6. The reference building (SFH15 from [5]) is adapted to 15 kWh/(m^2·a) heating demand in Innsbruck climate. For the validation the calculation results are compared with the results of other calculation tools (namely JAZcalc) and of simulation tools such as Delphi [7] with daily input data and Matlab/Simulink using the Carnot blockset [8] with hourly input data (Table 5).

Table 5: Systems for validation

Case	Functionality	Monovalent / bivalent	ϑ_{snk} [°C]	
			Heating	DHW
1	Heating	Monovalent	[24 28 35 40 55]	-
2	DHW	Monovalent	-	[45 50 55 60]
3	Heating & DHW	Monovalent	[28 35 40 55]	[55]
4	Heating & DHW	Bivalent	[28 35 40 55]	[55]

Table 6: Models/methods

Name in figures	Program platform	Method	Control strategy
PHPP on/off	Excel	Calculation	on/off
PHPP ideal	Excel	Calculation	ideal
JAZcalc	Excel	Calculation	on/off
Delphi	Delphi	Simulation with daily input data (PHI)	on/off
Simulink	Matlab / Simulink Carnot Blockset	Simulation with hourly input data	on/off

Air-sourced heat pumps

In Figure 10, the case 3 is shown for one of the several heat pumps. The electrical annual consumption of the system is plotted versus the sink temperature. The agreement between 'Simulink' and 'PHPP on/off' is quite good. The other two methods are too optimistic. Their resulting consumption is the range of that of the 'PHPP ideal'.

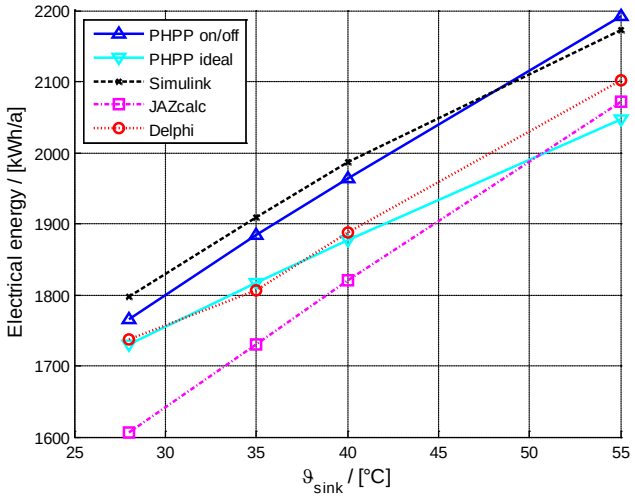

Figure 10: Electrical energy consumption of an air-sourced heat pump for heating and DHW demand (case 3). Example of a family house (SFH15) in Passive House standard in Innsbruck.

Heat pumps with ground heat exchanger (GHX)

The validation of heat pumps with GHX has been performed for the same conditions and cases. The depth of ground heat exchanger is 1m. The results for the case 4 are presented in Figure 11. With the exception of 'Delphi' which is too optimistic, all methods deliver almost the same results.

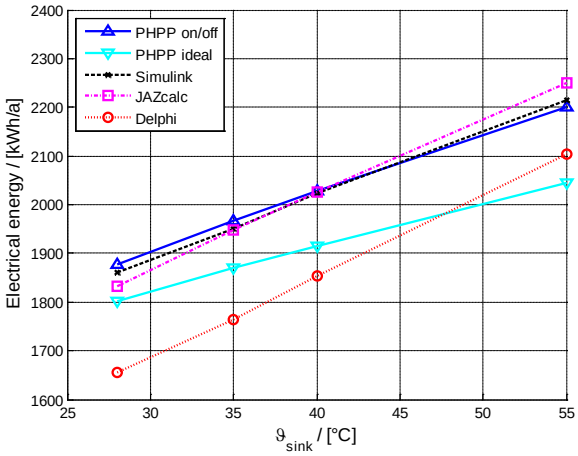

Figure 11: Electrical energy consumption of bivalent system for heating and DHW demand (case 4). Example of a family house (SFH15) in Passive House standard in Innsbruck

6. Conclusion

In conclusion, this new calculation tool for heat pumps gives the opportunity to the user of PHPP to calculate the annual primary energy demand and the SPF of several heat pump systems with little effort. An example of four heat pump systems with different sources is shown in table 3 and in Figure 12.

Table 3: Example of a family house in Passive House standard in Hamburg.

Variables	Heat pump source			
	Air	Ground water (GW)	Vertical ground heat exchanger (VGHX)	Horizontal ground heat exchanger (HGHX)
z / [m]	(-)	5	30	1
λ / [W/mK]	(-)	(-)	2	2
COP	3.9 (2/35)	5.2 (10/35)	3.8 (0/35)	3.8 (0/35)
SPF / [-]	2.31	2.63	2.42	2.38
W_{el} /[kWh/a]	923	811	883	897
$q_{specific}$ (1800h)			23.9 (W/m)	22.8 (W/m2)

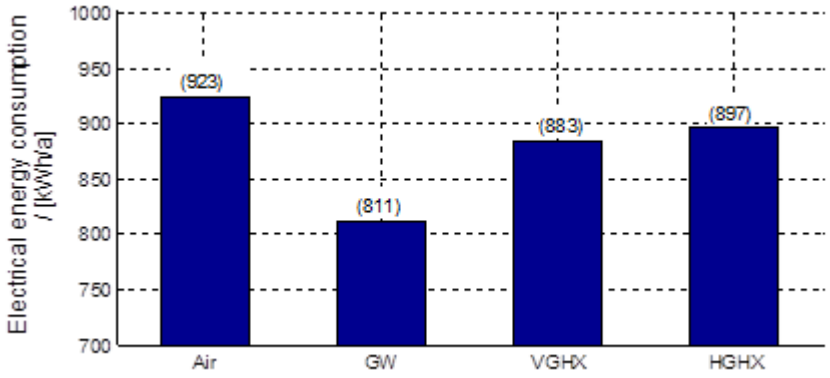

Figure 12: Electrical energy consumption of different heat pumps covering the heating demand (case 1/Table 1) with radiators (in 55 °C). Example of a family house in Passive House standard in Hamburg.

The comparison of the tool with simulations shows a good accuracy. Moreover, the additional incorporation of the 'ideal' control strategy, gives the opportunity to predict the minimum possible electrical energy demand. As the method for the vertical GHX is a steady state calculation, the results are conservative. The validation of solar thermal algorithm is still to be done. Future work should also address improving the accuracy of the climate data curve with regard to the air-sourced heat pumps. Furthermore, more types (geometries) of GHX may be implemented as well as cooling and solar heating.

7. Literature

[1] Energieinstitut Vorarlberg, Modellbeschreib Tool JAZcalc V63, www.guetesiegel-erdwaerme.at

[2] SIA384/3, http://www.sia.ch

[3] Verein Deutscher Ingenieure (VDI),Gebäude Energie Berater, Programm zur Berechnung der JAZ nach VDI 4650, http://www.gebinfo.de/QUlEPTI0Mzc4NiZNSUQ9MzAwMDEmVElYPS0x.html, 2009

[4] Rainer Pfluger, Berechnung des primärenergiekennwertes und der Jahresarbeitszahl aus den Messwerten der Laborprüfung für die Zertifizierung von Passivhaus-Kompaktgeräten, PHI, State 19.1.2007, internal document, Jan. 2007

[5] IEA SHC Task 44/HPP Annex 38 Solar and heat pumps, International Agency, http://www.iea-shc.org/task44/

[6] Wärmepumpen-Testzentrum WPZ, http://institute.ntb.ch/ies/competences/ heat-pump-test-center-wpz.html?L=1 , WPZ 2011

[7] Rainer Pfluger, Berechnungsalgorithmus zu Beitrag "Möglichkeiten und Potentiale unterschiedlicher Wärmequellen und Wärmesenken für Wärmepumpen und Kompaktgeräte" in Protokollband Nr. 26 des Arbeitskreises kosten günstige Passivhäuser, Phase III, Passivhaus Institut, Darmstadt 2004.

[8] Matlab simulink Carnot blockset, http://www.mathworks.com/

[9] Georgios Dermentzis, Fabian Ochs, Wolfgang Feist, Internal Report, PHPP Heat Pump Model, PHI, Darmstadt 2012.

Greek Symbols	
η_{ind}	Carnot performance factor
θ_{snk}	Sink temperature of the heat pump
θ_{src}	Source temperature of the heat pump
λ	Thermal conductivity of the ground
Latin symbols	
a_1, a_2, a_3	Coefficients for the approximation of heating capacity equation (3)
COP	Coefficient of Performance
DHW	Domestic hot water
GHX	Ground heat exchanger
P_{H_max}	Heating load of the building
P_{hp}	Heating capacity of a heat pump
Q_{dir}	Required direct electricity (Figure 2b)
Q_{HD}	Heating demand of the building
Q_{hp}	Heating energy supplied by the heat pump
SPF	Seasonal Performance Factor
$t_{end,heating}$	Duration of heating period
W_{dir}	Demand covered by direct electricity
W_{el}	Electrical energy consumption of the system
W_{el_hp}	Electrical energy consumption of the heat pump
z	Depth

A8. Investigation of the steady-state and transient behaviour of a ground source heat pump including model validation

Date: 19/04/2013
Author: Peter Pärisch

1. Abstract

The operation of ground coupled heat pumps in combination with solar collectors requires comprising knowledge of the component behaviour under non-nominal conditions. Especially higher source and lower sink temperatures, varying flow rates, material characteristics and sophisticated control strategies have to be taken into account.

Therefore stationary and dynamic tests of a typical brine/water heat pump have been carried out in order to analyse the behaviour under varying conditions. In details the heat pump efficiency depending on temperature and flow rate has been investigated. High source temperatures especially with low sink temperatures lead to a strong decrease in the exergetic efficiency which reduces the expected improvement of the COP significantly. And this effect depends strongly on the temperature difference between sink and source (temperature lift). The lower the temperature lift the stronger the drop in the exergetic efficiency. Varying flow rate only has an influence on temperature boundary conditions not on heat transfer coefficient. For simulations of systems with solar ground regeneration the polynomial coefficients of the YUM-model (TRNSYS type 401 (Afjei and Wetter 1997) must be determined by a sufficient data basis, which includes data on the source side up to 30 °C. The model algorithm based on these coefficients works accurately for the mass flow rate of the data basis but it is not applicable for other flow rates. For this purpose, e. g. the correction method from (Pahud and Lachal 2004) can be used and gives reasonable results. Based on this method the relative error in COP decreases from 5 % to about 2 %.

The measured start-up time constant of the heat pump is in the range of 10 to 20 s which is far quicker than the default value of 180 s of Type 401. By using the measured value instead of the default value the seasonal performance factor of the whole system improves from 3 to 4. Unfortunately this important parameter cannot be derived from manufacturer data as it is not integrated into the standard.

2. Introduction

The combination of solar thermal collectors with ground-coupled heat pump systems offers the possibility to reduce the annual electricity demand (e. g. (Bertram et al. 2011), (Tepe et al. 2003)) and to avoid uncertainties in the planning process (Bertram et al. 2008). However, the solar collector can be connected to the system in several ways: directly to the space heating system or the DHW preparation, to the heat source or to the evaporator of the heat pump. For each option different restrictions for the flow rates, operation temperatures and control strategies have to be taken into account.

In order to analyse these effects several tests have been carried out at the variable test facility for heat pumps and borehole heat exchangers at the ISFH (see (Pärisch et al. 2011) for further information). This test rig has been built up within the joint project Geo-Solar-WP

focusing on “High-efficient heat pump systems with geothermal and solar thermal energy sources” that is funded by the European Union and the Federal State of Lower Saxony.

In addition, the experiments will be supported by TRNSYS simulations. First of all, these simulations shall replicate the test itself. Secondly, they are used to analyse the performance of different simulation models and, third, thus allow studying the behaviour of different system combinations, like in (Bertram et al. 2012).

3. Heat pumps in combined solar and geothermal systems

Solar heat injection can either be realised on the source or the sink side of the heat pump. In both cases the operating temperatures of the heat pump will be influenced. By delivering heat to the source side the evaporator temperature will be increased, which has a positive effect on the heat pump efficiency. On the other hand heat delivered directly to the sink side avoids heat pump running time and can affect the average condenser temperature in both directions. For example, a solar DHW-system avoids heat pump running time for DHW preparation and thus will reduce the mean condenser temperature if the heating system operates on lower temperature levels.

3.1 Sensitivity of heat pump efficiency concerning flow and temperature variations

A brine/water heat pump (7.8 kW at B0W35) with thermostatic expansion valve has been measured in the test system with different flow rates and inlet and outlet temperatures. The hydraulic scheme including the measured values is shown in Fig. 1. The heat pump is connected to computer controlled hydraulic modules that regulate constant temperatures, constant heat flow rates and constant mass flow rates as well.

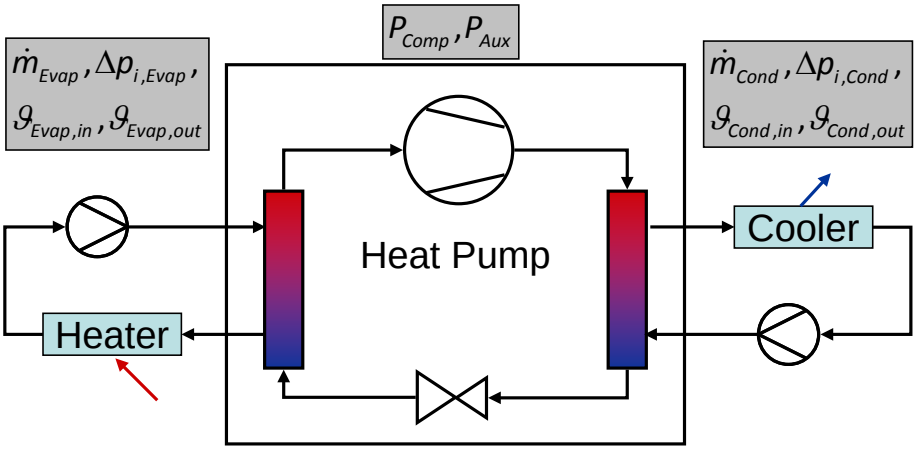

Fig. 1 Hydraulic scheme of the test system and measured values

Unlike the requirements in the European Standard DIN EN 14511-3:2012 the steady-state values are measured all with nominal flow rates and kept stable for 25 to 30 minutes. The standard deviations of the single temperature values of the sliding average during the steady-state are below 0.2 K. The realised uncertainties of the measurements can be seen in Table 7 in comparison to the standards values. The uncertainties of the pressure drops have a negligible influence on the uncertainty of the COP. The test equipment is leading to uncertainties of the COP value between 2 % and 4 %.

Table 7: Required and realised uncertainties of measurement [6]

Measured value	ISFH	DIN EN 14511-3
Heat flux	- (here 0.44-1.47 %)	5 %
Compressor power	0.04 kW (here 1.87-3.66 %)	1 %
COP	- (here 1.96-3.96 %)	-
Temperatures	0.064 K	0.15 K
Mass flow rate source	0.1 %	1 %
Mass flow rate sink	0.2 %	1 %
Concentration Brine	1.6 %	2 %
Pressure drop evaporator	(here ≈37,1 %)	5 %
Pressure drop condenser	(here ≈16,5 %)	5 %

The tests have been conducted for three different **condenser inlet temperatures** (45 °C, 35 °C and 25 °C) and eight different evaporator inlet temperatures (-5 °C to 30 °C in 5 K-steps).

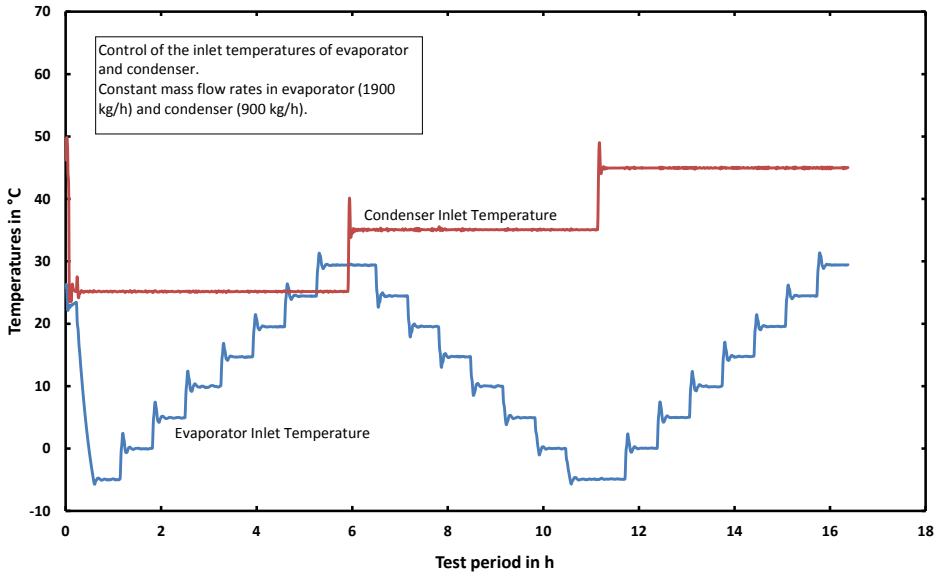

Fig. 2: Temperatures during a test sequence for the determination of the heat pump characteristics

The coefficient of performance COP for heat pumps for space heating without integrated circulation pumps follows from Eq. 1 according to DIN EN 14511-3:2012. The standard aims at making the heat pumps comparable. Therefore internal circulation pumps are added, if not

yet integrated, that only overcome the internal pressure drop Δp_i. The indices „Cond“, „Evap“, „Comp“ and „Aux“ stand for condenser, evaporator, compressor and controller.

$$COP = \frac{\dot{Q}_{Cond} + \frac{\Delta p_{i,Cond} \cdot V_{Cond}}{\eta_{P,Cond}}}{P_{Comp} + P_{Aux} + \frac{\Delta p_{i,Evao} \cdot V_{Evao}}{\eta_{P,Evap}} + \frac{\Delta p_{i,Cond} \cdot V_{Cond}}{\eta_{P,Cond}}} \quad \text{Eq. 1}$$

η_P is the efficiency of the circulation pumps for sink and source side that is calculated according to the latest version of DIN EN 14511-3:2012 depending on the hydraulic power of the circulation pumps P_{hydr} (in W):

$$\eta_P = 0{,}0721 \cdot P_{hydr}^{0{,}3183} \quad \text{Eq. 2}$$

Measured COP values according to Eq. 1 with its standard uncertainties are shown in Fig. 3 for different test conditions. The standard uncertainties of the COP lie between 2 and 4 %. It is obvious that the heat pump efficiency is better for higher source temperatures and lower sink temperatures which are both influenced by solar heat injection (no. 1 and 2 in Fig. 3).

1. Solar heat injection to the source side leads to higher evaporator temperatures and thereby has a positive effect on the efficiency of the heat pump. Furthermore, the heat source benefits indirectly from solar heat supply to the sink side due to less heat extraction from the ground.
2. However solar heat injection to the condenser side can affect the mean condenser temperature in both directions. A solar preheating of the return temperature of the heating system leads to higher inlet temperatures into the condenser and thereby to decreased COP-values. On the other hand the mean condenser inlet temperature will decrease if e. g. a significant part of the DHW-demand is covered by a solar collector and furthermore the temperature of the heat distribution system is below the mean temperature level for DHW preparation. Thus the operation conditions for the heat pump are improved and better COP-values will be reached.

It has to be stated that these considerations mainly focus on the COP or the seasonal performance factor of the heat pump (SPF_{HP}) itself. The effect on the SPF of the complete heating system (SPF_{SHP}) may be different.

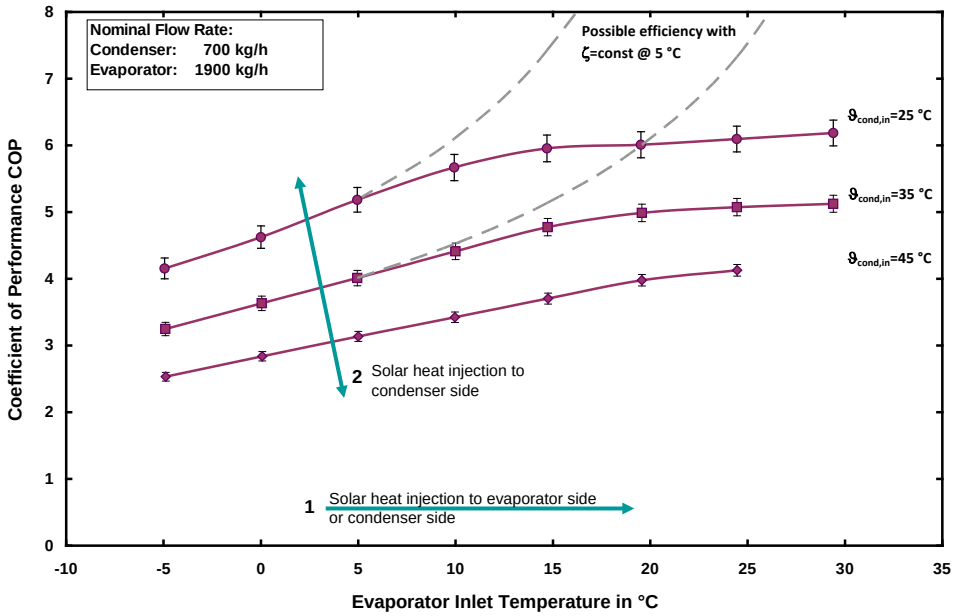

Fig. 3: Coefficient of performance at nominal mass flow rates for three different mean condenser temperatures over the evaporator inlet temperature and theoretic COP if exergetic efficiency ζ is assumed to be constant (e. g. @ 5 °C)

Furthermore Fig. 3 shows the expected COP if the quality grade or exergetic efficiency ζ (see (Baehr and Kabelac 2009) is assumed to be constant (here based on the values of 5 °C source temperature). The deviation between real and theoretic COP becomes huge for higher source temperatures which is obvious due to the design of the heat pump for typical operation conditions. However, the effect is contrary to the basic idea to improve the system performance by higher source temperatures.

3.2 Flow dependency of heat pump efficiency

Characteristic curves for different mass flow rates on source or sink side are shown in Fig. 4. The flow rate variation of the evaporator is presented in the right diagram and of the condenser side in the left diagram. The shift of the curves for the mass flow rate variation is caused by two effects, both influencing the heat transfer coefficient and the temperature levels of the inlet and outlet flows.

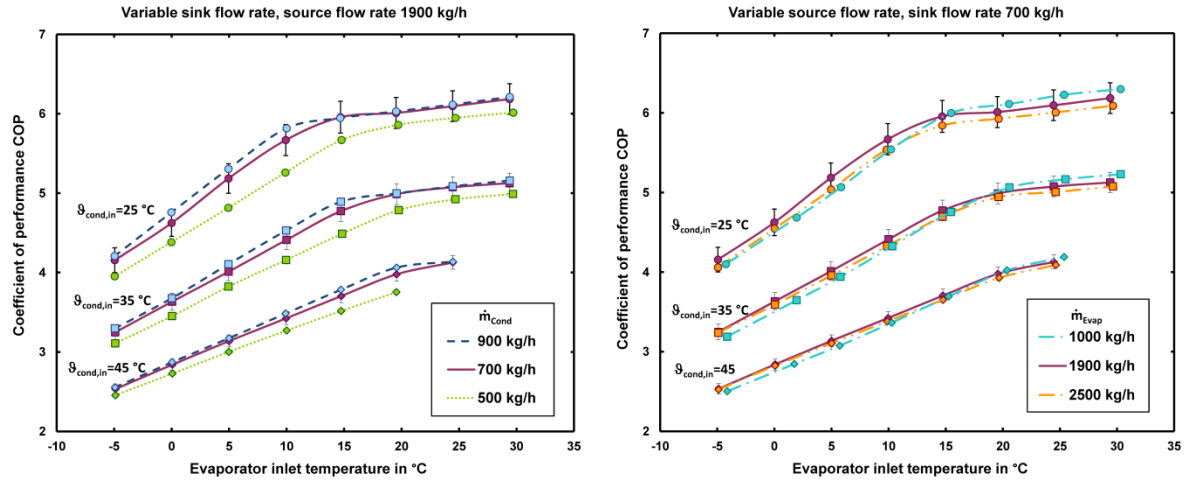

Fig. 4: Coefficient of performance at nominal mass flow rate in the evaporator over varying evaporator inlet temperatures for three different condenser flow rates and mean condenser temperatures

In order to divide between the two effects the exergetic efficiency ζ is calculated by dividing the COP by the maximum possible COP.

$$\zeta = \frac{COP}{COP_{\max}} \qquad \text{Eq. 3}$$

The maximum possible COP for Carnot cyclic processes follows from:

$$COP_{\max} = \frac{T_{Cond,m}}{T_{Cond,m} - T_{Evap,m}} \qquad \text{Eq. 4}$$

Here the thermodynamic mean temperature T_m after (Baehr and Kabelac 2009) for evaporator and condenser is used. Eq. 5 shows for example the thermodynamic mean temperature of the condenser.

$$T_{Cond,m} = \frac{T_{Cond,out} - T_{Cond,in}}{\ln\left(\frac{T_{Cond,out}}{T_{Cond,in}}\right)} \qquad \text{Eq. 5}$$

The exergetic efficiency allows eliminating the effect of the temperature difference. Thus the curves in Fig. 5 show that the effect of different flow rates on the exergetic efficiency is small. And this is independent whether the hydraulic power of the pressure drop Δp_i is considered or not. Hence, the heat pump efficiency is mainly depending on the temperature levels for the inlet and outlet flows, which are determined by the different flow rates.

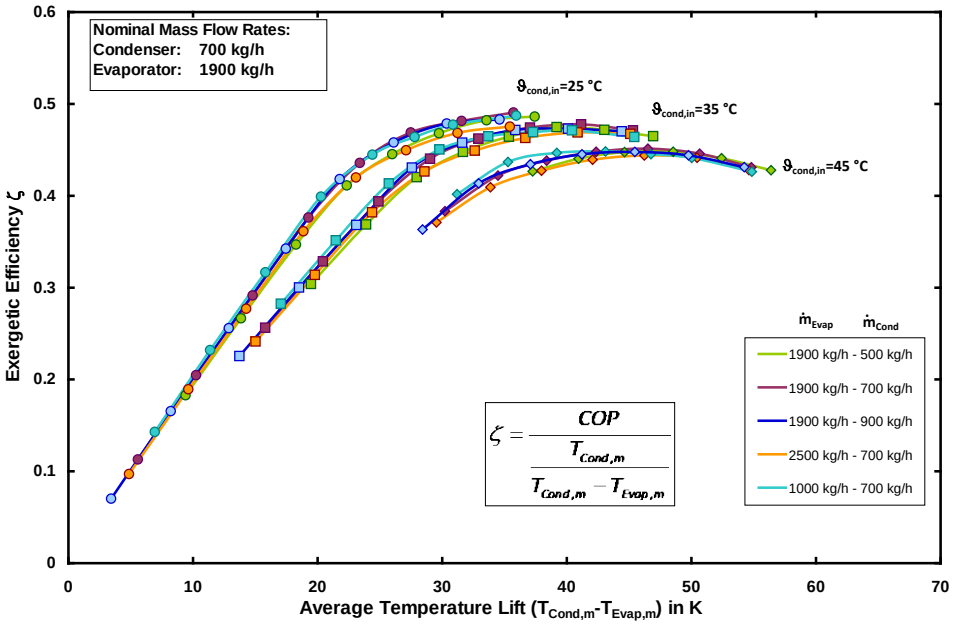

Fig. 5: Exergetic efficiency for different mean condenser temperatures and flow rates over the average temperature lift of the heat pump

The exergetic efficiency in Fig. 5 is plotted over the average temperature lift of the heat pump. The measured data point on the right side of each curve belongs to a source temperature of -5 °C and the source temperature is rising from the right to the left. The optima of the exergetic efficiency curves lie at a temperature lift of about 35 to 45 K between sink and source. A reduction of the temperature lift below the optimum by solar heat supply on the source side leads to a decrease in exergetic efficiency and the COP-values approximately reach constant values (see Fig. 3 and Fig. 4). The exergetic optimum is shifted to higher values with higher condenser temperatures.

To conclude, solar heat supplied to the source side of heat pump systems with high condenser temperatures is more valuable and leads to higher electricity savings than in systems with low condenser temperatures.

In order to quantify the COP improvement depending on the source temperature rise the COP characteristic curves are differentiated (see Fig. 6) with respect to the temperature difference. This relative COP-gain is related to electrical energy savings.

All the curves in Fig. 3 to Fig. 5 and especially in Fig. 6 express an effect that can't be neglected if a solar collector shall be connected to a ground coupled heat pump system: solar heat that is used to increase the evaporator inlet temperature does not always lead to significant improvements in the system performance (between 0.3 and 2.5 %/K). Especially for low temperature lifts between evaporator and condenser the possible gains from solar heat supply is abolished by characteristic heat pump behaviour. In addition, systems that combine both technologies should be equipped with controllers that use sophisticated algorithms which include the knowledge about heat pump characteristics in a broad temperature band (see (Haller and Frank 2011) for an example).

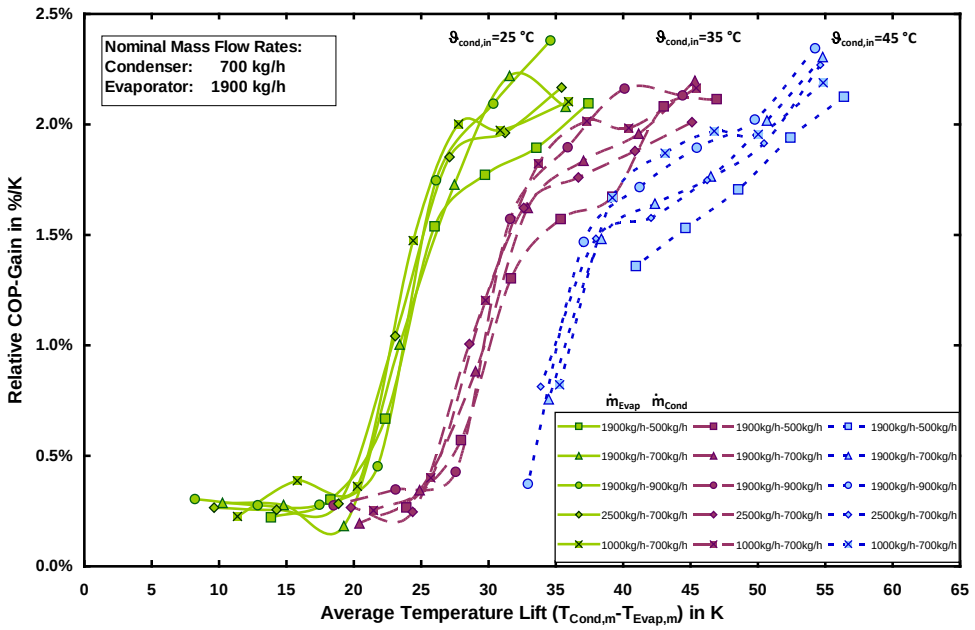

Fig. 6: Relative COP-gain per K increase of the source temperature as a function of average temperature lift for different configurations of flow rate and condenser inlet temperatures

3.3 Transient behaviour of heat pump

Most of the ground-coupled heat pumps for domestic applications run with constant compressor speed leading to intermittent operation in part load conditions. Depending on the system configuration and its design the combination with solar collectors can increase part load periods. Thus for the assessment of system configurations by simulations detailed knowledge about the start-up behavior of a heat pump is very important. The YUM model (type 401) describes the start-up behavior of the thermal power by a first order function with a time constant.

As it is not a standard parameter within DIN EN 14511-3:2012, the time constant has been determined at ISFH during a start-up period (see Fig. 7). The condenser heat flow rate rises after starting the heat pump with a time delay of about 6-9 s (sample time 3 s), which corresponds to the fluid volume of the condenser. Fig. 7 shows that the first order functions with a time constant of 10 s and a delay time between 8-10 s describe the measured values quite well, though the temperature response curve obviously shows a second order shape. In order to parameterize the YUM model that considers no delay time the error over the start-up period has to be minimized. This can be achieved by a time constant of 20 s.

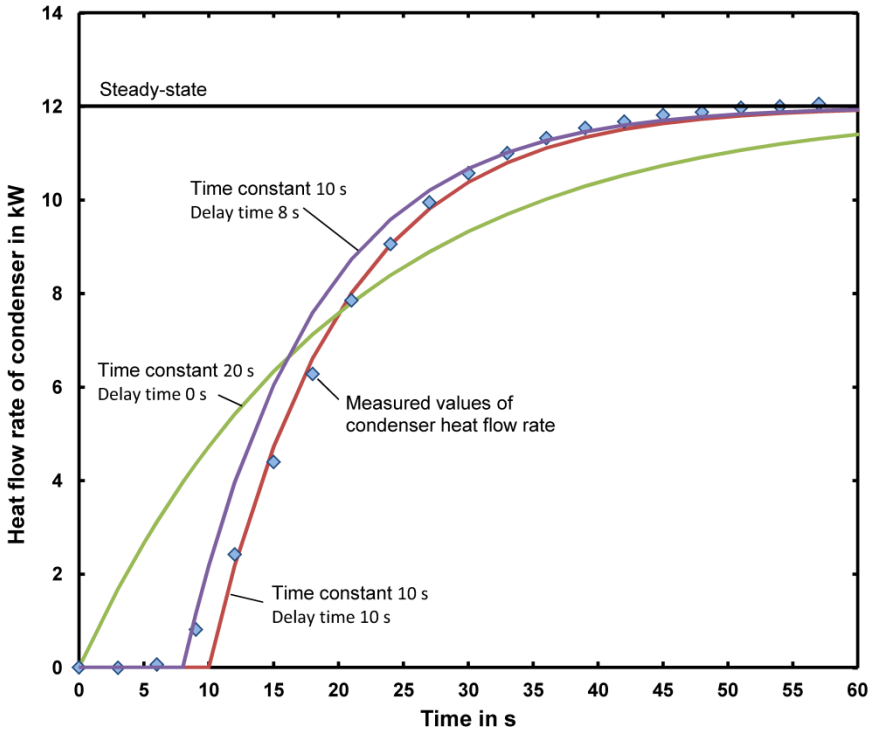

Fig. 7: Measured start-up behavior and different approximations (all first order)

Using 20 s instead of 180 s which is the default value for YUM model increases the SPF_{SHP} of a typical heat pump system from 3 to 4 and shows that it is an important parameter for transient system simulations.

4. Validation of YUM-heat pump model (TRNSYS Type 401)

The TRNSYS Type 401 (Afjei and Wetter 1997) is a black-box model for compression heat pumps that works with biquadratic polynomials describing the temperature dependency of the condenser power and the electric power. The 12 required coefficients (6 for condenser and 6 for electric power) are calculated by a multi-linear regression of manufacturer or test centre data. Of course the variation of the data, at least 12 points, should cover the whole temperature range of the expected heat pump operation to avoid extrapolation. As well, to cover a broader temperature range as it might occur in combined systems with solar thermal collectors the amount of interpolation nodes of the polynomials should be high. Here 23 interpolation nodes at nominal flow rates are used.

For the validation of Type 401 the measured mass flow rates and the inlet temperatures of evaporator and condenser of the experiments above (see Fig. 2) are given as input values into the model. Then the deviations between simulated and measured thermal and electric power and COP are compared (see Polynomial 700 Test 700 data in Fig. 8).

In general, Type 401 is made for heat pump operation with constant flow rates. However, in combined systems it might be necessary to run the components with varying flow rates. The investigations have shown that Type 401 works most precisely for constant flow rates and with polynomial coefficients determined on basis of the same operation conditions. For a system operation with varying flow rates (Pahud and Lachal 2004) show a method how the polynomial coefficients only from the reference case can be applied indeed.

The first boundary condition to derive the correction formulas is constant mean temperature:

$$\frac{\vartheta_{out} + \vartheta_{in}}{2} = \frac{\vartheta'_{out} + \vartheta'_{in}}{2} \qquad \text{Eq. 6}$$

The second boundary condition is constant heat flow rate. Assuming that the influence of the fluid heat capacity can be neglected due to Eq. 6 it follows simplified (here for the evaporator):

$$\dot{m}_{in} \cdot \left(\vartheta_{in} - \vartheta_{out}\right) = \dot{m}'_{ref} \cdot \left(\vartheta'_{in} - \vartheta'_{out}\right) \qquad \text{Eq. 7}$$

Based on these conditions, the method leads finally to the two following formulas, Eq. 8 for the corrected inlet temperature and Eq. 9 for the "re-corrected" outlet temperature:

$$\vartheta'_{in} = \vartheta'_{out} \cdot \frac{\dot{m}'_{\text{ref}} - \dot{m}_{in}}{\dot{m}'_{\text{ref}} + \dot{m}_{in}} + \vartheta_{in} \cdot 2 \cdot \frac{\dot{m}_{\text{in}}}{\dot{m}'_{\text{ref}} + \dot{m}_{in}} \qquad \text{Eq. 8}$$

$$\vartheta_{out} = \vartheta_{in} \cdot \frac{\dot{m}_{\text{in}} - \dot{m}'_{ref}}{\dot{m}'_{ref} + \dot{m}_{in}} + \vartheta'_{out} \cdot 2 \cdot \frac{\dot{m}'_{\text{ref}}}{\dot{m}'_{\text{ref}} + \dot{m}_{in}} \qquad \text{Eq. 9}$$

The validation of the YUM-Model including the flow rate correction according to (Pahud and Lachal 2004) is carried out in several steps:

1. The polynomial coefficients are determined from the steady-state data at constant flow rate conditions (condenser 500, 700 or 900 kg/h each with evaporator 1900 kg/h). Afterward the model with the polynomial coefficients is applied to the whole measured data set (including transient values see Fig. 2) with the **correct** flow rate in order to determine the uncertainty of the model (Abbreviations in Fig. 8 „Polynomial700 Test700", „Polynomial500 Test500" „Polynomial900 Test900"). These deviations represent the optimum and therefore the reference for a flow rate correction. The average relative deviation of the model for the three different condenser flow rates is shown in Table 8.

Table 8: Model uncertainty for condenser heat flow rate, electric power and COP, average for three flow rates (condenser 500, 700, 900 kg/h, evaporator 1900 kg/h) between measurement and simulation

		$\dot{Q}_{Cond}$	P_{el}	COP
Relative deviation	**%**	0.64%	-0.26%	1.14%
Standard deviation	**%**	3.6%	3.6%	5.4%

2. In the second step the model is fed with the coefficients derived with nominal flow rate but applied to the measured data set of another flow rate (abbreviations in *Fig. 8*„Polynomial700 Test500" „Polynomial700 Test900") in order to determine the error due to **"wrong" coefficients**. The errors of the condenser heat flow rate and the electric power increase from 1 up to 3 %. The error of the COP increases even up to 5 %.

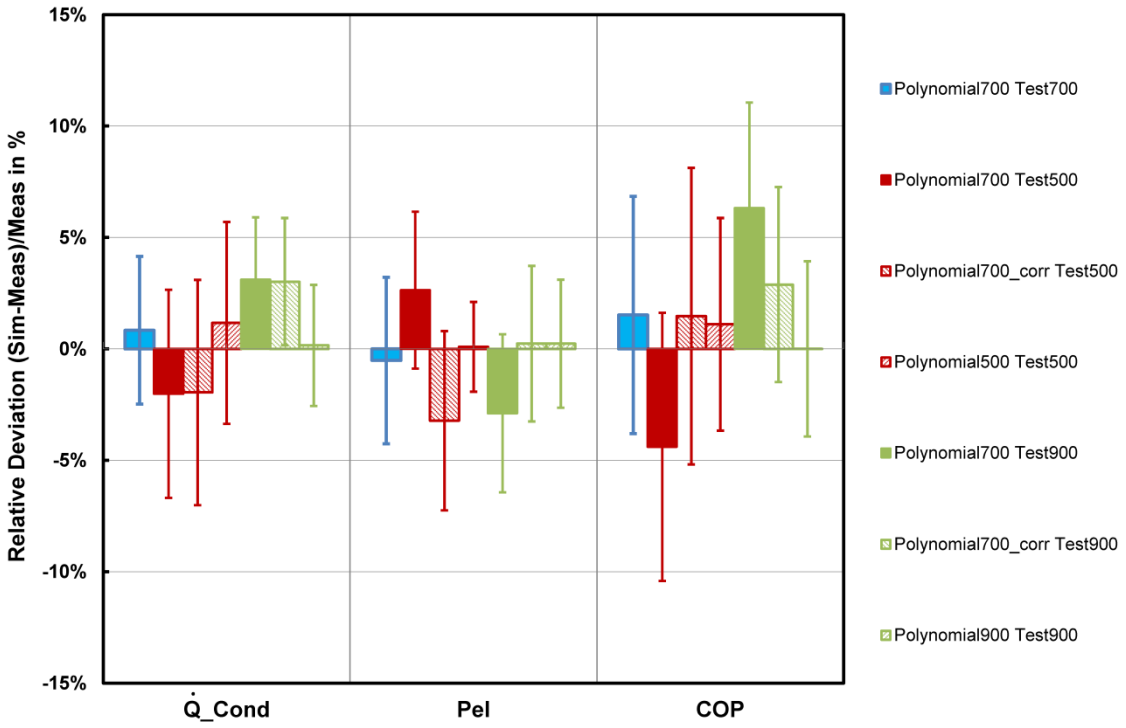

Fig. 8: Relative deviation and standard deviation between simulation and measurement for condenser heat flow rate, electric power and COP for different pairs of polynomial coefficients and flow rates

3. Finally the **flow rate correction** according to (Pahud and Lachal 2004) is analysed. Obviously the model error due to „wrong" coefficients obtained from 700 kg/h data applied to 500 kg/h and 900 kg/h data (abbreviation in *Fig. 8* „Polynomial700_corr Test500" „Polynomial700_corr Test900") decreases. The error of the COP is reduced from 5 % to about 2 %. The improvement considering $\dot{Q}_{cond}$ and P_{el} is less big. It can be stated that the correction methods is applicable and leads to better results.

5. References

Afjei, T. and Wetter, M. 1997. Compressor heat pump including frost and cycle losses. Version 1.1 Model description and implementing into TRNSYS. Zentralschweizerisches Technikum Luzern.

Baehr, H.D. and Kabelac, S. 2009. Thermodynamik. Springer.

Bertram, E., Glembin, J., Scheuren, J., Rockendorf, G. and Zienterra, G. 2008. Unglazed Solar Collectors in Heat Pump Systems: Measurement, Simulation and Dimensioning. (Lisbon, Portugal, Oct. 2008).

Bertram, E., Pärisch, P. and Tepe, R. 2012. Impact of solar heat pump system concepts on seasonal performance - Simulation studies. Proceedings of the EuroSun 2012 Conference (Rijeka, Croatia, 20.09. 2012).

Bertram, E., Stegmann, M. and Rockendorf, G. 2011. Heat Pump Systems with Borehole Heat Exchanger and Unglazed PVT Collector. Proceedings of the ISES Solar World Congress 2011 (Kassel, Germany, 08.-02.09. 2011).

DIN EN 14511-3 2012. Luftkonditionierer, Flüssigkeitskühlsätze und Wärmepumpen mit elektrisch angetriebenen Verdichtern für die Raumbeheizung und Kühlung - Teil 3: Prüfverfahren. Beuth.

DIN EN 14511-3 2008. Luftkonditionierer, Flüssigkeitskühlsätze und Wärmepumpen mit elektrisch angetriebenen Verdichtern für die Raumbeheizung und Kühlung - Teil 3: Prüfverfahren. Beuth.

Haller, M. and Frank, E. 2011. On the potential of using heat from solar thermal collectors for heat pump evaporators. Proceedings of the ISES Solar World Congress 2011 (Kassel, Germany, 08.-02.09. 2011).

Pahud, D. and Lachal, B. 2004. Mesure des performances thermiques d'une pompe à chaleur couplée sur les sondes géothermiques à Lugano (TI). Technical Report #40430 / 80266. Bundesamt für Energie.

Pärisch, P., Kirchner, M., Wetzel, W., Voß, S. and Tepe, R. 2011. Test system for the investigation of the synergy potential of solar collectors and borehole heat exchangers in heat pump systems. Proceedings of the ISES Solar World Congress 2011 (Kassel, 08.-02.09. 2011).

Tepe, R., Rönnelid, M. and Perers, B. 2003. Swedish Solar Systems in Combination with Heat Pumps. Proceedings of the ISES Solar World Congress 2003 (Göteborg, 2003).

A9. Heat Pump Model List

1. Heat Pump Model List

Name	Platform	Validation	Availability	Description	Literature	Author	Contact	HP-Type	Type of model	Calculation method		Transient effects	Capacity control
										thermal	temporal		
physical effect models													
ORNL Heat pump design model Mark VII	html online	yes	free access		http://www.ornl.gov/~wlj/hpdm/	DOE/ORNL		A/A	physical		STAT	no	
TRNSYS Type 877	TRNSYS 16	ongoing	proprietary ?		see Chapter A3	S. Bertsch, CH M. Haller, CH A. Heinz AT	Andreas Heinz, IWT Graz, AT	A/W, B/W, W/W	physical	C-Perf (compressor); NTU-HX	QSTAT	COND	in development
RDmes HP	html online	in the source published article	ask RDmes for your use	Parameter estimation based model. It can model any heat pump with the information of the catalogue data.	Jin, H. And J.D. Spitler. 2002. A Parameter Estimation Based Model of Water-To-Water Heat Pumps for use in Energy Calculation Programs. ASHRAE Transactions. 108(1): 3-17	Jin, H. Spitler J.D.	D. Carbonell RDmes, ES	W/W B/W reciprocating, scroll	physical	PHYS ParEst RefProp	QSTAT	no	no
LOREF	Matlab / Simulink	yes	proprietary (HSLU)	detailed model of evaporator with frosting	http://www.bfe.admin.ch/dokumentation/energieforschung/index.html?lang=de&publication=9671 LOREF report of SFOE switzerland	B. Wellig HSLU	Beat Wellig HSLU T+A, CH	A/all	physical		INT	no	no
TRNSYS Type 176	TRNSYS	yes		HP model for different kind of heat sources and heat sinks; consideration of defrosting; capacity control is possible;	http://www.ise.fraunhofer.de/veroeffentlichungen/nach-jahrgaengen/2001/simulationsmodell-fur-warmepumpen/at_download/file	A. Bühring, Fraunhofer ISE	Fraunhofer ISE	all	physical	C-Perf (compressor); NTU-HX	QSTAT	yes	yes
component performance map models													
TRNSYS Type 372	TRNSYS		to buy for everyone		http://www.transsolar.com/__software/download/en/ts_type_372_beta_en.pdf	M. Hornberger	Transsolar		grey box	C-PERF	QSTAT		no
KTH - Madani	EES	validated in wide range of conditions	proprietary (KTH)	separate models for variable speed compressor, single speed compressor, evaporator, condenser	Madani H., Claesson J. and Lundquist P., 2011. Capacity control in ground source heat pump systems part I: modeling and simulation. International Journal of Refrigeration, Volume 34, Issue 6, Pages 1338-1347	H. Madani KTH Stockholm	Hatef Madani KTH, SE	all	grey box	C-PERF+ RefProp	QSTAT		yes
INSEL-HP	INSEL	needed	shared fortran code	separate models for evaporator, condenser, single speed compressor with constant compressor efficiency	see Chapter A1	A. Dalibard HFT Stuttgart	A. Dalibard HFT-S, DE	all	grey box	C-PERF+ RefProp	QSTAT	no	no
HP performance map models													
TRNSYS Type 401 (201) (YUM)	TRNSYS		to buy for everyone	includes frost and cycle losses	http://www.transsolar.com/__software/download/en/ts_type_401_en.pdf	M. Wetter T. Afjei	Transsolar	all	black box	HP perf. map		COND	no
TRNSYS Types 504, 505, 665, 668	TRNSYS		TESS Library	all based on catalogue/measurement data and data interpolation and curve fits. Steady state models.	http://sel.me.wisc.edu/trnsys/components/componen.htm		C. Bales SERC, SE		black box	HP perf. map		no	no
TRNSYS Type 204	TRNSYS		proprietary	Dual-stage compressor heat pump including frost and cycle losses		M. Wetter T. Afjei	Thomas Afjei IEBau, CH	all	black box	HP perf. map		COND	no
Carnot-HP	Matlab / Simulink Carnot		open source	based on catalogue / measurement data with data interpolation		B. Hafner	Bernd Hafner Viessmann, DE	B/W	black box	HP perf. map		no	no
STASCH-HP (YUM)	Matlab / Simulink Carnot		IEBau	based on catalogue / measurement data with data interpolation, curve fit, includes frost and cycle losses	http://www.fhnw.ch/habg/iebau/afue/gruppe-gebaeudetechnik/standardschaltungen-waermepumpenanlagen	U. Schonhardt T. Afjei	Ralf Dott IEBau, CH	all	black box	HP perf. map		COND	no

POLYSUN	Applicatino software, Online service since 2012	SPF, Hetag	From Vela Solaris AG	Performance model suitable for usage with norm measurement values. Fully integrated in modular dynamic system modelling	www.velasolaris.com see Chapter A4	Vela Solaris AG	J. Marti	A/W, B/W, W/W	Grey box	Dynamic	Dynamic	Effective mass covers machine inertia	no

Name	Platform	Valida-tion	Availability	Description	Literature	Author	Contact	HP-Type	Type of model	Calculation method	Transient effects	Capacity control
calculation methods												
SIA 384/3:201x Entwurf 08-2011	open		in development	Heizungsanlagen in Gebäuden – Energiebedarf	see SIA	H.Huber IEBau, CH	Thomas Afjei IEBau, CH	all	black box SPF	HP-PERF	BIN	no	no
EN 15316-4-2:2008	open		to buy for everyone	Heating systems in buildings - Method for calculation of system energy requirements and system efficiencies - Part 4-2: Space heating generation systems, heat pump systems	see CEN			all	black box SPF	HP-PERF	BIN	no	no
ISO/WD 13612-2	open		in development	Building Environment Design — Heat pump systems for heating and cooling — Part 2: Energy calculation	see ISO			all	black box SPF	HP-PERF	BIN	no	yes
EN 14825:2012	open		to buy for everyone	Air conditioners, liquid chilling packages and heat pumps, with electrically driven compressors, for space heating and cooling - Testing and rating at part load conditions and calculation of seasonal performance	see CEN			all	black box Ref-SPF	HP-PERF	BIN	no	yes
ANSI/ASHRAE Standard 137-2009	open		to buy for everyone	Methods of Testing for Efficiency of Space-Conditioning/Water-Heating Appliances that Include a Desuperheater Water Heater (ANSI/ASHRAE Approved)	see ASHRAE			all	black box SPF	HP-PERF	BIN	no	
VDMA 24247 (Entwurf2010)	open		in development	Energieeffizienz von Kälteanlagen Teil 1: Klimaschutzbeitrag von Kälte- und Klimaanlagen – Verbesserung der Energieeffizienz – Verminderung von treibhausrelevanten Emissionen	see VDMA			A/A split	grey box COP	C-PERF	STAT	no	yes
ISO/DIS 15042:2005	open		in development	Multiple split-system air-conditioners and air-to-air heat pumps — Testing and rating for performance	see ISO			multi-split	black box SPF			no	yes
SPA3-528	MS Excel		no	calculations of SPF, developed by SP, air-to-air, air-to-water and liquid-to-water	see SP	SP	U. Pettersson, SP	all	black box				
Prestige	stand alone		to buy for everyone	Calculations of SPF, developed by SVEP, air-to-air, air-to-water and liquid-to-water, for domestic houses only	see SP	SVEP	U. Pettersson, SP	all	black box				

2. Heat Pump Model List – Legend

Abbreviation	Description	Weblink
Platform		
html online	Tool to be used over internet online	
TRNSYS	TRaNsient SYstems Simulation program	http://sel.me.wisc.edu/trnsys/
MATLAB / Simulink	MATrix LABoratory / Graphical Simulation environment	http://www.mathworks.com
INSEL	INtegrated Simulation Environment Language	http://www.insel.eu
MS Excel	Microsoft Excel	http://office.microsoft.com/excel/
EES	Engineering Equation Solver	http://www.fchart.com/ees/
POLYSUN	Originally the dynamic solar thermal simulation tool of University of Rapperswil, extended to cover heat pumps by Vela Solaris AG	http://www.velasolaris.com/
open	Open for all platforms and use, neutral description	
stand alone	stand-alone software without further specification	
HP-Type		
A/A	air-to-air heat pump, uses air as heat source and also air as heat sink	
A/W	air-to-water heat pump	
W/W	water-to-water heat pump	
B/W	brine-to-water heat pump	
W/A	water-to-air heat pump	
B/A	brine-to-air heat pump	
split	split system, where the evaporator and condenser part are mounted separately	
multi-split	split system, where the evaporator and condenser part are mounted separately and which uses more than one evaporator or more than one condenser	
all	all heat pump types possible	
Type of model		
physical	physical model of the represented physical effects	
grey box	empirical model of the represented effects with only few knowledge about inside details	
black box	empirical model of the represented effects without knowledge about inside details	
Ref-SPF	reference seasonal performance factor, derived from reference conditions	
SPF	seasonal performance factor	
Calculation method		
thermal	thermal model of the heat pump or its components	
temporal	time depending representation of the heat pump behaviour and temporal duration of the considered observation	
ParEst	Parameter Estimation based on a limited performance map data base	
C-PERF	calculation using Component PERFormance maps of the represented effects	
HP-PERF	calculation using Heat Pump PERFormance maps of the represented effects	
NTU-HX	Number of Transfer Units model for Heat eXchangers	
PHYS	calculation using PHYSical models of the represented effects	
STAT	STATic or steady state viewing not considering the element of time	
QSTAT	Quasi STATic viewing using difference equations where inside one timestep the viewing does not consider time, but considers time in the end of each timestep	
INT	INTegration of time using differential equations	
BIN	BIN-Method, where time is pre-evaluated according to defined boundary conditions and each relevant interval of boundary conditions is weighted by the frequency of its occurrence	
Transient effect		
COND	CONDenser = part of the heat pump where the condensation of the refrigerant takes place	
EVAP	EVAPorator = part of the heat pump where the evaporation of the refrigerant takes place	
COMP	COMPressor = part of the heat pump where the gaseous refrigerant is compressed	

3. Heat Pump Model List – Institutions

Abbreviation	Description	Weblink
IEBau	Institut Energy am Bau - Fachhochschule Nordwestschweiz (Institute of Energy in Building - University of applied Sciences Northwestern Switzerland)	www.fhnw.ch/iebau
HFT	Hochschule für Technik - Stuttgart (University of applied Sciences in Stuttgart)	www.hft-stuttgart.de
ORNL	Oak Ridge National Laboratory	www.ornl.gov
DOE	United States Department Of Energy	www.enery.gov
SPF	Institut für Solartechnik - Fachhochschule Ostschweiz (Institute for Solar Technology - University of Applied Sciences of Eastern Switzerland)	www.spf.ch
HSLU	Hochschule Luzern (Lucerne University of Applied Sciences and Arts)	www.hslu.ch
RDmes	Research and Development in Mechanical Engineering Solutions	www.rdmes.com
SFOE	Schweizerisches Bundesamt für Energie (Swiss Federal Office of Energy)	www.bfe.admin.ch
KTH	Kungliga Tekniska Högskolan (Swedish Royal Institute of Technology)	www.kth.se
SERC	Centrum for solarenergiforskning - Högskolan Dalarna (Solar Energy Research Center)	www.serc.se
SP	Sveriges Tekniska Forskningsinstitut (Technical Research Institute of Sweden)	www.sp.se
SVEP	Svenska Värmepumpföreningen (Swedish heat pump association)	www.svepinfo.se
TESS	Thermal Energy Systems Specialists	http://www.tess-inc.com/
SIA	Schweizerischer Ingenieur- und Architektenverein (Swiss engineers and architects association)	www.sia.ch
CEN	European Committee for Standardization	www.cen.eu
ISO	International Organization for Standardization	www.iso.org
ASHRAE	American Society of Heating, Refrigerating and Air-Conditioning Engineers	www.ashrae.org
VDMA	Verband Deutscher Maschinen- und Anlagenbau e.V. (German Engineering Federation)	www.vdma.org